CHARACTERIZATION OF THE INTERACTIONS BETWEEN INDOLICIDIN AND ITS ANALOGS WITH LIPOPOLYSACCHARIDE THROUGH CAPILLARY ELECTROPHORESIS

by

Tallon Milne

B.Sc., Simon Fraser University, 2013

A THESIS SUBMITTED IN PARTIAL FULFILLMENT OF THE REQUIREMENTS
FOR THE DEGREE OF
MASTER OF SCIENCE IN ENVIRONMENTAL SCIENCES

in

The Faculty of Graduate Studies
(Master of Environmental Science, *Chemistry*)

Thesis examining committee:

Heidi Huttunen-Hennelly (PhD), Associate Professor and Thesis Supervisor
Department of Physical Sciences (Chemistry)

Kingsley Donkor (PhD), Professor and Thesis Co-Supervisor
Department of Physical Sciences (Chemistry)

Jonathan Van Hamme (PhD), Associate Professor and Committee Member
Department of Biological Sciences

Christopher Harrison (PhD), Associate Professor and External Examiner
San Diego State University, Department of Chemistry and Biochemistry

August 2017

Thompson Rivers University

Thesis Supervisors: Associate Professor Heidi Huttunen-Hennelly & Professor Kingsley Donkor

ABSTRACT

Antimicrobial resistance is an emerging threat in the healthcare industry, endangering the efficacy of antimicrobials that have been used to save millions. Innovative research is required to establish a strong understanding of the non-covalent interactions between drugs and their receptors to advance drug development to slow this epidemic. The interaction between indolicidin (indol) and indolicidin45 (indol45) with lipopolysaccharide (LPS) was characterized using capillary electrophoresis (CE). Indol is a cationic antimicrobial peptide (AMP) that is isolated from the cytoplasmic granules of bovine neutrophils. Cationic AMPs are produced by organisms at infection sites and have a broad-spectrum of antimicrobial properties. The shortcoming of indol is that it is too toxic and hemolytic for therapeutic use. To improve the deficiencies of indol, it was previously altered through amino acid substitution. Indol45, a novel indol analog, was developed and has an increased antimicrobial potential and exhibits reduced hemolysis. LPS is the suspected target receptor for indol and indol45, located in the bacterial envelope. The equilibrium constant (K_b) for the interaction between indol and LPS, as well as, indol45 and LPS was determined using a range of CE techniques. Pre-incubation affinity CE (PI-ACE) was utilized over a temperature range of 20 – 30 °C to establish a K_b with thermodynamic parameters. Frontal analysis CE (FACE) was additionally employed to validate the K_b and the interactions binding stoichiometry. Ultimately, through PI-ACE, K_b values for the indol-LPS interaction ($3.13 \pm 0.77 \times 10^4\ M^{-1}$) and indol45-LPS interaction ($14.83 \pm 1.67 \times 10^4\ M^{-1}$) were determined at a physiological pH of 7.2. Both interactions were found

to be thermodynamically favourable and determined to be due to electrostatic forces. The FACE analysis verified previous results with a K_b close to PI-ACE findings. These results display that indol45 binds slightly stronger to LPS at equilibrium. This indicates that indol analogs with increased antimicrobial activity and less toxic properties have the potential to be novel drug candidates.

Keywords: Indolicidin / Lipopolysaccharide / Capillary electrophoresis / Equilibrium binding constant / Interaction studies

TABLE OF CONTENTS

ACKNOWLEDGEMENTS

I would like to express my deepest appreciation and gratitude to my supervisor, Dr. Heidi Huttunen-Hennelly, for her patience, her endless support, and her unwavering positivity. If I become only half the thinker, half the parent, and half the person that Heidi is, it will undoubtedly be one of my greatest accomplishments. I would also like to thank my co-supervisor, Dr. Kingsley Donkor, for providing endless help and guiding my research towards success. Without Kingsley, I would never have accomplished my thesis. A special thanks goes out to my last committee member Jonathan Van Hamme, for his interest in my research and the dedicated help he provided on my thesis. I am also grateful to Dr. Christopher Harrison, my external examiner, for all the time he provided and the thought-provoking feedback he offered.

A genuine thank you goes to Erika Dufort-Lefrancois for her continuous help and advice throughout my research, it will never be forgotten. You taught me the meaning of perseverance, determination, and dedication towards your goals.

I would also like to acknowledge the Men's Basketball program, the Graduate Student Research Mentor Fellowship, and the Ken Lepin Graduate Student Award from Thompson Rivers University for all of their financial assistance with my project.

Finally, I would be remiss if I didn't recognize the love and support of my girlfriend, Kacy Fehr. Thank you for the encouragement when I needed it most.

DEDICATION

To my parents

For their wisdom, guidance, and support.

LIST OF FIGURES

LIST OF TABLES

LIST OF IMPORTANT TERMS AND ABBREVIATIONS

ACE	Affinity capillary electrophoresis
AMP	Antimicrobial peptide
AMR	Antimicrobial resistance
BGE	Background electrolyte
CE	Capillary electrophoresis
CMC	Critical micelle concentration
D	Drug
DMSO	Dimethyl sulfoxide (neutral marker)
DP	Drug-protein complex
EOF	Electroosmotic flow
FACE	Frontal analysis capillary electrophoresis
h or hrs	Hours
ID	Internal diameter of capillary
Indol	Indolicidin
Indol45	Indolicidin analog
L	Litres
LPS	Lipopolysaccharide
L_t and L_d	Total capillary length and capillary length to detector
K or K_b	Equilibrium constant, also termed binding constant
MHC	Minimum hemolytic concentration
MIC	Minimum inhibitory concentration
min	Minutes
mol	Moles
OD	Outer capillary diameter
P	Protein

PI-ACE	Pre-incubation affinity capillary electrophoresis
ppm	Parts per million, mg-L^{-1} equivalent
R^2	Linear correlation coefficient
s	Seconds
UV	Ultraviolet
μ	Electrophoretic mobility
v/v	Volume per volume
WPW motif	Tryptophan-Proline-Tryptophan in a peptide sequence

CHAPTER 1: INTRODUCTION

Antimicrobial resistance (AMR) is an emerging threat occurring worldwide, endangering the efficacy of antimicrobials that have saved millions since their emergence in the 1940s.[1] Major advancements in medicine and surgery have been accomplished due to the prevention and treatment of infections with antimicrobials. After years of protection from microbial infections, the "golden age" of antimicrobials could be facing an impending disaster due to multidrug resistant organisms.[2] AMR can be attributed to the over prescription and misuse of these medications, as well as a shortage of drug development by the pharmaceutical industry.[3] Antimicrobials are; clinically overprescribed by physicians and thereby overused by patients, extensively employed as growth supplements for livestock, and even available in developing nations as over-the-counter drugs.[3] The pharmaceutical industry also has had an inadequate development of new antimicrobials due to economic and regulatory obstacles.[1,3]A coordinated effort to implement new management policies and provide extensive research is required to manage this crisis. Research focused on drug and receptor interactions is essential for pharmaceutical advancement. The following information about indolicidin (indol), an indolicidin analog (indol45), lipopolysaccharide (LPS), and capillary electrophoresis (CE) is not comprehensive, but presented for individuals whose expertise lies elsewhere.

INDOLICIDIN

New and innovative types of antimicrobials are required to prevent the increase of multidrug resistant organisms. One possible solution is cationic antimicrobial peptides (AMPs), often referred to as "nature's antibiotics".[4,5] Cationic AMPs are produced by many organisms as innate non-specific defence mechanisms

towards infections and show promise as novel anti-infective agents.[4,6] They have an astonishing range of antimicrobial activities, which include activity against most Gram-positive and Gram-negative bacteria, fungi, enveloped viruses, and even eukaryotic parasites.[6] They possess a broad spectrum of activity, which helps prevent them from becoming ineffective against multidrug resistant organisms. Indol is one such cationic AMP isolated from the cytoplasmic granules of bovine neutrophils.[6] Indol is composed of 13 amino acids and is antimicrobial tridecapeptide amidated at the C-terminus (ILPWKWPWWPWRR-NH_2) with a net charge of +4 at physiological pH (Figure 1.1).[5]

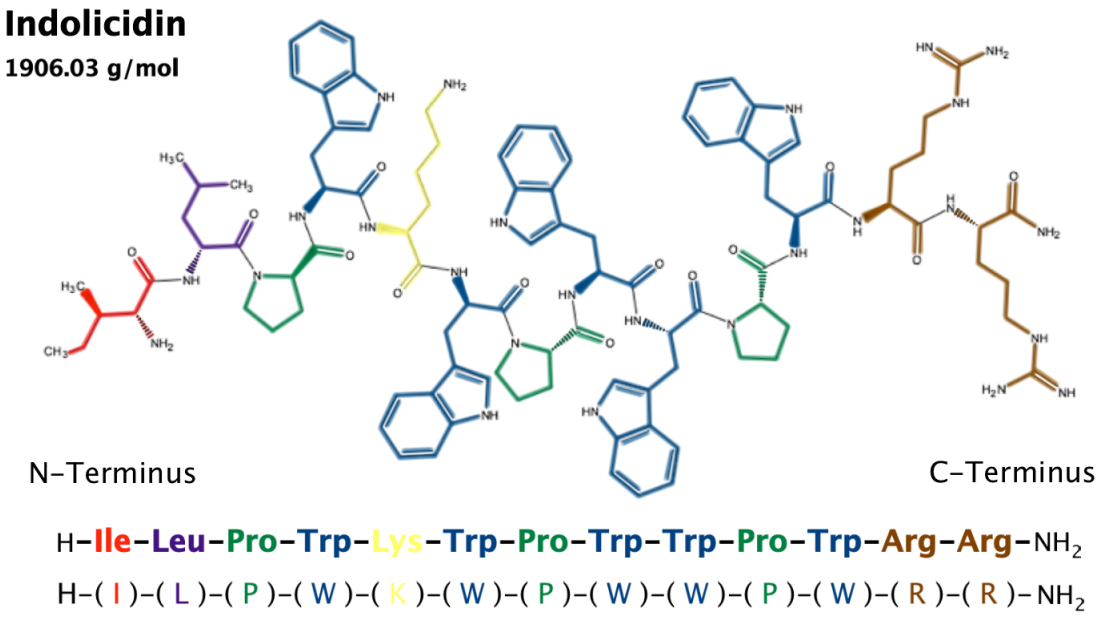

Figure 1.1: Structure of the antimicrobial peptide indolicidin.

Indolicidin is one of the smallest natural linear cationic AMPs known, with a unique extended boat-shaped structure unlike α-helical and β structure cationic peptides.[7,8] It also contains only six different amino acids with 38% being tryptophan, the highest percentage of tryptophan in any known peptide.[9] Indol

has displayed antimicrobial properties against Gram-positive and Gram-negative bacteria[6], protozoa[10], fungi[11], and the enveloped virus HIV-1[12]. Unfortunately, indol is also cytotoxic to rat and human T-lymphocytes[13] and lyses erythrocytes[11].

The properties and interactions of indol have been thoroughly researched but much is still unknown. The exact mechanism of antimicrobial and hemolytic attack indol displays is continuously being debated. Multiple studies have shown that indol exhibits toroidal pore formation or electroporative disruption of cell membranes, referred to as membrane permeabilization.[8,14–19] Other studies have shown that indol passes through the outer and inner membrane of Gram-negative bacteria by self-promoted uptake and then it binds to DNA and Ca^{2+} calmodulin-stimulated phosphodiesterase.[9,20] After indol binds to DNA in *E. coli* it results in filamentation, preventing replication which leads to cell lysis.[21] Ghosh et al. (2014) suggested that the PWWP motif within indol has significant importance in DNA binding.[22] The central PWWP motif of indol gives it a unique structural element where it wraps around and stabilizes DNA structures.[22] Indol has been shown to aggregate in aqueous solution, which correlated with the hemolytic properties of the peptide.[23,24] Rokitskaya et al. (2011) found that indol provoked erythrocyte lysis by disturbing metabolic regulation of osmotic balance.[25] The definitive antimicrobial mechanism of indol is still under debate, but evidently the biological action of indol is linked to membrane penetration or disruption. Therefore, an important part of future research involves the study of interactions between indol, its analogs, and LPS their proposed corresponding cell membrane receptor.[26]

Due to the short length of indol and large range of antimicrobial activity, it has great potential for development as an antimicrobial drug. However, in its

unaltered form, indol displays toxicity to both prokaryotes and eukaryotes preventing it from successful clinical application.[14,27] Consequently, many analogs have been developed from the parent structure of indol to make it less hemolytic while concurrently increasing its antimicrobial activity.[28–30] Podorieszach & Huttunen-Hennelly (2010) used solid phase peptide synthesis to develop five indol analogs by incrementally substituting the highly toxic and hydrophobic tryptophan for alanine to systematically and gradually decrease the toxic tryptophan residues and hence reduce the overall hydrophobicity of the AMP.[28] Their indolicidin analog, indol45, showed the greatest promise (more details to follow in the next section). Indol and indol45 were the main cationic AMPs examined throughout this study.

INDOL45

Indol45, (ILPWKWPWAPARR-NH_2), is an analog of indol where the 4th and 5th tryptophan residues are substituted for alanine (Figure 1.2). The novel indol analog, indol45, showed potential as a possible antimicrobial drug when compared to the parent AMP indol due to its increased therapeutic potential.[28] Indol45 displayed an increased antimicrobial activity against selected pathogens and decreased cytotoxicity with a 33 000-fold improvement in hemolytic index (defined as the Minimum Hemolytic Concentration (MHC) divided by the lowest Minimum Inhibitory Concentration (MIC)).[28] This allows indol45 a larger concentration range of safe activity than the parent AMP indol. Although a strong increase in antimicrobial activity was observed, exact binding interactions are relatively unknown. Research has focused on various indol analogs[16,23,31–36], however, the specific interaction between indol45 and LPS has not been investigated.

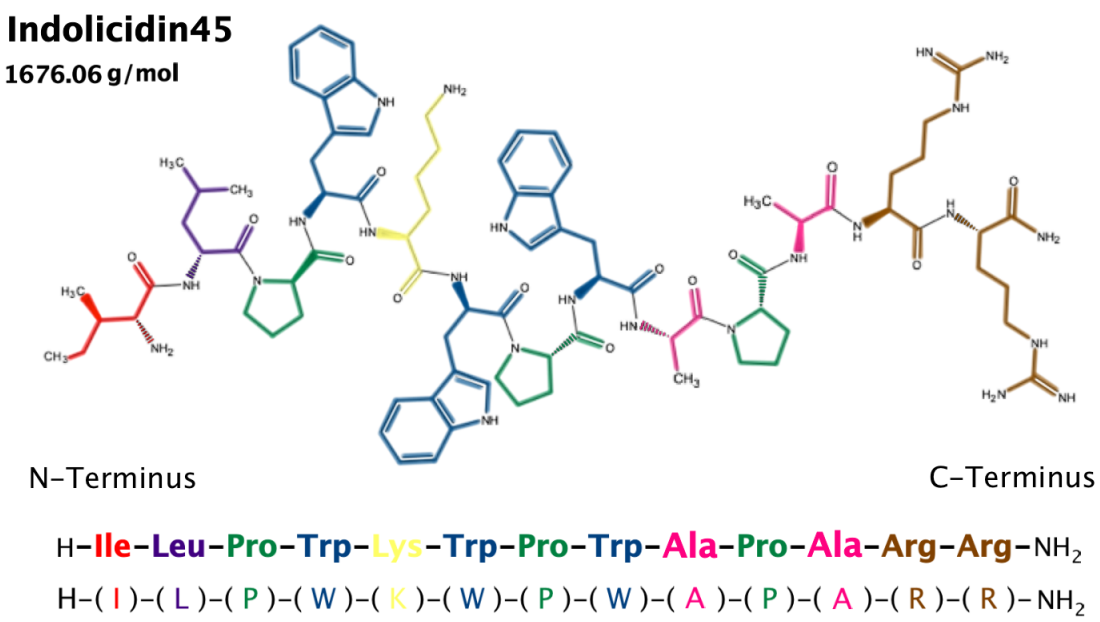

Figure 1.2: Structure of the indolicidin analog, Indol45.

Indol45 was developed in an effort to increase the antimicrobial activity of indol while minimizing hemolysis.[28] The focus was on tryptophan residues and their hydrophobic nature. By substituting tryptophan with alanine it would decrease the peptides' overall hydrophobicity. Indol has 5 tryptophan residues out of a total of 13 (38%), which is unlike any other AMP with typical abundances of only 1%.[37] By subsituting the last two tryptophan residues with alanine it removes the PWWP motif, which has been established as an important structural binding component for the DNA binding feature of indol.[22] It also removes one of the two WPW motifs from indol, which were determined to be critical for antimicrobial activity.[28] Podorieszach & Huttunen-Hennelly (2010) also found if a third tryptophan residue was removed, counting from the N-terminus, antimicrobial activity decreased.[28] Both motifs may factor into the mechanism of attack indol45 displays, however, the reduction in tryptophan content in indol analogs is definitely important for its dissociation into the cytosol. It is a delicate balance of

enough hydrophobicity to ensure the AMP can pass through the cell membrane and maitain its bioactivity, but not so much hydrophobicity (like indol) since that is linked to its hemolytic properties. Further assessment of indol45 is critical for understanding bacterial membrane interactions with peptides high in tryptophan. Knowing the full effects of tryptophan content in indol is critical for its continued drug development.

It has been shown that the negatively charged LPS layer of the outer membrane in Gram-negative bacteria prevents the translocation of AMPs.[38] To achieve access to the plasma membrane, AMPs are required to overcome the LPS permeability barrier first.[39,40] Thus, if AMPs such as indol/indol45 have LPS binding and neutralizing capabilities, it would provide a preparatory stage for their development as antibacterial drugs.[41]

LIPOPOLYSACCHARIDE

The Gram-negative bacteria cell wall is basically composed of two lipid bilayers, the outer membrane and the cytoplasmic membrane that are separated by the periplasmic space (Figure 1.3).[42] The outer membrane in common Gram-negative bacteria, like *E. coli*, is constructed of an outward directed layer consisting of LPS (also called endotoxin) and an inward layer of phospholipids.[42]

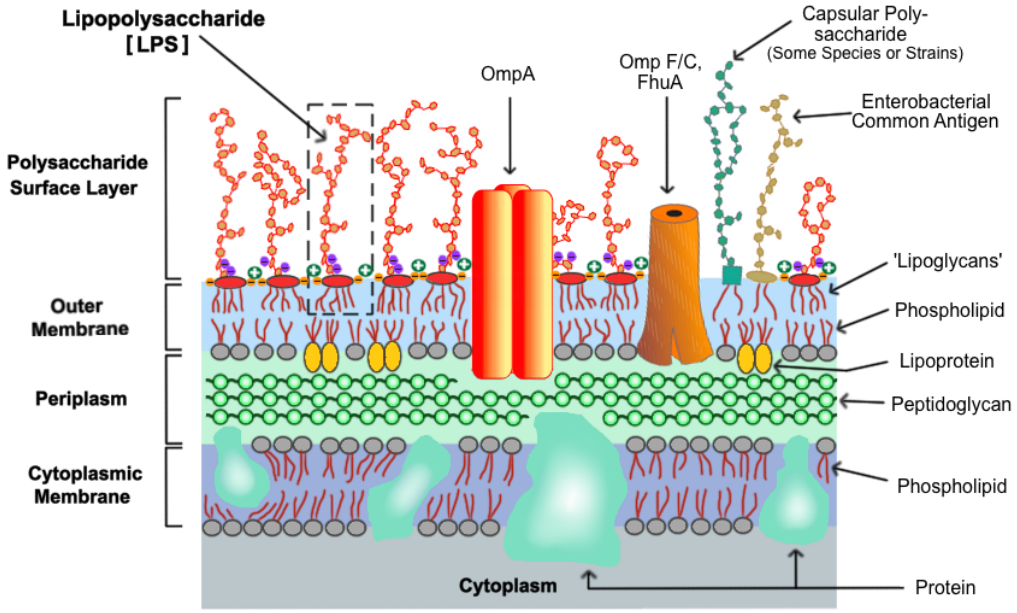

Figure 1.3: Structure of the Gram-negative bacterial cell envelope. Adapted from Alexander & Rietschel (2001).[42]

LPS makes up about 75% of the most outward membrane surface area with outer membrane proteins, capsular polysaccharides, and enterobacterial common antigens making up the rest.[42–44] Depending on bacterial species and strain, LPS can differ slightly in structure, however, every LPS molecule is comparable and made up of three sections: Lipid A, Core oligosaccharide region, and O-specific chain (Figure 1.4).

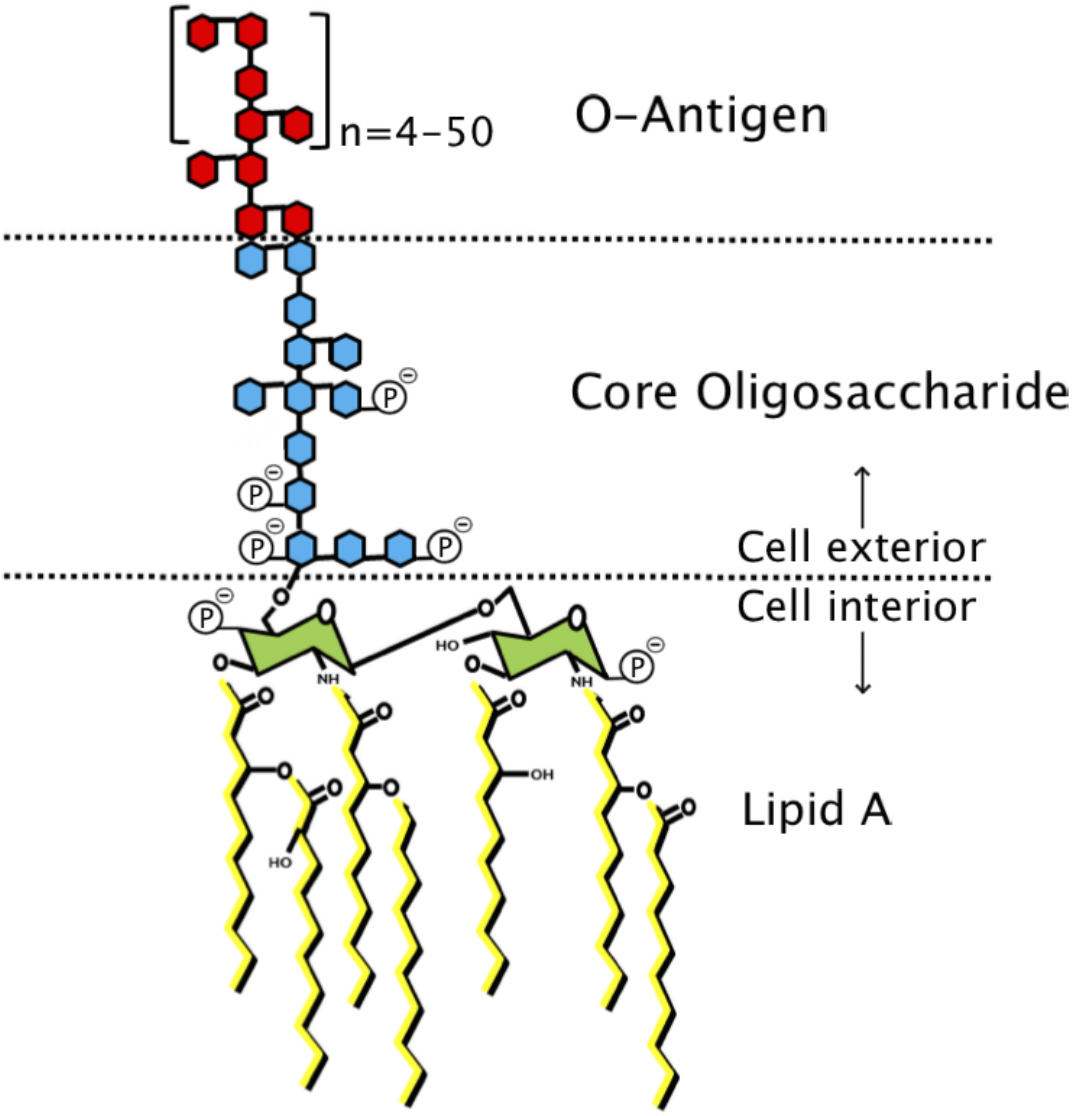

Figure 1.4: General chemical structure of LPS. Adapted from Dufort-Lefrancois (2015) while using Alexander & Rietschel (2001) for guidance.[42,45]

The hydrophobic Lipid A component of LPS anchors it to the outer bacterial membrane.[42,44] It consists of a backbone structure, which is a central β (1→6)-linked disaccharide unit composed of two D-glucosamine units attached to six acyl chains ("fatty acids") and one phosphate group on each glucosamine unit.[44] Lipid A is also the highly toxic section of LPS.[42] It is the key molecule associated

in the pathogenesis of endotoxin shock, which in humans results in septic shock due to the release of LPS from Gram-negative bacterial infections.[46–50]

The core oligosaccharide region of LPS is covalently linked to the Lipid A anchor and can be broken into an inner and outer core. The inner core shows the least structural variability and is composed of mainly the sugar unit 2-keto-3-deoxyoctulosonic acid.[42,44] The outer core consists of different hexoses like D-glucose, D-galactose, D-glucosamine, N-acetylglucosamine or N-acetylgalactosamine.[42] The O-specific chain, also called the O-antigen, is the largest section of LPS. It is hydrophilic and contains monosaccharide units that are highly species and strain specific.[44] It consists of up to 50 repeating oligosaccharide units formed of 2-8 monosaccharide subunits.[42]

There are countless species of Gram-negative bacteria all made up of differing proteins, phospholipids, and LPS molecules. Depending on the species or strain of bacteria, the actual structure of an LPS molecule can vary considerably. The exact structure of commercially available LPS samples is difficult to know, as preparations are heterogeneous. LPS also forms micelles when dissolved in solvent, which can present further challenges. Specifically, Sigma-Aldrich LPS from *E. coli* O111:B4 always forms micelles when dissolved in solvent, preventing single LPS units from being available during analysis.[51] Micelles formed from Sigma-Aldrich *E. coli* O111:B4 LPS have a critical micelle concentration (CMC) of 1.3-1.6 μM and aggregates of 43-49 molecules per micelles are formed.[52] With each LPS unit having a mass of 10-20 kDa, the aggregate mass range of LPS micelles is 430- 980 kDa.[53] However, these LPS micelles in an aqueous solvent would form such that the O-antigen hydrophilic sugars are facing outwards in the aqueous solvent and the inside hydrophobic pocket having the lipid A tails.

This is an excellent model to mimic a spherical Gram-negative bacterium in *in vivo* conditions.

The ideal situation to study the direct interaction of cationic AMPs with bacterial cell membranes would be to utilize intact live bacteria.[54] However, research is limited when working with live bacteria due to biosafety regulations. Investigating live bacterium-peptide interactions can be very time-consuming and complicated. As a result, using bacterial cell wall components and model bacterial cell membranes consisting of different lipids and other membrane constitutes is considered a viable alternative.[55] Utilizing only an individual receptor (LPS) to assess the peptides (indol/indo45) interactions can provide a simplified understanding of the whole process. Many biological features are not taken into account such as membrane potential, pH gradients, lipid heterogeneity, and membrane proteins.[55] To better understand the entire interaction mechanism, further research is required with more complicated model bacterial membranes or actual bacteria themselves.

CAPILLARY ELECTROPHORESIS

Drug discovery is a complicated, multistage process that requires techniques where large volumes of samples can be processed with a fast turnaround time.[56,57] In the past, the pharmaceutical industry has employed high performance liquid chromatography (HPLC) as the principal method due to its maturity in the industry and the lack of CE specialists.[56] CE however, is growing in popularity due to its tremendous versatility, convenient automation, and cost effectiveness with large sample sizes.[58]

CE is a powerful analytical technique used to separate and analyze molecules based on their movement within a small bore capillary. Traditional CE separation occurs within a narrow-bore capillary (10-100 μm internal diameter) filled with a background electrolyte (BGE) while under a high electric field (up to 30 kV). Two forces are responsible for CE separations, electroosmosis and electrophoresis.

Electroosmostic flow (EOF) is the bulk flow of solution, produced by the formation of a double layer on the surface of the fused silica capillary wall. Silanol groups on the interior capillary wall are deprotonated when a buffer of pH>2 is rinsed through the capillary inducing two distinct regions.[59] The negatively charged wall then immediately attracts the cations from the run buffer creating a "fixed layer". The next layer, called the "diffuse layer", is of hydrated cations, which migrate towards the negatively charged cathode during normal polarity. This migration of cations in the diffuse layer causes the bulk flow of solution in the same direction. The diffuse layer is the driving force of the EOF and contains more cations than anions. The electroosmotic mobility (μ_{eof}) is directly proportional to the dielectric constant (ε) of the BGE, the zeta potential of the capillary wall (ξ), and the electric field strength (E) as described in equation 1.1. It is also inversely proportional to the viscosity of the BGE (η).

$$\mu_{eof} = \frac{\nu_{eof}}{E} = \frac{\varepsilon\xi}{4\pi\eta} \qquad (1.1)$$

Electrophoretic migration of analytes is the movement of charged molecules due to the presence of an applied electric field. The electrophoretic mobility (μ_{ep}) of each analyte is based on its charge-to-size ratio and the viscosity of the BGE as

described in Equation 1.2. Where q is the charge of the analyte, η is the viscosity of the BGE, and r is the hydrodynamic radius. The electrophoretic velocity (υ_{ep}) of an analyte is directly related to its mobility and the applied electric field, E. Electric field strength is determined by dividing the applied voltage by the total length of the capillary, L_t. The electrophoretic velocity (υ_{ep}) can be measured experimentally with Equation 1.3. Where L_d is the capillary length from the inlet to the detection window and t_m is the analyte migration time.

$$\mu_{ep} = \frac{q}{6\pi\eta r} = \frac{\upsilon_{ep}}{E} \tag{1.2}$$

$$\upsilon_{ep} = \frac{L_d}{t_m} \tag{1.3}$$

The combination of the electroosmotic mobility (μ_{eof}) and the electrophoretic mobility (μ_{ep}) produces the analytes total apparent mobility (μ_{ap}):

$$\mu_{ap} = \mu_{eof} + \mu_{ep} \tag{1.4}$$

There are a number of different separation modes derived from CE. Some of the modes extend to capillary zone electrophoresis, micellar electrokinetic chromatography, capillary electrokinetic chromatography, capillary gel electrophoresis, capillary isoelectric focusing, microchip-based capillary electrophoresis (Microchip-based CE), and affinity capillary electrophoresis (ACE).[60]

These analytical CE methods have been used in pharmaceutical science for chiral separations, analyzing serum proteins and disease markers, DNA profiling for

criminal investigations, sequencing of nucleic acids and proteins, binding studies of analytes with ligands, and much more.[60–63] CE is also advantageous over HPLC due to its simplicity, rapid analysis, automation, ruggedness, different mechanisms for selectivity, and low cost.[60] The evolution of CE is occurring rapidly with publications in the field growing almost exponentially.[60]

Equilibrium Constants (K_b)

Determining the equilibrium constant (K_b) during drug discovery is critical to understand the interaction of non-covalent molecules. Biological systems, such as the human body, have numerous examples of non-covalent molecules continuously trying to achieve homeostasis or equilibrium. Elucidating the equilibrium constant, sometimes referred to as the binding constant, is critical when trying to understand the relationship between a receptor (R) and a ligand (L), or simply, a protein (P) and a drug (D).[64] The equilibrium equation of 1:1 binding is described below:

$$P + D \rightleftharpoons PD \tag{1.5}$$

The relationship of free protein (P) and drug (D) to complex (PD) can be expressed by the equation where $K=K_b$[65]:

$$K = \frac{[PD]}{[P][D]} \tag{1.6}$$

And the ratio (r) of complexed P to total P can be expressed as:

$$r = \frac{[PD]}{[P]+[PD]} = \frac{K[D]}{1+K[D]} \quad (1.7)$$

If multiple equilibria are considered, a more complex equation is required:[65–67]

$$\bar{r} = \sum_{i=1}^{i=m} \frac{n_i K_i (D_i)}{1+ K_i (D_i)} \quad (1.8)$$

$\bar{r}$ = The mean number of moles of *D* bound per mole of *P*
D_i = Free ligand concentration
n_i = Number of independent sites of class *i*
K_i = Association constant with *D*
m = Total number of classes

There have been a variety of techniques used to measure binding parameters for drug-protein interactions including, nuclear magnetic resonance (NMR), equilibrium dialysis, radioimmunoassay, fluorescence quenching, ultracentrifugation, and slab gel electrophoresis.[68] CE has also proved to be a versatile technique for studying equilibrium and dissociation constants in recent years.[56] There are multiple CE techniques available to elucidate equilibrium constants, which are all closely related. They should be considered complementary techniques with each method having specific advantages and disadvantages. Each technique is slightly different, however, they all provide valuable results. Different techniques include: ACE, Vacancy Affinity CE (VACE), Partial Filling Affinity CE (PFACE), Vacancy Peak (VP), Frontal Analysis CE (FACE)/Frontal Analysis Continuous CE (FACCE), and the Hummel-Dreyer method (HD).[69] ACE, VACE, and PFACE measure the change in mobility of the analytes while VP, FACE, FACCE, and HD all utilize the peak area or plateau height to determine the K_b.[69] After reviewing each of these CE

methods used for binding studies, combined with previous project results, the most suitable methods for studying the interaction between indol and its analog with LPS was ACE with a pre-incubation phase (PI-ACE) and FACE.

Pre-incubation Affinity Capillary Electrophoresis (PI-ACE)

ACE is recently the most commonly used CE method when evaluating protein-drug interactions.[70] PI-ACE simply adds a pre-incubation phase to ACE, making it suitable for slow binding kinetics such as the interaction between indol/indol45 and LPS.[45,71] The experimental design of PI-ACE when compared to ACE is almost the same, and the treatment of data are identical. Prior to analysis, P and D are pre-incubated for a set amount of time rather than one of these components being injected into the BGE where the other component is already present. Either P or D (LPS or indol/indol45, respectively) can be varied in pre-incubated samples while the other component stays constant. Close monitoring of the incubation time is critical in PI-ACE to establish repeatable results.

When assessing the results of PI-ACE studies the mobility of the injected species is the focus.[72] On the resulting electropherogram, the migration time of the analytes and complex is compared to the migration time of the neutral marker. The neutral marker (i.e., DMSO, acetonitrile, mesityl oxide), also referred to as the internal standard, designates the EOF of the solution. The electrophoretic mobility of the free and complexed drug provides all the required information to calculate the K_b. The equations as follows are for an assumed 1:1 binding of D to P.

$$\mu_i = \frac{[D_f]}{[D_f]+[DP]}\mu_f + \frac{[DP]}{[D_f]+[DP]}\mu_c \quad (1.9)$$

μ_i = Apparent electrophoretic mobility of D
μ_f = Mobility of the free drug (D)
μ_c = Mobility of the DP complex

Equation 1.9 can be rearranged as follows:

$$\frac{[DP]}{[D_f]} = K[P_f] = \left(\frac{\mu_f-\mu_i}{\mu_i-\mu_c}\right) \quad (1.10)$$

When employing Equation 1.10, μ_c must be determined experimentally but since the small molecular mass of the bound drug is not likely to significantly change the mobility of *P*, it is assumed that $\mu_c \cong \mu_p$.[62] Knowing the true mobility of the complex is almost impossible. From Equation 1.6 and 1.9, we obtain:[62,73]

$$\mu_i = \frac{\mu_f+\mu_c K[P_f]}{1+K[P_f]} \quad (1.11)$$

$$(\mu_i - \mu_f) = \frac{(\mu_c-\mu_f)K[P_f]}{1+K[P_f]} \quad (1.12)$$

Further rearrangement of Equation 1.12 results in:

$$\frac{1}{(\mu_i-\mu_f)} = \frac{1}{(\mu_c-\mu_f)K}\frac{1}{[P_f]} + \frac{1}{(\mu_c-\mu_f)} \quad (1.13)$$

$$\frac{[P_f]}{(\mu_i-\mu_f)} = \frac{1}{(\mu_c-\mu_f)}[P_f] + \frac{1}{(\mu_c-\mu_f)K} \quad (1.14)$$

$$\frac{(\mu_i - \mu_f)}{[P_f]} = -K(\mu_i - \mu_f) + K(\mu_c - \mu_f) \quad (1.15)$$

The PI-ACE experimental design requires monitoring the change of the migration time for the complexed species (t_c) compared with the marker (t_m) which indicates a change in the electrophoretic mobility (μ_i) of the complex.[69] The applied Voltage (V) used, total capillary length (L_t), and the effective length of the capillary (to the detector) (L_d) are also important parameters for the determination of μ_i as follows:

$$\mu_i = \left[\frac{L_d L_t}{V}\left(\frac{1}{t_c} - \frac{1}{t_m}\right)\right]\left(\frac{I}{I_o}\right) \quad (1.16)$$

During PI-ACE, the increasing concentration of the ligand in each sample introduces differences in the viscosity.[74] The correction (I/I_o) is included in Equation 1.16 in order to account for the viscosity effect. This is required if the neutral marker in each sample changes migration time in each run. The μ_{eff} can then be used to determine K_b based on the plotting forms shown in Table 1.1. The plotting methods described in Table 1.1 represent interactions with 1:1 binding stoichiometry. When these plots display high linearity it helps support the assumption of 1:1 binding. If multiple binding sites are present, the X-reciprocal plot will readily display nonlinearity.[62] A nonlinear regression model is then required to determine an accurate K_b. Multiple trends on the X-reciprocal plot can be a sign of more complicated stoichiometry and should be examined with other analytical methods such as NMR and/or UV spectroscopy, and mass spectrometry.[62,75,76]

Table 1.1: Regression plotting forms of binding constant (K_b)

Method	Plotting Equation (y axis vs x axis)	Determination of K_b	Equation
Nonlinear regression	$\frac{\mu_f-\mu_i}{\mu_i-\mu_c}$ vs $[P_f]$	*slope*	(1.10)
Double-reciprocal	$\frac{1}{(\mu_i-\mu_f)}$ vs $\frac{1}{[P_f]}$	$\frac{intercept}{slope}$	(1.13)
***Y*-Reciprocal**	$\frac{[P_f]}{(\mu_i-\mu_f)}$vs $[P_f]$	$\frac{slope}{intercept}$	(1.14)
***X*-Reciprocal**	$\frac{(\mu_i-\mu_f)}{[P_f]}$ vs $(\mu_i-\mu_f)$	*-slope*	(1.15)

μ_f, μ_c and μ_i are final/free drug, *DP* complex and apparent electrophoretic mobilities, respectively. $[P_f]$ is the free protein concentration. Table compiled from[62,73,77].

K_b values are typically presented in $(mol/L)^{-1}$ from the produced plots.[78,79] However, when a molecular mass of either the P or D cannot be determined, the K_b can be given in $(g/mL)^{-1}$. This is not optimal because it makes comparison of relative binding strengths difficult.[80]

Frontal Analysis Capillary Electrophoresis (FACE)

FACE is a reliable, simple, and accurate method that can be utilized to determine a K_b for drug-protein interactions.[69,81] It is sometimes favored over ACE because it does not require the assumption of 1:1 binding stoichiometry while ACE and PI-ACE does.[82,83] During FACE the capillary is filled with BGE and subsequently a large plug of sample is injected for 1-2 min. The sample plug consists of protein and drug at equilibrium, which results in large plateaus displayed rather than distinct peaks found in traditional ACE. Like all CE methods, experimental parameter optimization is required prior to analysis. In FACE, the mobility of the protein and complex is assumed to be similar while it is required that the

mobility of the drug differs sufficiently from them. This allows the free drug to leak out of the plug in a concentration equal to the free drug concentration in the injected sample. A K_b is determined by injecting pre-incubated samples of increasing concentrations of drug while keeping the concentration of protein constant. An electropherogram will then show two visible plateaus, one representing the free protein and complex, and the other representing the free drug. The height of the second aforementioned plateau represents the free drug concentration. The free drug concentration is calculated by comparing the height of the plateau to a previously made calibration curve. This calibration curve is obtained by injecting samples of increasing concentrations of only the drug. This data is used to graph the number of complexed molecules per molecule of protein as a function of the free drug concentration.[64] The result is a binding curve developed using nonlinear regression. The equations as follows are utilized to establish your binding curve.

$$\left[D_f\right] = \frac{C}{D} \times [D_{TOT}] \tag{1.17}$$

$$[D_b] = [D_{TOT}] - [D_f] \tag{1.18}$$

$$r = \frac{D_b}{[P]} \tag{1.19}$$

$[D_f]$ = Free drug concentration
C = Height of complex plateau
D = Height of plateau from drug standard curve
$[D_{TOT}]$ = Total drug concentration
$[D_b]$ = Bound drug concentration
[P] = Total protein concentration

r = Total drugs bound per protein

RESEARCH OBJECTIVES

The main objective of this thesis is to examine the binding interactions between indol/indol45 and LPS using two different CE methods to determine a K_b at physiological pH. A secondary focus is to develop a thermodynamic study using the K_b at multiple temperatures to verify the type of non-covalent interaction occurring between indol/indol45 and LPS. PI-ACE, the thermodynamic study, and FACE are presented in Chapters 2, 3 and 4, respectively. Each chapter explains the successes and failures encountered while using different CE techniques to verify the exact interaction occurring between indol/indol45 and LPS. Based on the optimized CE parameters outlined in this thesis, further studies of cationic AMPs with bacterial or mammalian cell wall components can continue to increase our understanding of this new class of potential drugs.

REFERENCES

1. World Health Organization. Global Action Plan on Antimicrobial Resistance. 2015:28.
2. Hancock REW. Peptide antibiotics. *Lancet*. 1997;349(9049):418.
3. Ventola CL. The antibiotic resistance crisis: part 1: causes and threats. *P T A peer-reviewed J Formul Manag*. 2015;40(4):277-283.
4. Hancock REW. Cationic peptides: Effectors in innate immunity and novel antimicrobials. *Lancet Infect Dis*. 2001;1(3):156-164. doi:10.1016/S1473-3099(01)00092-5.
5. Hancock REW, Diamond G. The role of cationic antimicrobial peptides in innate host defences. *Trends Microbiol*. 2000;8(9):402-410. doi:10.1016/S0966-842X(00)01823-0.
6. Selsted ME, Novotny MJ, Morris WL, Tang YQ, Smith W, Cullor JS. Indolicidin, a novel bactericidal tridecapeptide amide from neutrophils. *J Biol Chem*. 1992;267(7):4292-4295.
7. Nan YH, Park KH, Park Y, et al. Investigating the effects of positive charge and hydrophobicity on the cell selectivity, mechanism of action and anti-inflammatory activity of a Trp-rich antimicrobial peptide indolicidin. *FEMS Microbiol Lett*. 2009;292(1):134-140. doi:10.1111/j.1574-6968.2008.01484.x.
8. Rozek A, Friedrich CL, Hancock REW. Structure of the bovine antimicrobial peptide indolicidin bound to dodecylphosphocholine and sodium dodecyl sulfate micelles. *Biochemistry*. 2000;39(51):15765-15774. doi:10.1021/bi000714m.
9. Hsu CH, Chen C, Jou ML, et al. Structural and DNA-binding studies on the bovine antimicrobial peptide, indolicidin: Evidence for multiple conformations involved in binding to membranes and DNA. *Nucleic Acids Res*. 2005;33(13):4053-4064. doi:10.1093/nar/gki725.
10. Aley SB, Zimmerman M, Hetsko M, Selsted ME, Gillin FD. Killing of Giardia lamblia by cryptdins and cationic neutrophil peptides. *Infect Immun*. 1994;62(12):5397-5403.
11. Ahmad I, Perkins WR, Lupan DM, Selsted ME, Janoff AS. Liposomal entrapment of the neutrophil-derived peptide indolicidin endows it with in vivo antifungal activity. *BBA - Biomembr*. 1995;1237(2):109-114. doi:10.1016/0005-2736(95)00087-J.

12. Robinson WE, McDougall B, Tran D, Selsted ME. Anti-HIV-1 activity of indolicidin, an antimicrobial peptide from neutrophils. *J Leukoc Biol*. 1998;63(1):94-100.

13. Schluesener HJ, Radermacher S, Melms A, Jung S. Leukocytic antimicrobial peptides kill autoimmune T cells. *J Neuroimmunol*. 1993;47(2):199-202.

14. Falla TJ, Karunaratne DN, Hancock REW. Mode of Action of the Antimicrobial Peptide Indolicidin. *J Biol Chem*. 1996;271(32):19298-19303. doi:10.1074/jbc.271.32.19298.

15. Ladokhin a S, Selsted ME, White SH. Bilayer interactions of indolicidin, a small antimicrobial peptide rich in tryptophan, proline, and basic amino acids. *Biophys J*. 1997;72(2 Pt 1):794-805. doi:10.1016/S0006-3495(97)78713-7.

16. Halevy R, Rozek A, Kolusheva S, Hancock REW, Jelinek R. Membrane binding and permeation by indolicidin analogs studied by a biomimetic lipid/polydiacetylene vesicle assay. *Peptides*. 2003;24(11):1753-1761. doi:10.1016/j.peptides.2003.08.019.

17. Lee DG, Kim HK, Kim SA, et al. Fungicidal effect of indolicidin and its interaction with phospholipid membranes. *Biochem Biophys Res Commun*. 2003;305(2):305-310. doi:10.1016/S0006-291X(03)00755-1.

18. Shaw JE, Alattia JR, Verity JE, Privé GG, Yip CM. Mechanisms of antimicrobial peptide action: Studies of indolicidin assembly at model membrane interfaces by in situ atomic force microscopy. *J Struct Biol*. 2006;154(1):42-58. doi:10.1016/j.jsb.2005.11.016.

19. Zhao H, Mattila JP, Holopainen JM, Kinnunen PK. Comparison of the membrane association of two antimicrobial peptides, magainin 2 and indolicidin. *Biophys J*. 2001;81(5):2979-2991. doi:10.1016/S0006-3495(01)75938-3.

20. Sitaram N, Subbalakshmi C, Nagaraj R. Indolicidin, a 13-residue basic antimicrobial peptide rich in tryptophan and proline, interacts with Ca2+-calmodulin. *Biochem Biophys Res Commun*. 2003;309(4):879-884. doi:10.1016/j.bbrc.2003.08.095.

21. Subbalakshmi C, Sitaram N. Mechanism of antimicrobial action of indolicidin. *FEMS Microbiol Lett*. 1998;160(January):91-96. doi:10.1016/S0378-1097(98)00008-1.

22. Ghosh A, Kar RK umar, Jana J, et al. Indolicidin targets duplex DNA: structural and mechanistic insight through a combination of spectroscopy

and microscopy. *ChemMedChem*. 2014;9(9):2052-2058. doi:10.1002/cmdc.201402215.

23. Subbalakshmi C, Krishnakumari V, Nagaraj R, Sitaram N. Requirements for antibacterial and hemolytic activities in the bovine neutrophil derived 13-residue peptide indolicidin. *FEBS Lett*. 1996;395:48-52.

24. Tsai CW, Ruaan RC, Liu CI. Adsorption of antimicrobial indolicidin-derived peptides on hydrophobic surfaces. *Langmuir*. 2012;28(28):10446-10452. doi:10.1021/la301401v.

25. Rokitskaya TI, Kolodkin NI, Kotova EA, Antonenko YN. Indolicidin action on membrane permeability: Carrier mechanism versus pore formation. *Biochim Biophys Acta - Biomembr*. 2011;1808(1):91-97. doi:10.1016/j.bbamem.2010.09.005.

26. Nagpal S, Kaur KJ, Jain D, Salunke DM. Plasticity in structure and interactions is critical for the action of indolicidin, an antibacterial peptide of innate immune origin. *Protein Sci*. 2002;11(9):2158-2167. doi:10.1110/Ps.0211602.

27. Bowdish DME, Davidson DJ, Scott MG, Hancock REW. Immunomodulatory activities of small host defense peptides. *Antimicrob Agents Chemother*. 2005;49(5):1727-1732. doi:10.1128/AAC.49.5.1727-1732.2005.

28. Podorieszach AP, Huttunen-Hennelly HEK. The effects of tryptophan and hydrophobicity on the structure and bioactivity of novel indolicidin derivatives with promising pharmaceutical potential. *Org Biomol Chem*. 2010;8(I):1679-1687. doi:10.1039/b921248e.

29. Bhargava A, Osusky M, Hancock RE, Forward BS, Kay WW, Misra S. Antiviral indolicidin variant peptides: Evaluation for broad-spectrum disease resistance in transgenic Nicotiana tabacum. *Plant Sci*. 2007;172(3):515-523. doi:10.1016/j.plantsci.2006.10.016.

30. Sader HS, Fedler KA, Rennie RP, et al. Omiganan Pentahydrochloride (MBI 226), a Topical 12-Amino-Acid Cationic Peptide: Spectrum of Antimicrobial Activity and Measurements of Bactericidal Activity. *Antimicrob Agents Chemother*. 2004;48(8):3112-3118. doi:10.1128/AAC.48.8.3112.

31. Falla TJ, Hancock REW. Improved activity of a synthetic indolicidin analog. *Antimicrob Agents Chemother*. 1997;41(4):771-775.

32. Friedrich CL, Rozek A, Patrzykat A, Hancock REW. Structure and Mechanism of Action of an Indolicidin Peptide Derivative with Improved Activity against Gram-positive Bacteria. *J Biol Chem*. 2001;276(26):24015-24022. doi:10.1074/jbc.M009691200.

33. Subbalakshmi C, Bikshapathy E, Sitaram N, Nagaraj R. Antibacterial and Hemolytic Activities of Single Tryptophan Analogs of Indolicidin. *Biochem Biophys Res Commun*. 2000;274(3):714-716. doi:10.1006/bbrc.2000.3214.

34. Staubitz P, Peschel A, Nieuwenhuizen WF, et al. Structure-function relationships in the tryptophan-rich, antimicrobial peptide indolicidin. *J Pept Sci*. 2001;7:552-564. doi:10.1002/psc.351.

35. Yang ST, Shin SY, Hahm KS, Kim JI. Design of perfectly symmetric Trp-rich peptides with potent and broad-spectrum antimicrobial activities. *Int J Antimicrob Agents*. 2006;27(4):325-330. doi:10.1016/j.ijantimicag.2005.11.014.

36. Nan YH, Bang JK, Shin SY. Design of novel indolicidin-derived antimicrobial peptides with enhanced cell specificity and potent anti-inflammatory activity. *Peptides*. 2009;30(5):832-838. doi:10.1016/j.peptides.2009.01.015.

37. Lepthien S, Wiltschi B, Bolic B, Budisa N. In vivo engineering of proteins with nitrogen-containing tryptophan analogs. *Appl Microbiol Biotechnol*. 2006;73(4):740-754. doi:10.1007/s00253-006-0665-2.

38. Zasloff M. Antimicrobial peptides of multicellular organisms. *Nature*. 2002;415(January):389-395.

39. Yeaman MR, Yount NY. Mechanisms of antimicrobial peptide action and resistance. *Pharmacol Rev*. 2003;55(1):27-55. doi:10.1124/pr.55.1.2.

40. Peschel A. How do bacteria resist human antimicrobial peptides? *Trends Microbiol*. 2002;10(4):179-186. doi:10.1016/S0966-842X(02)02333-8.

41. Roman J, Massimo P. Endotoxin Neutralizing Peptides. *Curr Top Med Chem*. 2004;4(11):1173-1184.

42. Alexander C, Rietschel ET. Invited review: Bacterial lipopolysaccharides and innate immunity. *J Endotoxin Res*. 2001;7(3):167-202. doi:10.1177/09680519010070030101.

43. Rosenfeld Y, Shai Y. Lipopolysaccharide (Endotoxin)-host defense antibacterial peptides interactions: Role in bacterial resistance and prevention of sepsis. *Biochim Biophys Acta - Biomembr*. 2006;1758(9):1513-1522. doi:10.1016/j.bbamem.2006.05.017.

44. Raetz CR, Whitfield C. Lipopolysaccharide endotoxins. *Annu Rev Biochem*. 2002;71:635-700. doi:10.1146/annurev.biochem.71.110601.135414.

45. Dufort-Lefrancois E. Exploring Capillary Electrophoresis Methods for the Affinity Interaction of Indolicidin and Lipopolysaccharide. 2015.

46. Cohen J. The immunopathogenesis of sepsis. *Nature*. 2002;420(6917):885-891. doi:10.1038/nature01326.

47. Horii T, Kobayashi M, Sato K, Ichiyama S, Ohta M. An in-vitro study of carbapenem-induced morphological changes and endotoxin release in clinical isolates of Gram-negative bacilli. *J Antimicrob Chemother*. 1998;41(4):435-442. doi:10.1093/jac/41.4.435.

48. Beutler B, Milsark IW, Cerami AC. Passive immunization against cachectin/tumor necrosis factor protects mice from lethal effect of endotoxin. *Science (80-)*. 2017;229(4716):869-871.

49. Lehmann V, Freudenberg MA, Galanos C. Lethal toxicity of lipopolysaccharide and tumor necrosis factor in normal and D-galactosamine-treated mice. *J Exp Med*. 1987;165(3):657-663.

50. Morrison DC, Danner RL, Dinarello CA, et al. Bacterial endotoxins and pathogenesis of Gram-negative infections: current status and future direction. *J Endotoxin Res*. 1994;1:71-83.

51. Sigma-Aldrich. Lipopolysaccharides from escherichia coli O111:B4 Product Information. http://www.sigmaaldrich.com/technical-documents/protocols/biology/lipopolysaccharides.html. Accessed May 30, 2017.

52. Yu L, Tan M, Ho B, Ding JL, Wohland T. Determination of critical micelle concentrations and aggregation numbers by fluorescence correlation spectroscopy: Aggregation of a lipopolysaccharide. *Anal Chim Acta*. 2006;556(1):216-225. doi:10.1016/j.aca.2005.09.008.

53. Sigma-Aldrich. Glycobiology Analysis Manual, 2nd Edition. http://www.sigmaaldrich.com/technical-documents/articles/biology/glycobiology/lipopolysaccharides.html. Accessed May 30, 2017.

54. Hancock REW, Rozek A. Role of membranes in the activities of antimicrobial cationic peptides. *FEMS Microbiol Lett*. 2002;206(2):143-149. doi:10.1016/S0378-1097(01)00480-3.

55. Hallock KJ, Henzler Wildman K, Lee D-K, Ramamoorthy A. An innovative

procedure using a sublimable solid to align lipid bilayers for solid-state NMR studies. *Biophys J*. 2002;82(5):2499-2503. doi:10.1016/S0006-3495(02)75592-6.

56. Espada A, Molina-Martin M. Capillary electrophoresis and small molecule drug discovery: A perfect match? *Drug Discov Today*. 2012;17(7-8):396-404. doi:10.1016/j.drudis.2012.02.008.

57. Jordan AM, Roughley SD. Drug discovery chemistry: a primer for the non-specialist. *Drug Discov Today*. 2009;14(15-16):731-744. doi:10.1016/j.drudis.2009.04.005.

58. Altria K, Chen A, Clohs L. Capillary Electrophoresis as a Routine Analytical Tool in Pharmaceutical Analysis. *LC-GC Eur*. 2001;19(9):2-7.

59. Harris DC. *Quantitative Chemical Analysis*. Eigth. New York, NY: W.H. Freeman and Co.; 2010.

60. Sekhon BS. An overview of capillary electrophoresis: pharmaceutical, biopharmaceutical and biotechnology applications. *J Pharm Educ Res*. 2011;2(2):2-36.

61. Schou C, Heegaard NHH. Recent applications of affinity interactions in capillary electrophoresis. *Electrophoresis*. 2006;27(1):44-59. doi:10.1002/elps.200500516.

62. Tanaka Y, Terabe S. Estimation of binding constants by capillary electrophoresis. *J Chromatogr B Anal Technol Biomed Life Sci*. 2002;768(1):81-92. doi:10.1016/S0378-4347(01)00488-1.

63. Vesterberg O. History of electrophoretic methods. *J Chromatogr A*. 1989;480:3-19. doi:10.1016/S0021-9673(01)84276-X.

64. Østergaard J, Heegaard NHH. Capillary electrophoresis frontal analysis: principles and applications for the study of drug-plasma protein binding. *Electrophoresis*. 2003;24(17):2903-2913. doi:10.1002/elps.200305526.

65. Jiang C, Armstrong DW. Use of CE for the determination of binding constants. *Electrophoresis*. 2010;31(1):17-27. doi:10.1002/elps.200900528.

66. Scatchard G. Equilibrium in Non-Electrolyte Mixtures. *Chem Rev*. 1949;44(1):7-35. doi:10.1021/cr60137a002.

67. Klotz IM. Spectrophotometric investigations of the interactions of proteins with organic anions. *J Am Chem Soc*. 1946;68(11):2299-2304.

68. Liu X, Dahdouh F, Salgado M, Gomez FA. Recent advances in affinity

capillary electrophoresis. *J Pharm Sci*. 2009;98(2):394-410.

69. Busch MHA, Carels LB, Boelens HFM, Kraak JC, Poppe H. Comparison of five methods for the study of drug–protein binding in affinity capillary electrophoresis. *J Chromatogr A*. 1997;777:311-328. doi:10.1016/S0021-9673(97)00369-5.

70. Dvořák M, Svobodová J, Beneš M, Gaš B. Applicability and limitations of affinity capillary electrophoresis and vacancy affinity capillary electrophoresis methods for determination of complexation constants. *Electrophoresis*. 2013;34(5):761-767. doi:10.1002/elps.201200581.

71. Østergaard J, Heegaard NHH. Bioanalytical interaction studies executed by preincubation affinity capillary eletrophoresis. *Electrophoresis*. 2006;27(13):2590-2608. doi:10.1002/elps.200600047.

72. Vuignier K, Schappler J, Veuthey J-L, Carrupt P-A, Martel S. Drug-protein binding: a critical review of analytical tools. *Anal Bioanal Chem*. 2010;398(1):53-66. doi:10.1007/s00216-010-3737-1.

73. Rundlett KL, Armstrong DW. Examination of the origin, variation, and proper use of expressions for the estimation of association constants by capillary electrophoresis. *J Chromatogr A*. 1996;721(1):173-186. doi:10.1016/0021-9673(95)00774-1.

74. Fang N, Chen DDY. Behavior of interacting species in capillary electrophoresis described by mass transfer equation. *Anal Chem*. 2006;78(6):1832-1840. %3CGo.

75. Liu J, Abid S, Hail ME, Lee MS, Hangeland J, Zein N. Use of affinity capillary electrophoresis for the study of protein and drug interactions. *Analyst*. 1998;123(July):1455-1459. doi:10.1039/a800285a.

76. Deeb S El, Wätzig H, El-Hady DA. Capillary electrophoresis to investigate biopharmaceuticals and pharmaceutically-relevant binding properties. *TrAC - Trends Anal Chem*. 2013;48:112-131. doi:10.1016/j.trac.2013.04.005.

77. El-Hady D, Kühne S, El-Maali N, Wätzig H. Precision in affinity capillary electrophoresis for drug-protein binding studies. *J Pharm Biomed Anal*. 2010;52:232-241. doi:10.1016/j.jpba.2009.12.022.

78. Li ZM, Wei CW, Zhang Y, Wang DS, Liu YN. Investigation of competitive binding of ibuprofen and salicylic acid with serum albumin by affinity capillary electrophoresis. *J Chromatogr B Anal Technol Biomed Life Sci*. 2011;879(21):1934-1938. doi:10.1016/j.jchromb.2011.05.020.

79. Li M, Wang Q, Ling X, et al. Interactions between N-terminal extracellular tail of CCR4 and natural products of licorice using capillary electrophoresis. *Chromatographia*. 2013;76(13-14):811-819. doi:10.1007/s10337-013-2474-y.

80. Fu H, Li J, Meng W, Dong R, Dai R, Deng Y. Study of binding constant of toll-like receptor 4 and lipopolysaccharide using capillary zone electrophoresis. *Electrophoresis*. 2011;32(6-7):749-751. doi:10.1002/elps.201000618.

81. Østergaard J, Hansen SH, Jensen H, Thomsen AE. Pre-equilibrium capillary zone electrophoresis or frontal analysis: Advantages of plateau peak conditions in affinity capillary electrophoresis. *Electrophoresis*. 2005;26(21):4050-4054. doi:10.1002/elps.200500287.

82. Hancock REW, Sahl H-G. Antimicrobial and host-defense peptides as new anti-infective therapeutic strategies. *Nat Biotechnol*. 2006;24(12):1551-1557. doi:10.1038/nbt1267.

83. Vuignier K, Schappler J, Veuthey JL, Carrupt PA, Martel S. Improvement of a capillary electrophoresis/frontal analysis (CE/FA) method for determining binding constants: Discussion on relevant parameters. *J Pharm Biomed Anal*. 2010;53(5):1288-1297. doi:10.1016/j.jpba.2010.07.024.

CHAPTER 2: PRE-INCUBATION AFFINITY CAPILLARY ELECTROPHORESIS

INTRODUCTION

Antimicrobial resistance (AMR) is a global crisis that poses health risks to the entirety of our society.[1] The era of antimicrobials could be facing an impending disaster due to the emergence of multi-drug resistant organisms.[2] Novel antibiotic alternatives need to be investigated to prevent a global pandemic. One class of drugs called cationic antimicrobial peptides (AMPs) show promise as robust anti-infective agents.[3] These cationic AMPs are produced by many organisms as innate non-specific defence mechanisms towards infections.[3] They have an astonishing range of antimicrobial activities, which include activity against most Gram-positive and Gram-negative bacteria, fungi, enveloped viruses, and even eukaryotic parasites.[4] The broad spectrum of activity coupled with multiple modes of antimicrobial action, cationic AMPs are less affected by antibiotic-resistance mechanisms that can limit the use of other antibiotics.[5] Indolicidin (indol) (ILPWKWPWWPWRR-NH_2) is one such AMP derived from cytoplasmic granules of bovine neutrophils.[4] Indol is a short 13-amino acid cationic AMP with a linear structure.[4] It consists of six different amino acids with 38% being tryptophan and 23% being proline. It uniquely has the highest percentage of tryptophan of any known peptide and is a potent AMP, active against a variety of microorganisms.[6]

The exact mode of antimicrobial attack indol displays is continuously debated, but multiple different mechanisms have been observed. It has displayed membrane permeabilization, self-promoted uptake, binding to Ca^{2+} calmodulin-stimulated phosphodiesterase, and binding to DNA preventing RNA and DNA

synthesis leading to cell lysis.[6–15] The downfall with indol is the cytotoxic nature it displays towards human T-lymphocytes and that it lyses erythrocytes.[16,17] The parent structure of indol, however, represents an excellent foundation for the synthesis of analogs with increased antimicrobial activity and reduced cytotoxicity. One such analog was examined, indol45 (ILPWKWPWAPARR-NH_2), which took the original structure of indol and replaced its 4th and 5th tryptophan residues with alanine.[18]

After substituting the highly toxic and hydrophobic tryptophan for alanine, indol45 displayed an increase in antimicrobial activity and a decrease in cytotoxicity.[18] Thus demonstrating potential as a possible antimicrobial drug when compared to the parent AMP indol, due to its increased therapeutic potential. For drug discovery purposes, determination of an equilibrium constant (K_b), which provides the strength of interaction between the drug and the receptor, is critical in the development of any pharmaceutical.[19] As of now, a K_b for indol45 with its projected receptor, lipopolysaccharide (LPS), has yet to be reported.[20] Also, minimal information on the K_b for indol has been reported with no study comparing the two peptides.[21] Due to the lack of efficient and accurate analytical techniques to characterize the extent of the interaction between indol/indol45 with its target molecule LPS, the development of new techniques to measure binding parameters is warranted.

Pharmaceutical development and analysis require techniques that produce large amounts of information in a short turnaround time.[22] Capillary electrophoresis (CE) is one such technique with a growing reputation of being able to analyze large sample groups with fast and simple methods.[23] CE has also proven to be a reliable technique for elucidating accurate K_b values in many different drug-

protein interactions.[22] Out of a multitude of different CE methods used for K_b analysis, affinity capillary electrophoresis (ACE) is the most commonly used in recent years.[24] ACE uses CE to dissociate between the migration times of the free ligand, the receptor, and the ligand-receptor complex.[19] In conventional ACE, increasing concentrations of the receptor is added into the background electrolyte (BGE) that has a constant amount of the ligand, thereby, causing a shift in migration time relative to the neutral marker.[19,25] Subsequent analysis of migration times via X-reciprocal, Y-reciprocal, and Double-reciprocal plots can then be used to determine a K_b.

Due to slow binding kinetics between indol and LPS, a pre-incubation phase prior to ACE analysis has been determined to provide more precise K_b data.[21,26] This method, called Pre-incubation ACE (PI-ACE), provided the best results for the interaction between indol/indol45 with LPS in a BGE with a pH of 7.2. By keeping the pH of the system at 7.2, it simulated physiological conditions. PI-ACE is very similar to ACE, with only small changes to the experimental design and an identical assessment of data. Prior to CE analysis, the ligand and target receptor are combined for a set amount of time before injection into the capillary. Our study adapted the standard PI-ACE methodology in order to minimize protein adsorption in the inner capillary wall, which is a concern when studying proteins via CE. In doing so we altered the traditional equation with LPS being held constant and indol/indol45 being added in increasing concentrations. The K_b was determined through analysis of the electrophoretic mobility of the free and bound receptor.[19] The effective electrophoretic mobility (μ_{eff}) is used in combination with the concentration of the ligand to ultimately determine K_b. The μ_{eff} was determined using a neutral marker of the electroosmotic flow (EOF) in

order to compare the change in electrophoretic mobility of the complex (μ_c) with electrophoretic mobility of the free receptor (μ_f). The following equations are used:[27,28]

$$\mu_{eff} = \mu_i - \mu_f \quad (2.1)$$

$$\mu_i = \left[\frac{L_d L_t}{V}\left(\frac{1}{t_c} - \frac{1}{t_m}\right)\right]\left(\frac{I}{I_o}\right) \quad (2.2)$$

$$\mu_f = \left[\frac{L_d L_t}{V}\left(\frac{1}{t_f} - \frac{1}{t_m}\right)\right] \quad (2.3)$$

Where:
μ_{eff} is the effective change in electrophoretic mobility
μ_i is the apparent electrophoretic mobility of the complex
μ_f is the electrophoretic mobility of the receptor (this value is constant for each data set)
L_d is the length of the capillary to the detector window (cm)
L_t is the total length of the capillary (cm)
V is the voltage (V)
t_c is the migration time of the complex (s)
t_m is the migration time of the marker (s)
t_f is the migration time of the receptor (s)
I is the measured current at zero additive concentration (A)
I_o is the measured current at given additive concentration (A)

Equation 2.1 is manipulated to generate plots which serve to determine the value of K_b. The different plotting forms are shown in Table 2.1.

Table 2.1: Linear regression plotting forms of binding constant (K_b).

Method	Plotting Equation (y-axis vs x-axis)	Determination of K_b
Double-reciprocal	$\frac{1}{\mu_{eff}}$ vs $\frac{1}{[indol]}$	$\frac{intercept}{slope}$
***Y*-Reciprocal**	$\frac{[indol]}{\mu_{eff}}$ vs $[indol]$	$\frac{slope}{intercept}$
***X*-Reciprocal**	$\frac{\mu_{eff}}{[indol]}$ vs μ_{eff}	$-slope$

μ_{eff} is the change in electrophoretic mobility of the complex, $[indol]$ is the indol concentration in μM or M. Table compiled from[27–29].

When using linear regression plotting there is one drawback with ACE, or in our case PI-ACE. A 1:1 binding stoichiometry must be assumed. Using nonlinear regression is one possible technique to overcome this problem. The literature also states that depending on the linear regression method, the data can sometimes show different stoichiometries. When two distinct trends occur in the X-reciprocal plot, it may indicate a 2:1 binding interaction.[29] Frontal analysis capillary electrophoresis (FACE) however, is one CE technique used to eliminate any assumed 1:1 binding. This will be examined in the Chapter 4 but preliminary results using PI-ACE represent a reasonable K_b for the interaction of both indol and indol45 with LPS.

EXPERIMENTAL

Chemicals and reagents

All chemicals were of analytical grade unless otherwise indicated. Indol (95.95% purity) and indol45 (94.99% purity) were obtained from GL Biochem Ltd. (Shanghai, China). LPS, isolated from *E. coli* O111:B4, and monobasic sodium

phosphate ($NaH_2PO_4 \cdot H_2O$) were obtained from Sigma-Aldrich Ltd. (Oakville, Ontario, Canada). Dibasic sodium phosphate ($Na_2HPO_4 \cdot H_2O$) was obtained from Caledon Laboratories (Georgetown, Ontario, Canada). Dimethyl sulfoxide (DMSO), used as an EOF marker was acquired from BDH Chemicals (Toronto, Ontario, Canada). Deionized water used to prepare solutions was 18 MΩ water filtered by Barnstead™ Easypure™ RoDi. Indol, indol45, and LPS solutions were filtered through 0.45 μm cellulose acetate syringe filters (Canadian Life Science, Ontario, Canada) to decrease protein loss due to adsorption in Nylon® syringe filters. All other reagents and BGEs were filtered through 0.45 μm Nylon® syringe filters (Canadian Life Science, Ontario, Canada) before being used in the CE instrument. All reagents and stock solutions of BGEs were prepared and stored at room temperature (~23 °C).

BGE and Sample preparation

A phosphate buffer was used as the BGE with a pH of 7.2 (±0.1), to most closely resemble a physiological pH. 100 mM phosphate buffer was prepared by mixing 100 mM monobasic sodium phosphate ($NaH_2PO_4 \cdot H_2O$) and 100 mM dibasic sodium phosphate ($Na_2HPO_4 \cdot H_2O$) to a pH of 7.2. The BGE pH was determined using a Mettler Toledo FE20 – FiveEasy™ pH meter (Mettler Toledo, Switzerland).

Stock solutions of 230 mg/L indol, 230 mg/L indol45, and 700 mg/L LPS were prepared using the 100 mM phosphate buffer. These solutions were all filtered using 0.45 μm cellulose acetate syringe filters. The solutions were then stored in the refrigerator (~4 °C) for a maximum of 30 days.

To investigate the interaction between indol and indol45 with LPS, respectively, different concentrations of indol and indol45 were tested to determine the formation of a complex. Indol and indol45 samples were diluted from 0 to 200 mg/L in 500 μL vials then mixed with LPS stock diluted to a concentration of 50 mg/L. DMSO, used as a neutral marker, was then added to samples at a concentration of 0.01% v/v (Table 1.1). Samples were then gently vortexed and incubated at 25 °C for 2 h each. To ensure all samples incubated for a consistent 2 h, samples were made every 15 min and analyzed after the 2 h incubation period. Subsequent samples were analyzed in 15 min intervals thereafter. The range of concentrations was previously determined to be most effective for an interaction to occur and complex formation to materialize.

Table 2.2: Preparation of PI-ACE samples showing volume (μL) of stock LPS, Indol, Buffer and DMSO, and mix time for each sample.

Indol Concentration (mg/L)	230 ppm Indol stock (μL)	LPS Concentration (mg/L)	700 ppm LPS stock (μL)	100 mM PO_4^{2-} buffer, pH 7.36 (μL)	0.1v/v DMSO (μL)	Mix time (± 00:10)
0	0	0	0	198	2.0	11:30
0	0	50	14.3	183.7	2.0	11:45
10	8.7	50	14.3	175.0	2.0	12:00
20	17.4	50	14.3	166.3	2.0	12:15
30	26.1	50	14.3	157.6	2.0	12:30
40	34.8	50	14.3	148.9	2.0	12:45
50	43.5	50	14.3	140.2	2.0	13:00
100	87.0	50	14.3	96.7	2.0	13:15
150	130.4	50	14.3	53.3	2.0	13:30
200	173.9	50	14.3	9.8	2.0	13:45

Table 2.3: Preparation of PI-ACE samples showing volume (μL) of stock LPS, Indol45, Buffer and DMSO, and mix time for each sample.

Indol45 Concentration (mg/L)	230 ppm Indol45 stock (μL)	LPS Concentration (mg/L)	700 ppm LPS stock (μL)	100 mM PO_4^{2-} buffer, pH 7.36 (μL)	0.1v/v DMSO (μL)	Mix time (± 00:10)
0	0	0	0	198	2.0	11:30
0	0	50	14.3	183.7	2.0	11:45
10	8.7	50	14.3	175.0	2.0	12:00
20	17.4	50	14.3	166.3	2.0	12:15
30	26.1	50	14.3	157.6	2.0	12:30
40	34.8	50	14.3	148.9	2.0	12:45
50	43.5	50	14.3	140.2	2.0	13:00
100	87.0	50	14.3	96.7	2.0	13:15
150	130.4	50	14.3	53.3	2.0	13:30
200	173.9	50	14.3	9.8	2.0	13:45

Apparatus

The CE instrument used in this study was a Beckman Coulter MDQ (Fullerton, CA, USA) with ultraviolet (UV) detector set to 214 nm with direct absorbance. The capillary tubing (Polymicro Technologies, Phoenix, AZ, USA) used for PI-ACE analysis was an uncoated fused silica capillary with an internal diameter of 50.3 (+/- 0.2), external diameter of 366.2 μm (+/- 0.2), 47.7 cm effective length (inlet to detector), and 58 cm total length. A circulating liquid fluorocarbon coolant provided temperature regulation, keeping the capillary cartridge at the desired temperature. Pressure injection was utilized for sample introduction with a duration of 5 s at 1.0 psi. The conditions used for ACE analysis were as follows: voltage, 20 kV; detection, 214 nm; temperature, 25.0 ± 0.1 °C. Data was collected and analyzed with Beckman System Gold software.

Procedures

Before PI-ACE analysis, new capillaries were conditioned with 1.0 M NaOH for 60 min at 20 psi then 0.1 M NaOH for 30 min at 20 psi. Prior to each incubation process, the capillary was also rinsed with H_2O, 0.1 M NaOH, H_2O, and BGE (all for 10 min at 20 psi). Finally, before each sample injection, the capillary was rinsed with 0.1 M NaOH for 4.0 min, H_2O for 2.0 min, and then BGE for 4.0 min (each at 20 psi). An extensive capillary rinse was required to ensure a reduction in protein adsorption to the uncoated capillary wall.[29] Each pre-incubated sample was then injected for 5 s at 1.0 psi. The electrophoresis was carried out using normal polarity for 15 min to complete detection of all species.

RESULTS AND DISCUSSION

This interaction study was launched to establish a precise analytical method to investigate the interaction between indol/indol45 and LPS using PI-ACE at a physiological pH. The goal was to establish an accurate K_b for indol with LPS, as well as indol45 with LPS, with further verification of the equilibrium constant via thermodynamic analysis (Chapter 3) and FACE (Chapter 4). Comparison of K_b values determined from multiple CE techniques provides method validation and confidence in the binding stoichiometry. A thermodynamic study assessing the interaction at multiple temperatures also characterizes the type of non-covalent interaction via the Van't Hoff equation and Gibbs equation, and will be discussed.

In order to accurately determine the strength of interaction and a definitive K_b between indol/indol45 and LPS, a change in migration time of the indol/indol45-LPS complex must be observed when the concentration of indol/indol45 increases. The change in electrophoretic mobility (μ_{eff}) is calculated by using the

neutral marker and complex peak migration times to assess the change in mobility of the complex as LPS binds to an increasing concentration of indol/indol45. Linear regression analysis of double reciprocal, Y-reciprocal, and X-reciprocal were developed from each peptides data set (Table 2.4 & Table 2.5).

Table 2.4: Compilation of regression and binding constant values for 2, 6 and 12 h incubation data for the interaction of constant concentration of LPS with varying concentration of indol at 25 °C.

Indol					
Incubation time (hrs ± 0.5)	**Regression Type (Reciprocal)**	**Regression Equation**	**Correlation (R^2)**	**K_b (M^{-1}) × 10^4**	**Average K_b (M^{-1}) × 10^4**
2	*Double*	y = 3113.3x + 94.667	0. 9599	3.04	2.47
	Y	y = 76.438x + 3508.7	0.9604	2.18	
	X	y = -0.0219x + 0.0003	0.8179	2.19	
6	*Double*	y = 2427.6x + 95.202	0. 9327	3.92	2.47
	Y	y = 55.148x + 3358.7	0. 9126	1.64	
	X	y = -0.0185x + 0.0003	0. 6877	1.85	
12	*Double*	y = 3153.7x + 160.93	0. 9646	5.10	4.44
	Y	y = 147.95x + 3577.6	0. 9322	4.14	
	X	y = -0.0408x + 0.0003	0. 7363	4.08	

Table 2.5: Compilation of regression and binding constant values for 2, 6 and 12 h incubation data for the interaction of constant concentration of LPS with varying concentration of indol45 at 25 °C.

Indol45					
Incubation time (hrs ± 0.5)	**Regression Type (Reciprocal)**	**Regression Equation**	**Correlation (R^2)**	**K_b (M^{-1}) × 10^4**	**Average K_b (M^{-1}) × 10^4**
2	*Double*	y = 1341.3x + 243.51	0. 91199	18.2	15.3
	Y	y = 231.11x + 1712.7	0. 98785	13.5	
	X	y = -0.1436x + 0.0006	0. 77999	14.4	
6	*Double*	y = 583.99x + 85.466	0. 94235	14.6	15.0
	Y	y = 88.087x + 490.96	0. 98612	17.9	
	X	y = -0.1255x + 0.0015	0. 82712	12.6	
12	*Double*	y = 1245.1x + 168.74	0. 95490	13.6	13.9
	Y	y = 173.22x + 1104.3	0. 99791	15.7	
	X	y = -0.1252x + 0.0008	0. 86795	12.5	

Every reciprocal plot displayed a clear trend, with double reciprocal and Y-reciprocal plots having R^2 values ≥ 0.90 and the X-reciprocal plot produced a slightly lower correlation with R^2 values ≥ 0.68 (Appendix A). Three runs were completed at equilibrium, this data set was compiled into an average K_b value (n=3) for each peptide (Table 2.6).

Table 2.6: Compilation of regression and binding constant values at equilibrium for the interaction of constant concentration of LPS with varying concentrations of indol and indol45 at 25 °C (n=3).

Peptide	Regression Type (Reciprocal)	Average K_b (M^{-1}) × 10^4	Average K_b (M^{-1}) × 10^4
Indol	*Double*	4.02 ± 1.03	3.13 ± 0.77
	Y	2.65 ± 1.31	
	X	2.71 ± 1.20	
Indol45	*Double*	15.62 ± 2.70	14.83 ± 1.67
	Y	15.95 ± 1.88	
	X	12.91 ± 0.64	

Several experimental factors were taken into consideration when developing this interaction study. A phosphate buffer (pH 7.2) was chosen for analysis due to its strong buffering capacity and how it best simulated physiological conditions. The phosphate buffer concentration was found to be most effective at 100 mM based on previous studies[21] and the production of sharp peaks with a high baseline resolution. DMSO was chosen as the neutral marker because of its difference in mobility from the analytes and of the easily recognizable peaks it displayed. A thorough rinse protocol was also required to reduce protein adsorption to the inner capillary wall.

In PI-ACE interaction studies, protein adsorption has been shown within the inner capillary wall causing low precision of binding data.[29,30] This can be avoided with appropriate rinsing procedures. Early attempts of method development resulted in large peaks occurring randomly due to possible protein

adsorption, which resulted in poor binding data (Figure 2.1). When limited rinsing was performed on the uncoated capillary, large amounts of protein were found to interact with the inner capillary wall then release in large aggregates resulting in poor peak resolution.

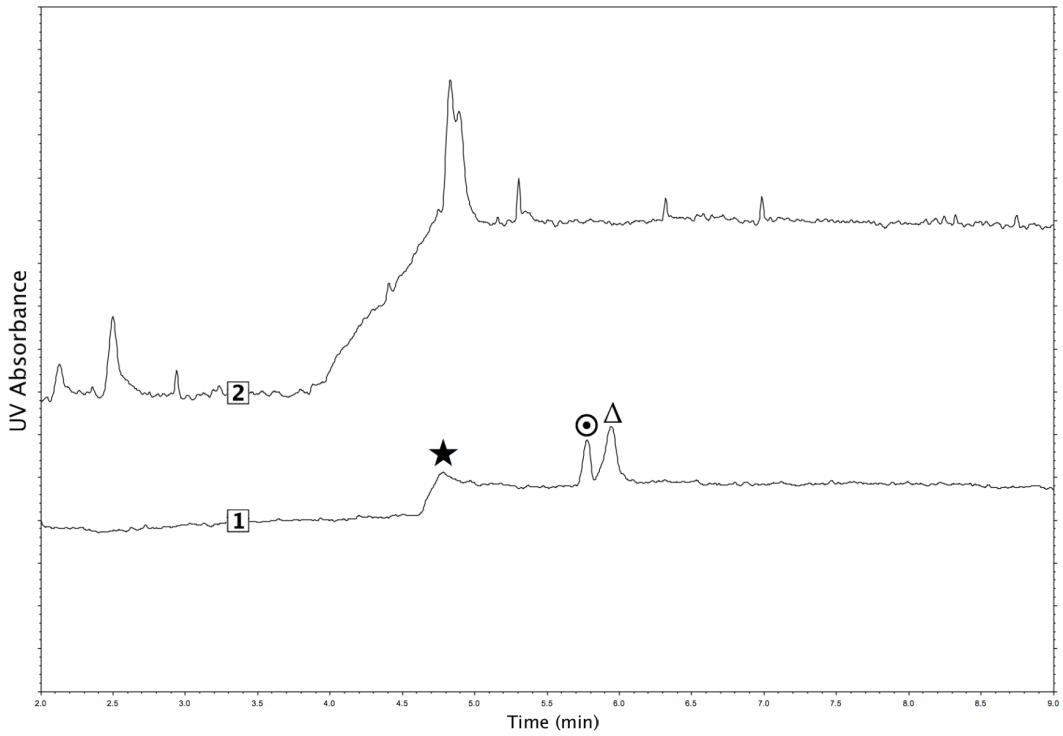

Figure 2.1: Electropherogram of two runs at 40 mg/L indol combined with 50 mg/L LPS and DMSO (0.1%v/v) incubated for 6 h. [⊙]: DMSO (neutral marker), [Δ]: LPS/LPS-indol complex, [★]: Free indol. 1) Accurate run with limited protein adsorption on the capillary wall 2) Protein adsorption on the capillary wall resulting in poor baseline resolution. With an inadequate rinse protocol protein adsorption occurred on the inner capillary wall resulting in unusable binding data. Samples were injected for 5 s duration at 1.0 psi, 20 kV separation voltage, normal polarity, UV detection at 214 nm, BGE of 100 mM PO_4^{-2} (pH 7.2).

Figure 2.2 shows an overlay of the PI-ACE electropherograms for the binding experiments between indol and LPS. A distinct indol-LPS complex forms after

the neutral marker with excess indol appearing as the concentration is increased. The excess indol peak indicates that LPS has reached saturation or equilibrium.

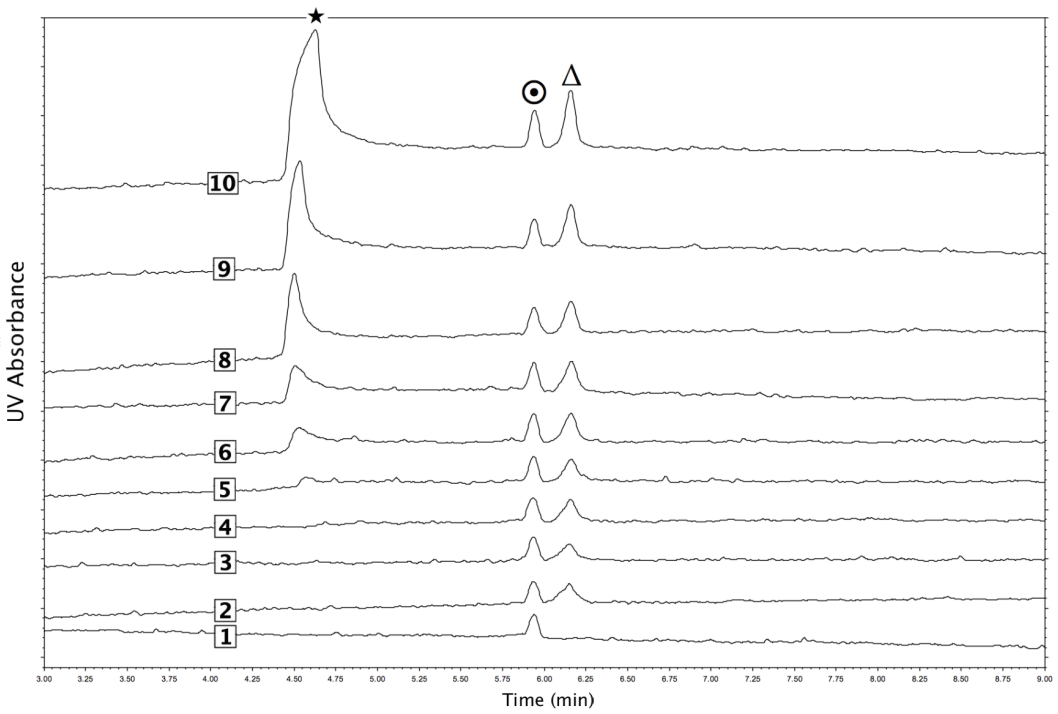

Figure 2.2: Overlay of electropherograms from samples pre-incubated for 6 h of 50 mg/L LPS combined with varying concentrations of indol and DMSO (0.1%v/v). [⊙]: DMSO (neutral marker), [Δ]: LPS/LPS-indol complex, [★]: Free indol. Indol concentrations were: 1) 0 (DMSO only), 2) 0, 3) 10, 4) 20, 5) 30, 6) 40, 7) 50, 8) 100, 9) 150, 10) 200 mg/L. Samples were injected for 5 s duration at 1.0 psi, 20 kV separation voltage, normal polarity, UV detection at 214 nm, BGE of 100 mM PO_4^{-2} (pH 7.2).

Figure 2.3 shows an overlay of the PI-ACE electropherograms for the binding experiments between indol45 and LPS. In Figure 2.3 you can observe the indol45-LPS complex drastically increase in size with little excess indol45 appearing, which could result from strong binding at equilibrium or saturation not fully being met. With close examination of the complex peak however, a small shoulder after the peak can be observed, which was hypothesized to be the

excess indol45 (Electropherograms 9 and 10 in Figure 2.3). The shoulder increases in size when concentrations of indol45 are increased, displaying possible excess indol45. This only occurs at very high concentrations of indol45 indicating a very strong interaction between indol45 and LPS.

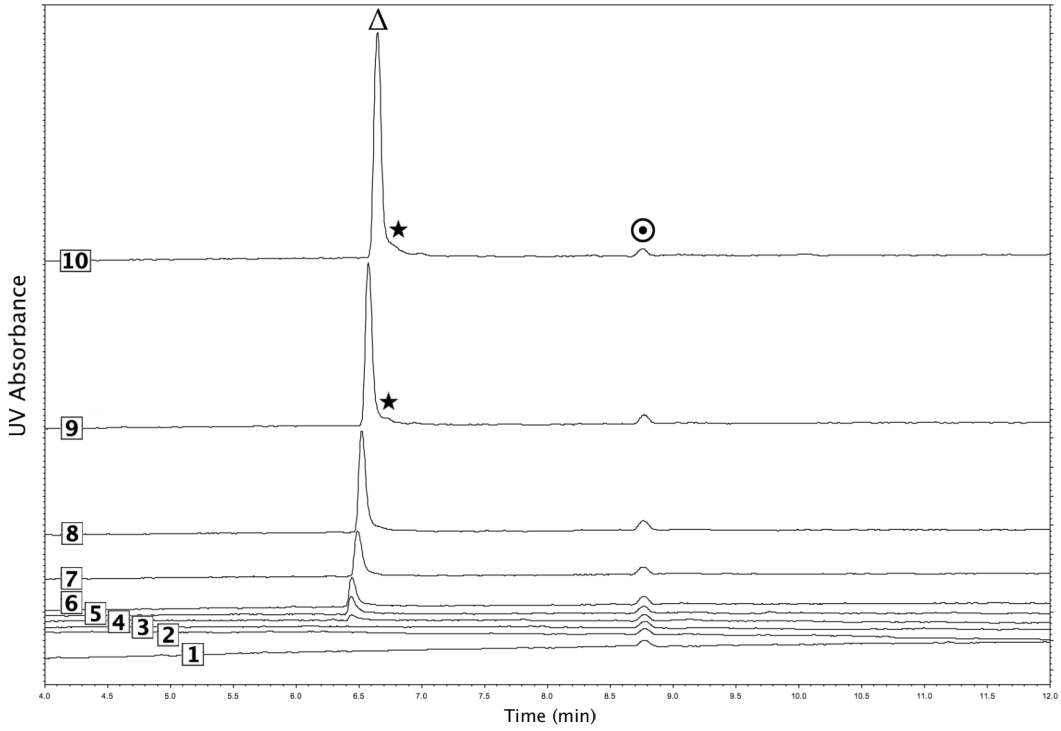

Figure 2.3: Overlay of electropherograms from samples pre-incubated for 6 h of 50 mg/L LPS combined with varying concentrations of indol45 and DMSO (0.1%v/v). [⊙]: DMSO (neutral marker), [Δ]: LPS/LPS-indol45 complex. [★]: Free indol45. Indol45 concentrations were: 1) 0 (DMSO only), 2) 0, 3) 10, 4) 20, 5) 30, 6) 40, 7) 50, 8) 100, 9) 150, 10) 200 mg/L. Samples were injected for 5 s duration at 1.0 psi, 20 kV separation voltage, normal polarity, UV detection at 214 nm, BGE of 100 mM PO_4^{-2} (pH 7.2).

When comparing the migration of the indol-LPS complex to the indol45-LPS complex in Figures 2.2 and 2.3, it can be observed that the indol45-LPS complex results in a shorter migration time. The indol-LPS complex appears after the neutral marker while the indol45-LPS complex appears before the neutral

marker. This is theorized to be due to the difference in binding strength. Indol45 has a higher K_b with LPS compared to indol, and therefore stronger binding at equilibrium, which results in a complex that has indol45 more strongly bound to LPS, than indol to LPS. With inherently anionic LPS micelles, the cationic peptides make the micelles less negative or perhaps in the case of indol45-LPS slightly positive. This reasoning is supported by the larger indol45-LPS complex peak, which also appears at a shorter migration time, coming out before the neutral marker, since the indol45-LPS complex moves more quickly toward the negatively charged cathode. Indol, on the other hand, has a lower K_b and is less strongly bound to LPS at equilibrium, resulting in a predominately more anionic complex. This is observed at the detector as a smaller complex peak with a longer migration time that appears after the neutral marker.

Incubation time for our PI-ACE study was precisely recorded due to slow binding kinetics between indol/indol45 and LPS, respectively. Previous analyses have shown that equilibrium was not reached until after 10 h[21], however the experiments appear to reach equilibrium for both indol and indol45 after 2 h. The data displayed in Table 2.6 reflects the average K_b and will be focused on henceforth. The electropherograms at each incubation time showed minimal changes in mobility of the indol-LPS and indol45-LPS complexes. Previous research also recorded minimal changes in mobility[21], which showed that small changes in migration time can have a large influence on K_b values. Although there are conflicting results regarding the amount of time required to reach equilibrium, both studies show K_b constants at a magnitude of $M^{-1} \times 10^4$ or more, displaying a strong affinity between indol/indol45 and LPS.

When comparing the binding affinity between indol and indol45 with LPS, the strength of interaction between indol45-LPS (K_b: 14.83 ± 1.67 × 10^4 M^{-1}) was determined to be stronger than indol-LPS (K_b: 3.13 ± 0.77 × 10^4 M^{-1}). This indicates indol45 is bound to LPS approximately five times more strongly at equilibrium than indol. This stronger binding by indol45 could help explain the results of prior bioactivity studies, which showed that indol45 had a much lower minimum inhibitory concentration than that of indol against select bacteria.[18] This is most likely because of the change in hydrophobicity between indol and indol45 after the change in amino acid content. Indol45 is less hydrophobic due to the substitution of the 4th and 5th tryptophan residues for alanine. Due to the known increased in antimicrobial activity of indol45 compared to indol, it can be hypothesized that indol45 binds more strongly to LPS moieties in the bacterial cell membrane. In terms of bactericidal activity, two mechanisms of action could be proposed. Either the binding of indol45 to LPS weakens the bacterial cell membrane resulting in cell lysis or indol45 crosses the bacterial envelope into the cytosol and exerts its bactericidal activity intracellularly. Indol45 should be more comfortable in the cytosol compared to indol due to its less hydrophobic nature. If indol45 does pass through the bacterial membrane into the cytosol then the antimicrobial activity could be due to DNA binding, via the one remaining WPW motif, preventing DNA and RNA replication and ultimately leading to cell death. The exact mode of action of indol and indol45 still remains unclear, although it is generally accepted that for bacteria, the bacterial membrane is the main target. However, new evidence[6,7,18], indicates intracellular targets are important in antimicrobial mechanisms.[8] Thus, the principle that these AMPs target membranes indiscriminately is flawed. Knowing that indol is more hydrophobic than indol45, begs the question as to how is indol45 binding more strongly to LPS? This will be examined in Chapter 3 through a thermodynamic

study where the nature of binding between indol/indol45 with LPS can be determined, i.e., is it hydrophobic, electrostatic, hydrogen bonding or a Van der Waals interaction.

CONCLUSION

The interaction between indol/indol45 and LPS, respectively, was determined at a physiological pH using a PI-ACE methodology. The results displayed a binding constant between indol-LPS (K_b: 3.13 ± 0.77 × 10^4 M^{-1}) and indol45-LPS (K_b: 14.83 ± 1.67 × 10^4 M^{-1}), which both indicate strong interactions. The indol-LPS K_b also compares closely to previous investigation.[21] Based on the linearity of the X-reciprocal plots, the interactions were found to have a 1:1 binding stoichiometry. Although the correlation was not as strong as the Y-reciprocal and double reciprocal plots, the X-reciprocal plot displayed one specific trend, which supports 1:1 binding (Appendix A). The best correlations were found in the Y-reciprocal and double reciprocal plots, with R^2 values of ≥ 0.90. The data also indicated that equilibrium was reached after 2 h with the K_b values minimally increasing or decreasing from 2 to 12 h. More replicates and further analyses by FACE would provide support to the PI-ACE methodology and a more reliable K_b due to FACE not being limited by a 1:1 binding stoichiometry. The FACE experiments will be discussed in Chapter 4.

These findings display the potential for indol and indol45 as possible pharmaceutical options with indol possibly being used as a parent structure to develop analogs from. Based on the increased antimicrobial activity and decreased cytotoxicity of indol45 compared to indol[18], coupled with the observed increase in binding strength to LPS, indol45 and other possible indol analogs could be a potential help towards the growing AMR epidemic.

REFERENCES

1. World Health Organization. Global Action Plan on Antimicrobial Resistance. 2015:28.
2. Hancock REW. Peptide antibiotics. *Lancet*. 1997;349(9049):418.
3. Hancock REW. Cationic peptides: Effectors in innate immunity and novel antimicrobials. *Lancet Infect Dis*. 2001;1(3):156-164. doi:10.1016/S1473-3099(01)00092-5.
4. Selsted ME, Novotny MJ, Morris WL, Tang YQ, Smith W, Cullor JS. Indolicidin, a novel bactericidal tridecapeptide amide from neutrophils. *J Biol Chem*. 1992;267(7):4292-4295.
5. Hancock REW, Sahl H-G. Antimicrobial and host-defense peptides as new anti-infective therapeutic strategies. *Nat Biotechnol*. 2006;24(12):1551-1557. doi:10.1038/nbt1267.
6. Hsu CH, Chen C, Jou ML, et al. Structural and DNA-binding studies on the bovine antimicrobial peptide, indolicidin: Evidence for multiple conformations involved in binding to membranes and DNA. *Nucleic Acids Res*. 2005;33(13):4053-4064. doi:10.1093/nar/gki725.
7. Sitaram N, Subbalakshmi C, Nagaraj R. Indolicidin, a 13-residue basic antimicrobial peptide rich in tryptophan and proline, interacts with Ca2+-calmodulin. *Biochem Biophys Res Commun*. 2003;309(4):879-884. doi:10.1016/j.bbrc.2003.08.095.
8. Subbalakshmi C, Sitaram N. Mechanism of antimicrobial action of indolicidin. *FEMS Microbiol Lett*. 1998;160(January):91-96. doi:10.1016/S0378-1097(98)00008-1.
9. Shaw JE, Alattia JR, Verity JE, Privé GG, Yip CM. Mechanisms of antimicrobial peptide action: Studies of indolicidin assembly at model membrane interfaces by in situ atomic force microscopy. *J Struct Biol*. 2006;154(1):42-58. doi:10.1016/j.jsb.2005.11.016.
10. Zhao H, Mattila JP, Holopainen JM, Kinnunen PK. Comparison of the membrane association of two antimicrobial peptides, magainin 2 and indolicidin. *Biophys J*. 2001;81(5):2979-2991. doi:10.1016/S0006-3495(01)75938-3.
11. Falla TJ, Karunaratne DN, Hancock REW. Mode of Action of the Antimicrobial Peptide Indolicidin. *J Biol Chem*. 1996;271(32):19298-19303. doi:10.1074/jbc.271.32.19298.

12. Rozek A, Friedrich CL, Hancock REW. Structure of the bovine antimicrobial peptide indolicidin bound to dodecylphosphocholine and sodium dodecyl sulfate micelles. *Biochemistry*. 2000;39(51):15765-15774. doi:10.1021/bi000714m.

13. Ladokhin a S, Selsted ME, White SH. Bilayer interactions of indolicidin, a small antimicrobial peptide rich in tryptophan, proline, and basic amino acids. *Biophys J*. 1997;72(2 Pt 1):794-805. doi:10.1016/S0006-3495(97)78713-7.

14. Halevy R, Rozek A, Kolusheva S, Hancock REW, Jelinek R. Membrane binding and permeation by indolicidin analogs studied by a biomimetic lipid/polydiacetylene vesicle assay. *Peptides*. 2003;24(11):1753-1761. doi:10.1016/j.peptides.2003.08.019.

15. Lee DG, Kim HK, Kim SA, et al. Fungicidal effect of indolicidin and its interaction with phospholipid membranes. *Biochem Biophys Res Commun*. 2003;305(2):305-310. doi:10.1016/S0006-291X(03)00755-1.

16. Ahmad I, Perkins WR, Lupan DM, Selsted ME, Janoff AS. Liposomal entrapment of the neutrophil-derived peptide indolicidin endows it with in vivo antifungal activity. *BBA - Biomembr*. 1995;1237(2):109-114. doi:10.1016/0005-2736(95)00087-J.

17. Schluesener HJ, Radermacher S, Melms A, Jung S. Leukocytic antimicrobial peptides kill autoimmune T cells. *J Neuroimmunol*. 1993;47(2):199-202.

18. Podorieszach AP, Huttunen-Hennelly HEK. The effects of tryptophan and hydrophobicity on the structure and bioactivity of novel indolicidin derivatives with promising pharmaceutical potential. *Org Biomol Chem*. 2010;8(I):1679-1687. doi:10.1039/b921248e.

19. Vuignier K, Schappler J, Veuthey J-L, Carrupt P-A, Martel S. Drug-protein binding: a critical review of analytical tools. *Anal Bioanal Chem*. 2010;398(1):53-66. doi:10.1007/s00216-010-3737-1.

20. Nagpal S, Kaur KJ, Jain D, Salunke DM. Plasticity in structure and interactions is critical for the action of indolicidin, an antibacterial peptide of innate immune origin. *Protein Sci*. 2002;11(9):2158-2167. doi:10.1110/Ps.0211602.

21. Dufort-Lefrancois E. Exploring Capillary Electrophoresis Methods for the Affinity Interaction of Indolicidin and Lipopolysaccharide. 2015.

22. Espada A, Molina-Martin M. Capillary electrophoresis and small molecule drug discovery: A perfect match? *Drug Discov Today*. 2012;17(7-8):396-404.

doi:10.1016/j.drudis.2012.02.008.

23. Altria K, Chen A, Clohs L. Capillary Electrophoresis as a Routine Analytical Tool in Pharmaceutical Analysis. *LC-GC Eur*. 2001;19(9):2-7.

24. Dvořák M, Svobodová J, Beneš M, Gaš B. Applicability and limitations of affinity capillary electrophoresis and vacancy affinity capillary electrophoresis methods for determination of complexation constants. *Electrophoresis*. 2013;34(5):761-767. doi:10.1002/elps.201200581.

25. Liu X, Dahdouh F, Salgado M, Gomez FA. Recent advances in affinity capillary electrophoresis. *J Pharm Sci*. 2009;98(2):394-410.

26. Østergaard J, Heegaard NHH. Bioanalytical interaction studies executed by preincubation affinity capillary eletrophoresis. *Electrophoresis*. 2006;27(13):2590-2608. doi:10.1002/elps.200600047.

27. Rundlett KL, Armstrong DW. Examination of the origin, variation, and proper use of expressions for the estimation of association constants by capillary electrophoresis. *J Chromatogr A*. 1996;721(1):173-186. doi:10.1016/0021-9673(95)00774-1.

28. Tanaka Y, Terabe S. Estimation of binding constants by capillary electrophoresis. *J Chromatogr B Anal Technol Biomed Life Sci*. 2002;768(1):81-92. doi:10.1016/S0378-4347(01)00488-1.

29. El-Hady D, Kühne S, El-Maali N, Wätzig H. Precision in affinity capillary electrophoresis for drug-protein binding studies. *J Pharm Biomed Anal*. 2010;52:232-241. doi:10.1016/j.jpba.2009.12.022.

30. Graf M, Galera García R, Wätzig H. Protein adsorption in fused-silica and polyacrylamide-coated capillaries. *Electrophoresis*. 2005;26(12):2409-2417. doi:10.1002/elps.200410360.

CHAPTER 3: PI-ACE THERMODYNAMIC ANALYSIS

INTRODUCTION

Antimicrobial resistance (AMR) is a continuous problem in the health care industry with the rapid development of multi-drug resistant bacteria jeopardizing our current antibiotics.[1,2] Resistance arises from changes in bacterial genes, extending from chromosomal mutations to acquisition of exogenous genetic material.[2] Every bacterium has a negatively charged membrane with hydrophilic head groups and hydrophobic cores.[3,4] Cationic antimicrobial peptides (AMPs) are produced by many organisms as non-specific defences against infections and are well suited to interact with bacterial membranes making them valuable in the fight against AMR.[3,5] Many known AMPs are positively charged and have the ability to fold into three-dimensional amphiphilic structures allowing them to interact with negatively charged membranes.[3] These AMPs have an astonishing range of antimicrobial activities, which include activity against most Gram-positive and Gram-negative bacteria, fungi, enveloped viruses, and even eukaryotic parasites.[3,6,5] The cationic AMP indolicidin (indol) (ILPWKWPWWPWRR-NH_2) is a short 13 amino acid peptide derived from the cytoplasmic granules of bovine neutrophils.[6] The downfall of indol is the cytotoxicity it displays towards human T-lymphocytes and how it lyses erythrocytes.[7,8] One indol analog was examined, indol45 (ILPWKWPWAPARR-NH_2), which took the original structure of indol and replaced its 4^{th} and 5^{th} tryptophan residues with alanine.[9] Indol45 has shown promise as a superior alternative when compared to indol with an increase in antimicrobial activity and a decrease in cytotoxicity.[9]

Non-covalent interactions between proposed drugs, such as indol and indol45, with receptors, such as lipopolysaccharide (LPS), require a detailed understanding to move forward in the drug development process.[10] The PI-ACE method described in Chapter 2 is an effective technique used to assess these interactions. Determining an equilibrium constant (K_b) is one way to better understand the interaction between proposed drugs and target receptors. The K_b of indol/indol45 and LPS was determined in Chapter 2 using PI-ACE. This established if there was an interaction between indol/indol45 and LPS, as well as the strength of the interaction. To reliably establish the type of interaction between indol/indol45 and LPS, a thermodynamic analysis must be completed. This assessment requires the PI-ACE method to be carried out at multiple different temperatures to assess the change in migration times and resulting change in K_b values. These data are then used to develop a thermodynamic model that explains entropic and enthalpic properties as well as favourable/unfavourable conditions in the indol/indol45 and LPS interaction. The thermodynamic data provides the change in enthalpy (ΔH°), the change in entropy (ΔS°), and the change in Gibbs Free Energy (ΔG°). Using the calculated ΔH° and ΔS° values, the type of interaction can be predicted i.e., hydrophobic, electrostatic, hydrogen bonding, or Van der Waals.[11] The value of ΔG° is then established to determine the spontaneity of the interaction.[11]

The K_b value of an interaction is closely related to the temperature, ΔH°, ΔS°, and ΔG° values.[11] A Van't Hoff plot is used to assess the K_b value of an interaction at different temperatures and establishes the ΔH° and ΔS° coefficients (Table 3.1). The Gibbs Free Energy equation is then used to determine a ΔG° value. With the following equations you can calculate each desired constant:[11]

$$ln\,K_b = -\frac{\Delta H^\circ}{RT} + \frac{\Delta S^\circ}{R} \quad (3.1)$$

$$\Delta G^\circ = -RT\ln K_b \quad (3.2)$$

$$\Delta G^\circ = \Delta H^\circ - T\Delta S^\circ \quad (3.3)$$

Where:
R is the universal gas constant
T is the temperature (K)
ΔH° is enthalpy change
ΔS° is entropy change
ΔG° is the change in Gibbs Free Energy

The Van't Hoff plot's linear regression line provides the slope (ΔH°) and the y-intercept (ΔS°). These are then input into Equation 3.3 to yield the ΔG°.[11]

Table 3.1: Nature of interaction based on enthalpy and entropy change.

ΔH°	ΔS°	Interaction
+	+	Hydrophobic
-	+	Electrostatic
-	-	Hydrogen Bonding & Van der Waals

ΔH° and ΔS° are calculated from the Van't Hoff plot. After placed into the above equations and solved for, they provide the type of interaction based on their sign.[11]

A negative ΔG° indicates a spontaneous interaction while a positive ΔG° describes a non-spontaneous interaction.[11]

EXPERIMENTAL

Chemicals and reagents

All chemicals were of analytical grade unless otherwise indicated. Indol (95.95% purity) and Indol45 (94.99% purity) were obtained from GL Biochem Ltd. (Shanghai, China). LPS, isolated from *E. coli* O111:B4, and monobasic sodium phosphate ($NaH_2PO_4 \cdot H_2O$) were obtained from Sigma-Aldrich Ltd. (Oakville, Ontario, Canada). Dibasic sodium phosphate ($Na_2HPO_4 \cdot H_2O$) was obtained from Caledon Laboratories (Georgetown, Ontario, Canada). Dimethyl sulfoxide (DMSO), used as an EOF marker was acquired from BDH Chemicals (Toronto, Ontario, Canada). Deionized water used to prepare solutions was 18 MΩ water filtered by Barnstead™ Easypure™ RoDi. Indol, indol45, and LPS solutions were filtered through 0.45 μm cellulose acetate syringe filters (Canadian Life Science, Ontario, Canada) to decrease protein loss due to adsorption in Nylon® syringe filters. All other reagents and BGEs were filtered through 0.45 μm Nylon® syringe filters (Canadian Life Science, Ontario, Canada) before being used in the CE instrument. All reagents and stock solutions of BGEs were prepared and stored at room temperature (~23 °C).

BGE and Sample preparation

A phosphate buffer was used as the BGE with a pH of 7.2 (±0.1), to most closely resemble a physiological pH. 100 mM phosphate buffer was prepared by mixing 100 mM monobasic sodium phosphate ($NaH_2PO_4 \cdot H_2O$) and 100 mM dibasic sodium phosphate ($Na_2HPO_4 \cdot H_2O$) to a pH of 7.2. The BGE pH was determined using a Mettler Toledo FE20 – FiveEasy™ pH meter (Mettler Toledo, Switzerland).

Stock solutions of 230 mg/L indol, 230 mg/L indol45, and 700 mg/L LPS were prepared using the 100 mM phosphate buffer. These solutions were all filtered using 0.45 μm cellulose acetate syringe filters. The solutions were then stored in the refrigerator (~4 °C) for a maximum of 30 days.

To investigate the interaction between indol and indol45 with LPS, different concentrations of indol and indol45 were tested to determine the formation of a complex. Indol and indol45 samples were diluted from 0 to 200 mg/L in 500 μL vials then mixed with LPS stock diluted to a concentration of 50 mg/L. DMSO, used as a neutral marker, was then added to samples at a concentration of 0.01% v/v (Table 1.1). Samples were then gently vortexed and incubated at 25 °C for 2 h each. To ensure all samples incubated for a consistent 2 h, samples were made every 15 min and analyzed after the 2 h incubation period. Subsequent samples were analyzed in 15 min intervals thereafter. The range of concentrations was previously determined to be most effective for an interaction to occur and complex formation to materialize.

Table 3.2: Preparation of PI-ACE samples showing volume (µL) of stock LPS, Indol, Buffer and DMSO, and mix time for each sample.

Indol Concentration (mg/L)	230 ppm Indol stock (µL)	LPS Concentration (mg/L)	700 ppm LPS stock (µL)	100 mM PO_4^{2-} buffer, pH 7.36 (µL)	0.1v/v DMSO (µL)	Mix time (± 00:10)
0	0	0	0	198	2.0	11:30
0	0	50	14.3	183.7	2.0	11:45
10	8.7	50	14.3	175.0	2.0	12:00
20	17.4	50	14.3	166.3	2.0	12:15
30	26.1	50	14.3	157.6	2.0	12:30
40	34.8	50	14.3	148.9	2.0	12:45
50	43.5	50	14.3	140.2	2.0	13:00
100	87.0	50	14.3	96.7	2.0	13:15
150	130.4	50	14.3	53.3	2.0	13:30
200	173.9	50	14.3	9.8	2.0	13:45

Table 3.3: Preparation of PI-ACE samples showing volume (µL) of stock LPS, Indol45, Buffer and DMSO, and mix time for each sample.

Indol45 Concentration (mg/L)	230 ppm Indol45 stock (µL)	LPS Concentration (mg/L)	700 ppm LPS stock (µL)	100 mM PO_4^{2-} buffer, pH 7.36 (µL)	0.1v/v DMSO (µL)	Mix time (± 00:10)
0	0	0	0	198	2.0	11:30
0	0	50	14.3	183.7	2.0	11:45
10	8.7	50	14.3	175.0	2.0	12:00
20	17.4	50	14.3	166.3	2.0	12:15
30	26.1	50	14.3	157.6	2.0	12:30
40	34.8	50	14.3	148.9	2.0	12:45
50	43.5	50	14.3	140.2	2.0	13:00
100	87.0	50	14.3	96.7	2.0	13:15
150	130.4	50	14.3	53.3	2.0	13:30
200	173.9	50	14.3	9.8	2.0	13:45

Apparatus

The CE instrument used in this study was a Beckman Coulter MDQ (Fullerton, CA, USA) with ultraviolet (UV) detector set to 214 nm with direct absorbance. The capillary tubing (Polymicro Technologies, Phoenix, AZ, USA) used for PI-ACE analysis was an uncoated fused silica capillary with an internal diameter of 50.3 (+/- 0.2), external diameter of 366.2 μm (+/- 0.2), 47.7 cm effective length (inlet to detector), and 58 cm total length. A circulating liquid fluorocarbon coolant provided temperature regulation, keeping the capillary cartridge at the desired temperature. Pressure injection was utilized for sample introduction with a duration of 5 s at 1.0 psi. The conditions used for ACE analysis were as follows: voltage, 20 kV; detection, 214 nm; temperature, 20.0 – 30.0 ± 0.1 °C. Data was collected and analyzed with Beckman System Gold software.

Procedures

Before PI-ACE analyses, new capillaries were conditioned with 1.0 M NaOH for 60 min at 20 psi then 0.1 M NaOH for 30 min at 20 psi. Prior to each incubation process, the capillary was also rinsed with H_2O, 0.1 M NaOH, H_2O, and BGE (all for 10 min at 20 psi). Finally, before each sample injection, the capillary was rinsed with 0.1 M NaOH for 4.0 min, H_2O for 2.0 min, and then BGE for 4.0 min (each at 20 psi). An extensive capillary rinse was required to ensure a reduction in protein adsorption to the uncoated capillary wall[12]. Each pre-incubated sample was then injected for 5 s at 1.0 psi. The electrophoresis was carried out using normal polarity for 15 min to complete detection of all species. An analysis was completed in triplicates at three temperatures (20.0 °C, 25.0 °C, and 30.0 °C).

RESULTS AND DISCUSSION

This study was designed to confirm the type of interaction that was occurring between indol/indol45 and LPS. PI-ACE at one temperature provides a basic K_b, however, this lacks the power to establish an accurate interaction type. A thermodynamic analysis is required using the previously developed PI-ACE method at multiple temperatures to produce data, which can be utilized to determine the interaction type. An overlay of the electropherograms for indol and indol45 with LPS, assessed at three different temperatures can be found in Appendix B. Linear regression is then used to establish double reciprocal, Y-reciprocal, and X-reciprocal plots. Each regression model provides a K_b value at multiple temperatures, which can be incorporated into a Van't Hoff plot. This graph provides data that is then inserted into Equation 3.1 and 3.3 to yield ΔH°, ΔS°, and ΔG° values.

The Van't Hoff plots for indol and indol45 are shown in Figure 3.1 below and the ΔH°, ΔS°, and ΔG° values determined from the interaction between indol/indol45 and LPS, are displayed in Table 3.4.

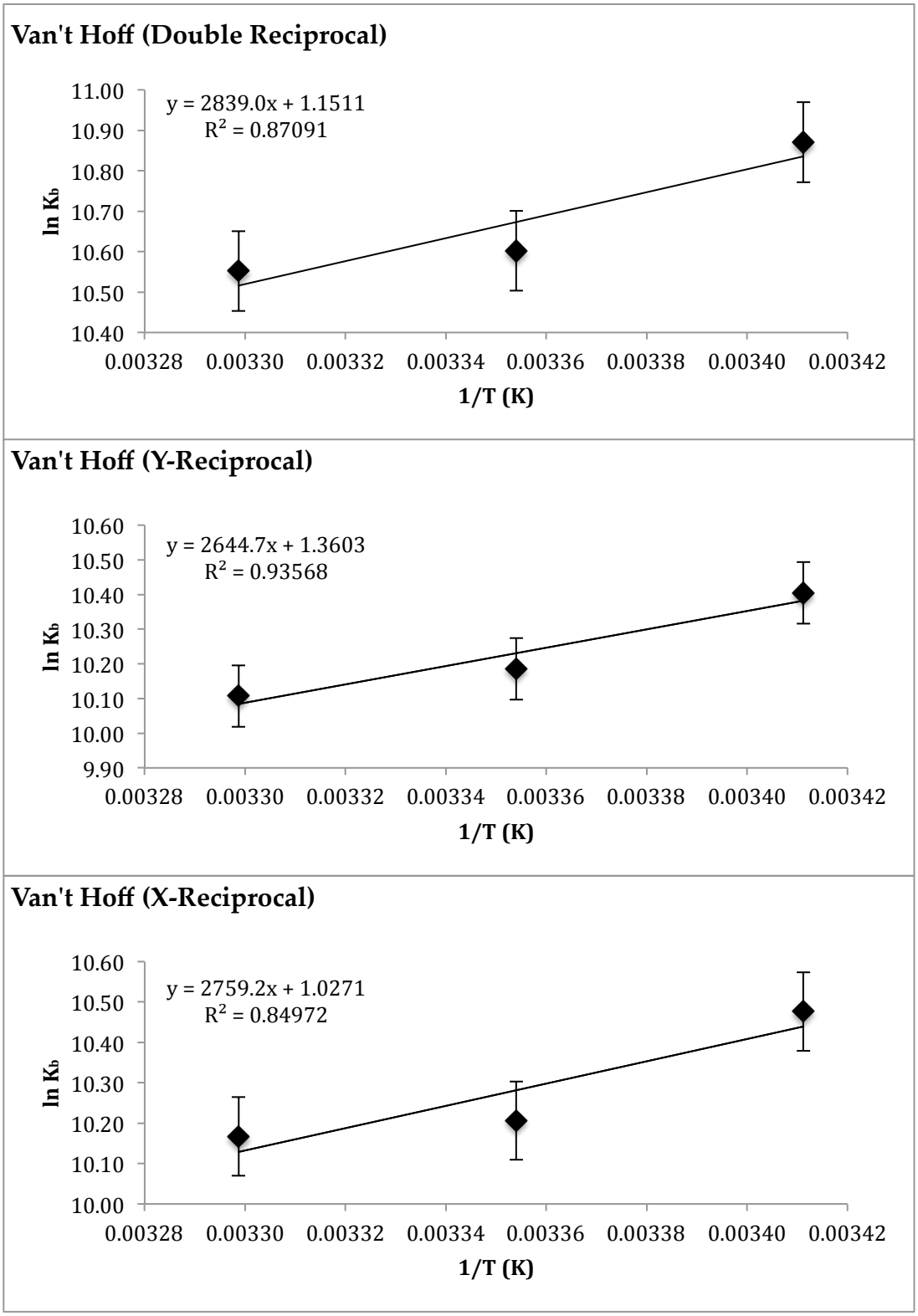

Figure 3.1: The Van't Hoff plots for the indol-LPS interaction produced using the average binding constants calculated from the double, Y-, and X-reciprocal plots at 20, 25, 30°C (n=3).

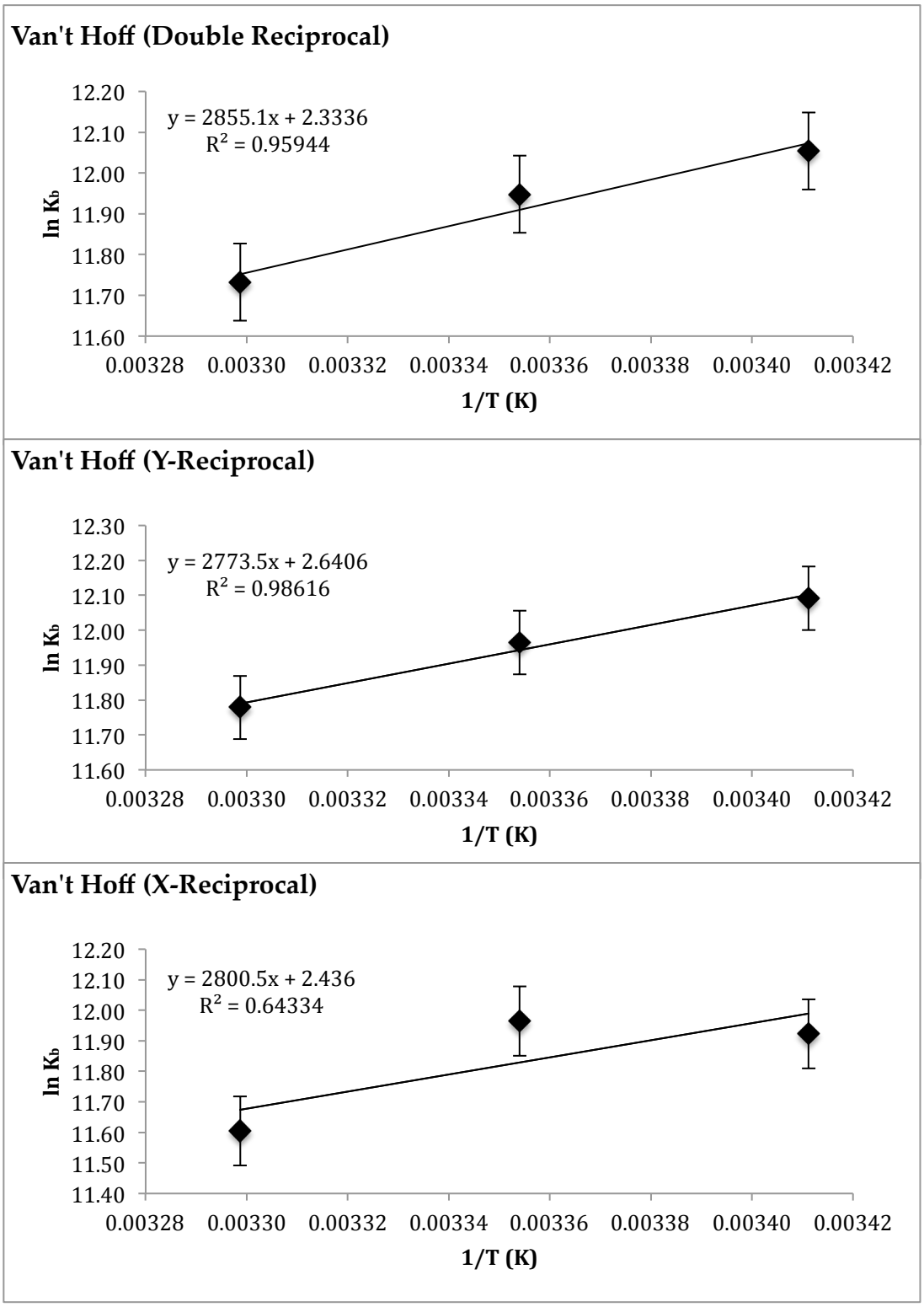

Figure 3.2: The Van't Hoff plots for the indol45-LPS interaction produced using the average binding constants calculated from the double, Y-, and X-reciprocal plots at 20, 25, 30°C (n=3).

As shown in Figure 3.1 and 3.2, the Van't Hoff relationship was also found to be linear and the ΔH° was determined from the slope while the ΔS° was ascertained from the intercept. The data are compiled in Table 3.4.

Table 3.4: Compilation of thermodynamic parameters (n=3).

Peptide	Regression Type (Reciprocal)	ΔH° (kJ×mol^{-1})	ΔS° (kJ×deg^{-1}mol^{-1})	ΔG° (kJ×mol^{-1})
Indol	*Double*	-23.60	9.57 × 10^{-3}	20°C = -26.41 25°C = -26.46 30°C = -26.51
	Y	-21.99	11.3 × 10^{-3}	20°C = -25.30 25°C = -25.36 30°C = -25.42
	X	-22.94	8.54 × 10^{-3}	20°C = -25.44 25°C = -25.49 30°C = -25.53
	Average	-22.85 ± 0.81	9.81 ± 1.40 × 10^{-3}	20°C = -25.72 ± 0.60 25°C = -25.77 ± 0.60 30°C = -25.82 ± 0.60
Indol45	*Double*	-23.74	19.4 × 10^{-3}	20°C = -29.43 25°C = -29.52 30°C = -29.62
	Y	-23.06	22.0 × 10^{-3}	20°C = -29.50 25°C = -29.61 30°C = -29.72
	X	-23.28	20.3 × 10^{-3}	20°C = -29.22 25°C = -29.32 30°C = -29.42
	Average	-23.36 ± 0.35	20.5 ± 1.30 × 10^{-3}	20°C = -29.38 ± 0.14 25°C = -29.48 ± 0.15 30°C = -29.59 ± 0.15

The enthalpy change for the interaction between indol and LPS was found to be $\Delta H^{\circ} = -22.85 \pm 0.81$ kJ×mol^{-1} and the entropy change was determined to be $\Delta S^{\circ} = 9.81 \pm 1.40 \times 10^{-3}$ kJ×deg^{-1}mol^{-1}. The Gibbs Free Energy change was calculated to be negative, indicating that the interaction was spontaneous. The enthalpy change of the interaction between indol45 and LPS was found to be $\Delta H^{\circ} = -23.36 \pm 0.35$ kJ×mol^{-1} while the entropy change was determined to be $\Delta S^{\circ} = 20.5 \pm 1.30 \times 10^{-3}$ kJ×deg^{-1}mol^{-1}. The Gibbs Free Energy change for indol45 and LPS was also negative, indicating a spontaneous interaction.

When comparing the thermodynamic parameters associated between indol and LPS as well as indol45 and LPS, a similar pattern is obvious in each interaction. Both interactions display a negative ΔH°, a negligible (minimally positive) ΔS°, and a negative ΔG° value but differ in magnitude. They both indicate a spontaneous electrostatic interaction. The nature of this electrostatic interaction could be between the positively charged arginine and lysine amino acids in indol and indol45, to the negatively charged phosphate groups on LPS. Figure 3.3 is a visual representation depicting such possible electrostatic interactions. This type of electrostatic interaction was hypothesized, and is now supported by the experimental data. Furthermore, Rozek et al. (2000) also found that indol and indol analogs bind to bacterial micelle models via electrostatic interactions using NMR studies.[13,14]

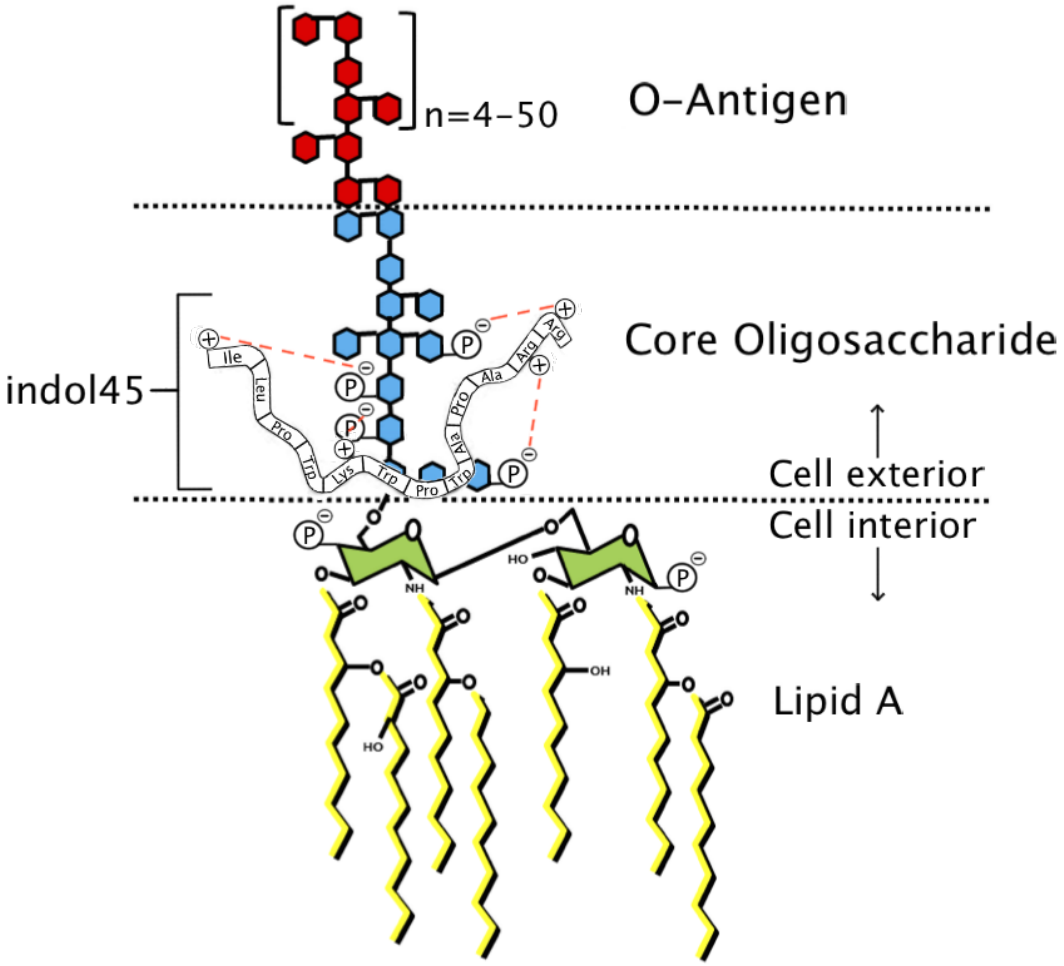

Figure 3.3: Positively charged indol45 interacting with the negatively charged phosphate groups located on the core oligosaccharide portion of LPS. The red dashed lines indicate electrostatic interactions. Adapted from Dufort-Lefrancois (2015) while using Alexander & Rietschel (2001) for guidance.[15,16]

As mentioned above, the results are in agreement with a hypothesized electrostatic interaction between indol/indol45 and LPS. This also supports that the interaction between indol/indol45 and LPS, cannot entirely be due to a hydrophobic interaction, although it does not preclude it either. When developing indol45, the substitution of the 4th and 5th tryptophan residues for alanine made it less hydrophobic, but maintained the cationic charge of +4, which would again support that both indol and indol45 could bind to LPS via a

similar electrostatic interaction.[14,17] Since indol45 has a lower hydrophobicity, a possible explanation for its stronger interaction to LPS could be due to an apparent increase in hydrophilic interactions, such as dipole-dipole or hydrogen bonding. Furthermore, the five bulky hydrophobic tryptophan rings in indol may actually interfere with the peptides' ability to physically create these critical hydrophilic electrostatic interactions.

As the temperature increased, the K_b went slightly down in both interactions between indol/indol45 and LPS, respectively. This is also not entirely surprising since higher temperatures can result in more motion or conformational flexibility of the peptides, and hence result in an equilibrium that would slightly favour the unbound species. Indol45 displayed a more negative ΔH° and ΔG°, and negligible ΔS°, indicating that the binding process was more favourable than that of indol.

CONCLUSION

The type of interaction between indol/indol45 and LPS was determined at a physiological pH through thermodynamic analysis using PI-ACE. The results displayed an enthalpy change of $\Delta H^\circ = -22.85 \pm 0.81$ kJ×mol^{-1}, an entropy change of $\Delta S^\circ = 9.81 \pm 1.40 \times 10^{-3}$ kJ×deg^{-1}mol^{-1}, and a negative Gibbs' Free energy change for the interaction between indol and LPS. Between indol45 and LPS there was an enthalpy change of $\Delta H^\circ = -23.36 \pm 0.35$ kJ×mol^{-1}, an entropy change of $\Delta S^\circ = 20.54 \pm 1.30 \times 10^{-3}$ kJ×deg^{-1}mol^{-1}, and a negative Gibbs' Free energy change as well. These results indicate a spontaneous electrostatic interaction between both indol and indol45 with LPS, respectively. Indol45 had a slightly more negative ΔH° and ΔG° with a larger ΔS° value, indicating a more favourable interaction. Every Van't Hoff plot displayed a clear linear trend with double reciprocal and Y-

reciprocal plots showing the highest correlation, with an $R^2 \geq 0.87$. More replicates at additional temperatures and further analysis by FACE would provide greater support to this thermodynamic analysis.

These findings provide a stronger understanding of the interaction that occurs between indol/indol45 and LPS. This data can be built upon for further improvement of indol analogs as possible antimicrobial drugs. Knowing an electrostatic interaction occurs at equilibrium is extremely valuable for comprehending how indol and indol45 attack bacteria. This can be utilized to further assess the potential of these cationic AMPs and possibly lead to drug development.

REFERENCES

1. Ventola CL. The antibiotic resistance crisis: part 1: causes and threats. *P T A peer-reviewed J Formul Manag*. 2015;40(4):277-283.
2. Waterer GW, Wunderink RG. Increasing threat of Gram-negative bacteria. *Crit Care Med*. 2001;29(4):N75-N81.
3. Hancock REW. Cationic peptides: Effectors in innate immunity and novel antimicrobials. *Lancet Infect Dis*. 2001;1(3):156-164. doi:10.1016/S1473-3099(01)00092-5.
4. Rosenfeld Y, Shai Y. Lipopolysaccharide (Endotoxin)-host defense antibacterial peptides interactions: Role in bacterial resistance and prevention of sepsis. *Biochim Biophys Acta - Biomembr*. 2006;1758(9):1513-1522. doi:10.1016/j.bbamem.2006.05.017.
5. Hancock REW. Peptide antibiotics. *Lancet*. 1997;349(9049):418.
6. Selsted ME, Novotny MJ, Morris WL, Tang YQ, Smith W, Cullor JS. Indolicidin, a novel bactericidal tridecapeptide amide from neutrophils. *J Biol Chem*. 1992;267(7):4292-4295.
7. Ahmad I, Perkins WR, Lupan DM, Selsted ME, Janoff AS. Liposomal entrapment of the neutrophil-derived peptide indolicidin endows it with in vivo antifungal activity. *BBA - Biomembr*. 1995;1237(2):109-114. doi:10.1016/0005-2736(95)00087-J.
8. Schluesener HJ, Radermacher S, Melms A, Jung S. Leukocytic antimicrobial peptides kill autoimmune T cells. *J Neuroimmunol*. 1993;47(2):199-202.
9. Podorieszach AP, Huttunen-Hennelly HEK. The effects of tryptophan and hydrophobicity on the structure and bioactivity of novel indolicidin derivatives with promising pharmaceutical potential. *Org Biomol Chem*. 2010;8(I):1679-1687. doi:10.1039/b921248e.
10. Vuignier K, Schappler J, Veuthey J-L, Carrupt P-A, Martel S. Drug-protein binding: a critical review of analytical tools. *Anal Bioanal Chem*. 2010;398(1):53-66. doi:10.1007/s00216-010-3737-1.
11. Ross PD, Subramanian S. Thermodynamics of Protein Association Reactions: Forces Contributing to Stability. *Biochemistry*. 1981;20(11):3096-3102.
12. El-Hady D, Kühne S, El-Maali N, Wätzig H. Precision in affinity capillary electrophoresis for drug-protein binding studies. *J Pharm Biomed Anal*.

2010;52:232-241. doi:10.1016/j.jpba.2009.12.022.

13. Rozek A, Friedrich CL, Hancock REW. Structure of the bovine antimicrobial peptide indolicidin bound to dodecylphosphocholine and sodium dodecyl sulfate micelles. *Biochemistry*. 2000;39(51):15765-15774. doi:10.1021/bi000714m.

14. Halevy R, Rozek A, Kolusheva S, Hancock REW, Jelinek R. Membrane binding and permeation by indolicidin analogs studied by a biomimetic lipid/polydiacetylene vesicle assay. *Peptides*. 2003;24(11):1753-1761. doi:10.1016/j.peptides.2003.08.019.

15. Dufort-Lefrancois E. Exploring Capillary Electrophoresis Methods for the Affinity Interaction of Indolicidin and Lipopolysaccharide. 2015.

16. Alexander C, Rietschel ET. Invited review: Bacterial lipopolysaccharides and innate immunity. *J Endotoxin Res*. 2001;7(3):167-202. doi:10.1177/09680519010070030101.

17. Rozek A, Powers JPS, Friedrich CL, Hancock REW. Structure-Based Design of an Indolicidin Peptide Analogue with Increased Protease Stability. *Biochemistry*. 2003;42(48):14130-14138. doi:10.1021/bi035643g.

CHAPTER 4: FRONTAL ANALYSIS CAPILLARY ELECTROPHORESIS

INTRODUCTION

The rapid emergence of antimicrobial resistance (AMR) is putting extreme pressure on the pharmaceutical industry to produce novel antibiotic replacements.[1,2] These alternative antibiotics require extensive research due to their complex nature in how they attack invading pathogens. Understanding different interactions, specifically non-covalent, between proposed drugs and proteins is critical for the early stages of drug development.[3,4] Due to strict regulatory barriers in the pharmaceutical industry, multiple methods are required to investigate and validate these interactions.[1] Elucidating an equilibrium constant (K_b) is a valuable way to understand how proposed drugs, such as indol and indol45, interact with receptors, such as lipopolysaccharide (LPS). To further validate the PI-ACE research on the K_b between indol/indol45 and LPS, respectively, multiple capillary electrophoresis (CE) techniques were used for comparison. The second technique, called frontal analysis capillary electrophoresis (FACE), has been employed previously for many different interaction studies.[3,5–8]

FACE is a simple, yet robust, method that can be utilized to determine a K_b for drug-protein interactions.[6,9] It is comparable to PI-ACE with both CE methods injecting samples into the BGE that include the ligand, receptor, and the resulting ligand-receptor complex. FACE however, is sometimes favored over PI-ACE and ACE because it can be utilized to determine the number of binding sites and clarify the assumption of a 1:1 binding stoichiometry.[7,10] Using a more complex binding model, FACE can also effectively be utilized to assess multiple

interaction types and binding sites (Equation 1.8 (Chapter 1)).[7,10] FACE uses longer injection times (1-2 min) to produce obvious plateaus because data analysis is completed through plateau height measurement. PI-ACE uses a short injection (5-10 s) to produce peaks because data analysis is accomplished through migration time assessment (Figure 4.1).

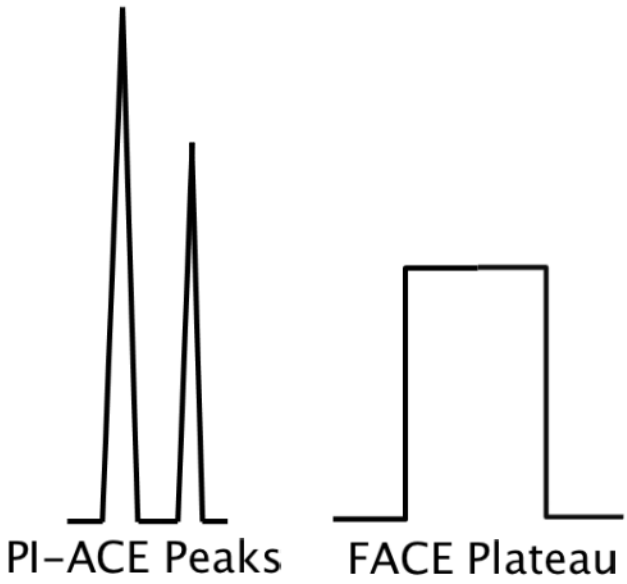

Figure 4.1: Schematic diagram of the short injection time associated with PI-ACE and the long injection time in FACE.

During FACE it is also assumed that the receptor and ligand-receptor complex have similar mobility, however, it is required that the mobility of the ligand differs sufficiently from the mobility of the complex.[6] With the difference in mobility, the free ligand leaks out of the injected plug in a concentration equal to the free ligand concentration in the injected sample (Figure 4.2).[6] This guarantees that there is an obvious difference in plateau heights to establish accurate K_b data.

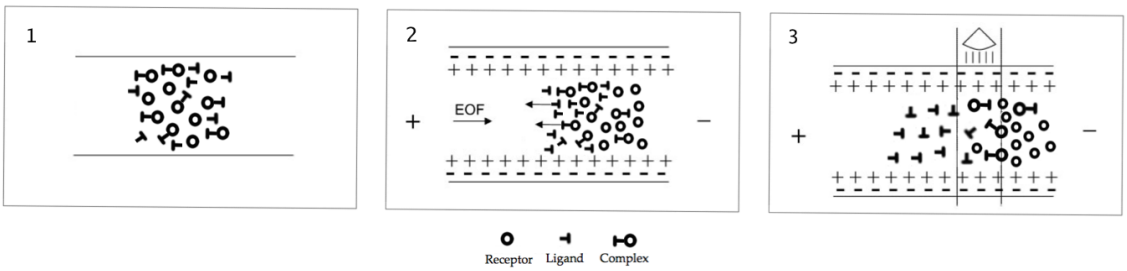

Figure 4.2: Schematic diagram of FACE separation. 1) Sample is at equilibrium immediately upon injection into the capillary. 2) Separation of ligand and receptor occurs on route to the detector. 3) At the detector the free ligand has separated from the receptor and complex. Figure adapted from Østergaard & Heegaard (2003).[5]

A K_b is determined by injecting pre-incubated samples of increasing concentrations of ligand while keeping the concentration of receptor constant. An electropherogram will then show two visible plateaus, one representing the free receptor and complex, and the other representing the free ligand (Figure 4.3). The height of the latter aforementioned plateau represents the free ligand concentration. The free ligand concentration is calculated by comparing the height of the complex plateau to a previously made calibration curve, also referred to as a standard curve. This calibration curve is obtained by injecting samples of increasing concentrations of only ligand. This data can then be used to graph the number of complexed molecules per molecule of receptor as a function of the free ligand concentration.[5] The result is a binding isotherm developed using nonlinear regression. The following equations are used:[6]

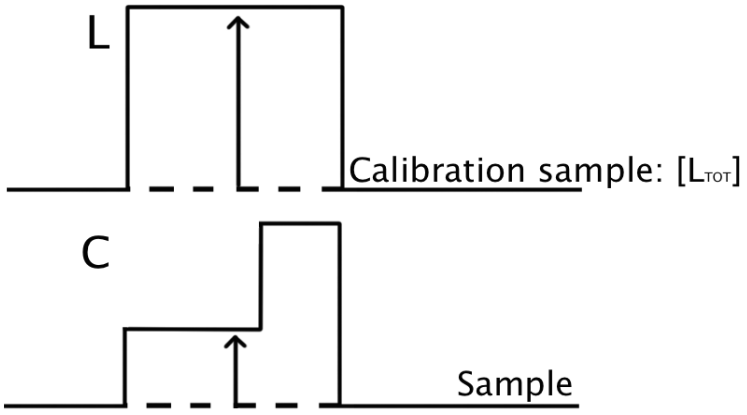

Figure 4.3: Illustration of the measurement and calibration procedure for FACE. Figure adapted from Busch et al. (1997).[6]

$$[L_f] = \frac{C}{L} \times [L_{TOT}] \quad (4.1)$$

$$[L_b] = [L_{TOT}] - [L_f] \quad (4.2)$$

$$r = \frac{L_b}{[\mathrm{Rt}]} \quad (4.3)$$

Where:
$[L_f]$ is free ligand concentration
C is height of complex plateau
L is height of plateau from ligand standard curve
$[L_{TOT}]$ is total ligand concentration
$[L_b]$ is bound ligand concentration
$[R_t]$ is total receptor concentration (LPS)
r is total ligands bound per receptor

EXPERIMENTAL

Chemicals and reagents

All chemicals were of analytical grade unless otherwise indicated. Indol (95.95% purity) and Indol45 (94.99% purity) were obtained from GL Biochem Ltd. (Shanghai, China). LPS, isolated from *E. coli* O111:B4, and monobasic sodium phosphate ($NaH_2PO_4 \cdot H_2O$) were obtained from Sigma-Aldrich Ltd. (Oakville, Ontario, Canada). Dibasic sodium phosphate ($Na_2HPO_4 \cdot H_2O$) was obtained from Caledon Laboratories (Georgetown, Ontario, Canada). Deionized water used to prepare solutions was 18 MΩ water filtered by Barnstead™ Easypure™ RoDi. Indol, indol45, and LPS solutions were filtered through 0.45 μm cellulose acetate syringe filters (Canadian Life Science, Ontario, Canada) to decrease protein loss due to adsorption in Nylon® syringe filters. All other reagents and BGEs were filtered through 0.45 μm Nylon® syringe filters (Canadian Life Science, Ontario, Canada) before being used in the CE instrument. All reagents and stock solutions of BGEs were prepared and stored at room temperature (~23 °C).

BGE and Sample preparation

A phosphate buffer was used as the BGE with a pH of 7.2 (±0.1), to greatest resemble a physiological pH. The 100 mM phosphate buffer was prepared by mixing 100 mM monobasic sodium phosphate ($NaH_2PO_4 \cdot H_2O$) and 100 mM dibasic sodium phosphate ($Na_2HPO_4 \cdot H_2O$) to a pH of 7.2. This 100 mM phosphate buffer was diluted to a 10 mM phosphate buffer for analysis. The BGE pH was determined using a Mettler Toledo FE20 – FiveEasy™ pH meter (Mettler Toledo, Switzerland).

Stock solutions of 600 mg/L indol, 600 mg/L indol45, and 570 mg/L LPS were prepared by dissolving the samples directly into the 10 mM phosphate buffer.

These solutions were all filtered using 0.45 μm cellulose acetate syringe filters. The solutions were then stored in the refrigerator (~4 °C) for a maximum of 30 days. A calibration curve was required for both indol and indol45 so that the plateau height obtained during analysis could be use to determine the free indol/indol45 concentration. Indol samples were made in increasing concentrations from 100 mg/L to 600 mg/L (equivalent of 52 μM to 315 μM). Indol45 samples were also made in increasing concentrations from 100 mg/L to 600 mg/L (equivalent of 60 μM to 358 μM).

Apparatus

The CE instrument used in this study was a Beckman Coulter MDQ (Fullerton, CA, USA) with ultraviolet (UV) detector set to 214 nm with direct absorbance. The capillary tubing (Polymicro Technologies, Phoenix, AZ, USA) used for FACE analysis was an uncoated fused silica capillary with an internal diameter of 50.3 (+/- 0.2), external diameter of 366.2 μm (+/- 0.2), 47.7 cm effective length (inlet to detector), and 58 cm total length. A circulating liquid fluorocarbon coolant provided temperature regulation, keeping the capillary cartridge at the desired temperature. Pressure injection was utilized for sample introduction with a duration of 120 s at 1.0 psi. The conditions used for FACE analysis were as follows: voltage, 10 kV; detection, 214 nm; temperature, 25.0 $\pm$ 0.1 °C. Data was collected and analyzed with Beckman System Gold software.

Procedures

Before FACE analysis, new capillaries were conditioned with 1.0 M NaOH for 60 min at 20 psi then 0.1 M NaOH for 30 min at 20 psi. Prior to each incubation process, the capillary was also rinsed with of H_2O, 0.1 M NaOH, H_2O, and BGE (all for 10 min at 20 psi). Finally, before each sample injection, the capillary was

rinsed with 0.1 M NaOH for 14.0 min, H_2O for 2.0 min, and then BGE for 4.0 min (each at 20 psi). An extensive capillary rinse was required to ensure a reduction in protein adsorption to the uncoated capillary wall[11]. During FACE, a large rinsing step is necessary due to the large plug of cationic AMP being introduced into the capillary. A higher concentration of peptide compared to PI-ACE is also used, which compounds the need for a longer rinse protocol. Each sample was injected for 120 s at 1.0 psi, which was previously established as the optimized time to produce adequate plateaus for indol.[12] The electrophoresis was carried out using normal polarity for 20 min to complete detection of all species. All runs were generated as triplicates. Following completion of reasonable calibration curves for both indol and indol45, samples within a similar concentration range were analyzed through varying the indol/indol45 concentration and keeping the LPS concentration constant.

RESULSTS AND DISCUSSION

FACE was employed for this study to add validation and confidence to the K_b established through PI-ACE for indol/indol45 and LPS. The goal was to develop a FACE method to verify previous results and confirm the previously assumed 1:1 binding stoichiometry. By compiling results from the PI-ACE analysis, the thermodynamic assessment, and the FACE procedure, a strong foundation can be established of the equilibrium dynamics between indol/indol45 and LPS, respectively.

Indol45 Standard Curve

When using FACE, a standard curve is required to determine an accurate concentration of bound ligand. This allows the receptor (LPS), to be held constant

while the ligand (indol or indol45) concentration is varied to establish K_b binding data. The plateau height of the indol/indol45-LPS complex and free LPS (C) is measured and then divided by the plateau height of only indol/indol45 (L), determined from the standard curve, which is then multiplied by the total concentration of indol/indol45 (L_{TOT}) as seen in Equation 4.1. This provides the free ligand concentration (L_f), which can then be subtracted from L_{TOT} to equal the bound ligand concentration (L_b). The L_b divided by the total receptor concentration (R_t) provides the total ligands bound per receptor (r), which is evaluated against [L_f] using nonlinear regression to produce the K_b value. This binding isotherm displays the affinity between indol/indol45 and LPS, respectively.

When producing the standard curve for indol and indol45 the plateaus produced were adequate, however, indol had a less than desirable shape due to possible protein adsorption to the silanol groups on the inner capillary wall (Figure 4.4 & 4.5). The standard curve for indol is displayed in Figure 4.6 and indol45 is shown in Figure 4.7. They were completed in duplicate at a temperature of 25 °C.

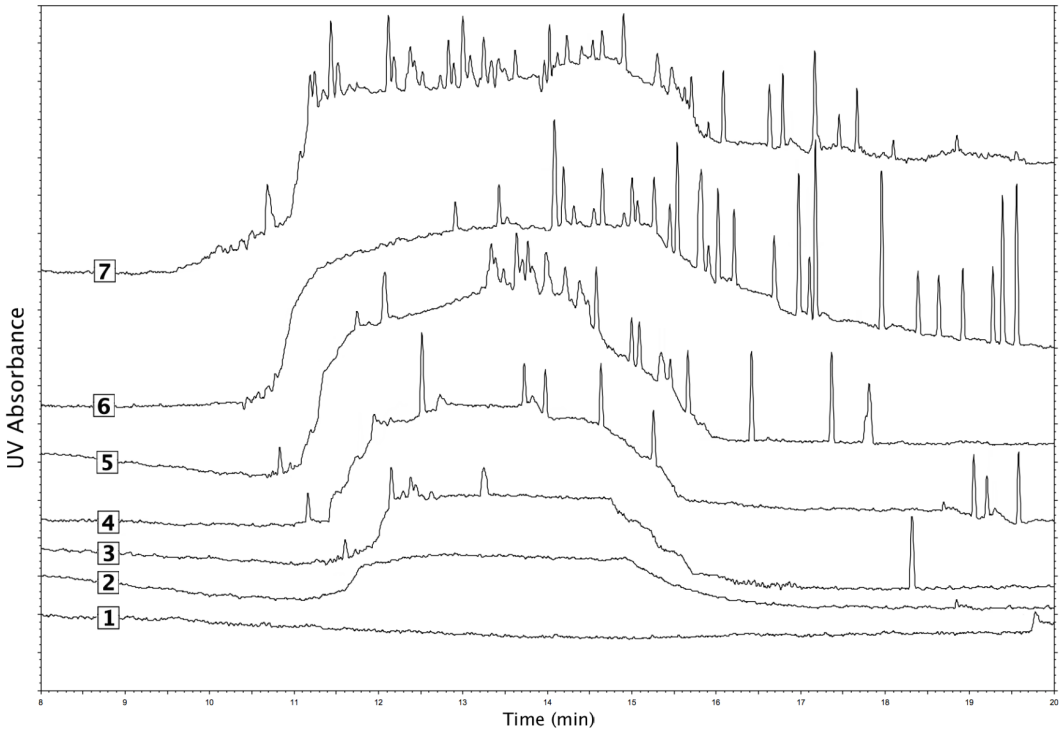

Figure 4.4: Overlay of electropherograms of varying concentrations of indol in 10 mM phosphate buffer (pH 7.2). Indol concentrations are: 1) 0, 2) 100, 3) 200, 4) 300, 5) 400, 6) 500, 7) 600 mg/L. Samples were injected for 120 s duration at 1.0 psi, 10 kV separation voltage, normal polarity, UV detection at 214 nm, BGE 10 mM PO_4^{-2} (pH 7.2).

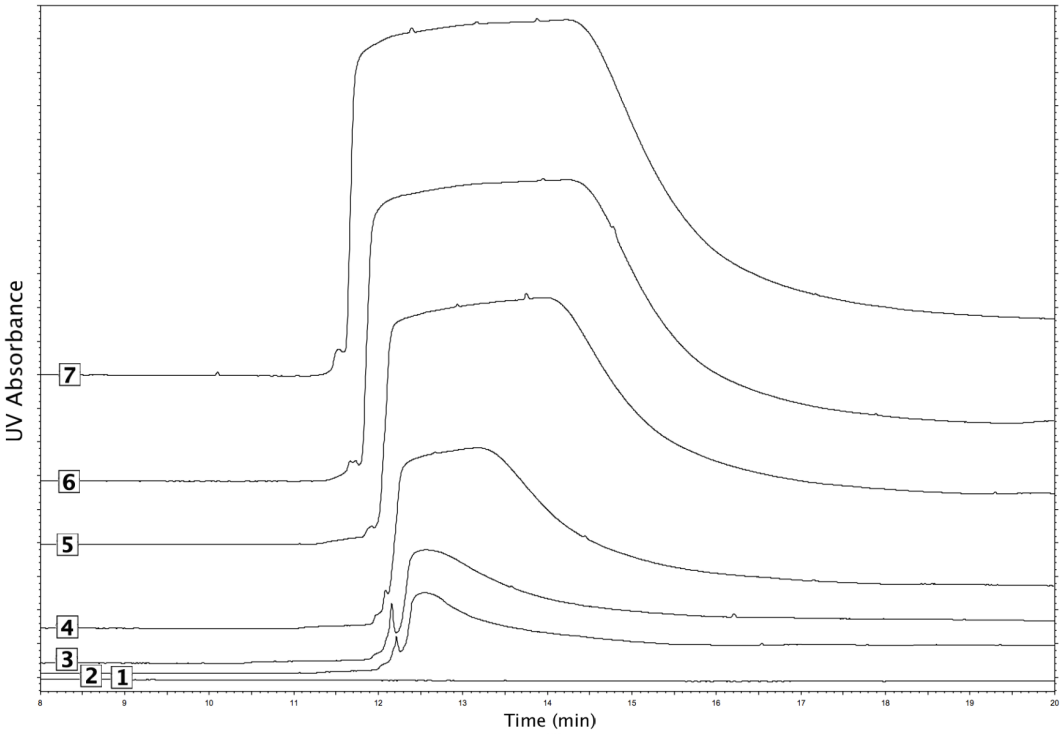

Figure 4.5: Overlay of electropherograms of varying concentrations of indol45 in 10 mM phosphate buffer (pH 7.2). Indol45 concentrations are: 1) 0, 2) 100, 3) 200, 4) 300, 5) 400, 6) 500, 7) 600 mg/L. Samples were injected for 120 s duration at 1.0 psi, 10 kV separation voltage, normal polarity, UV detection at 214 nm, BGE 10 mM PO_4^{-2} (pH 7.2).

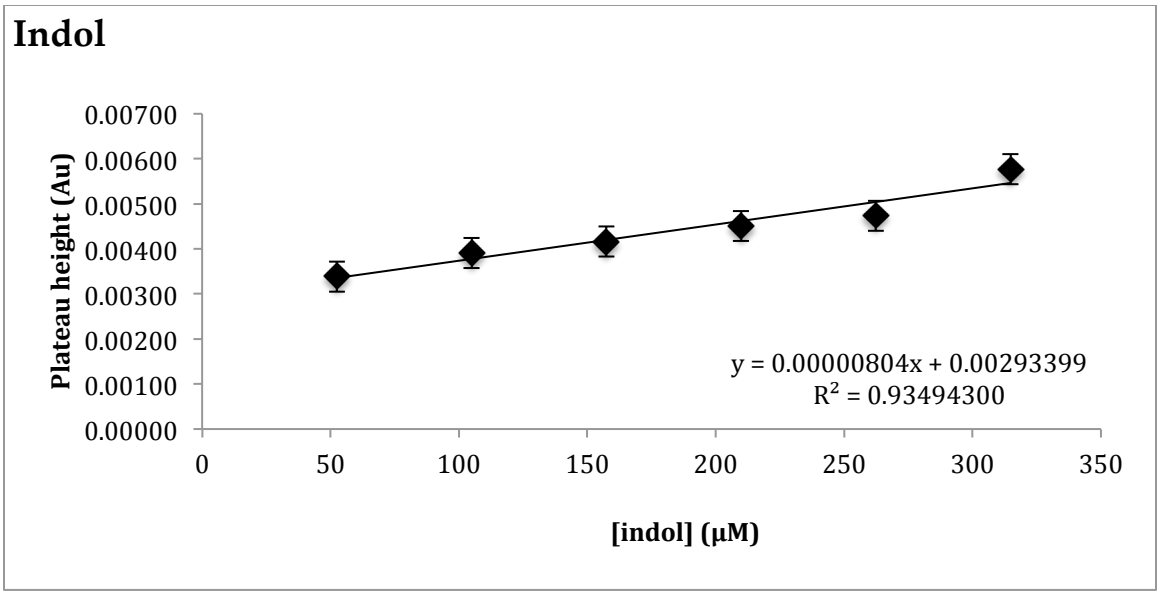

Figure 4.6: Indol standard curve.

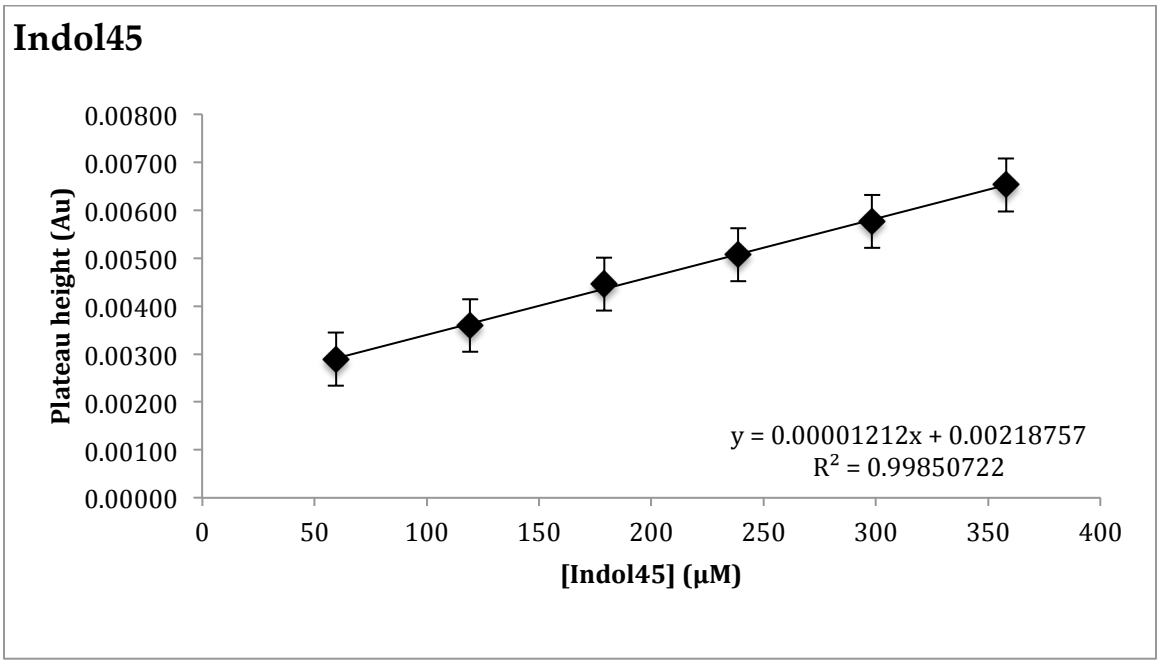

Figure 4.7: Indol45 standard curve.

FACE Analysis

After completion of the standard curve for both ligands, analyses could be completed for the interaction between indol/indol45 and LPS, respectively. In

FACE it is required that the mobility of indol/indol45 is different than that of LPS and the formed complex, which have similar mobility, to achieve an accurate K_b. This allows free indol/indol45 to leak out of the injection plug and create different height plateaus when it reaches the detector. The plateau height of the complex is used to ultimately calculate the total amount of indol or indol45 bound per LPS unit. Our analyses used a constant amount of LPS while the concentration of indol/indol45 was increased. Based on previous PI-ACE results it was also determined equilibrium was reached after 2 h. Thus, samples were incubated for 2 h at 25 °C then pressure assisted injected. Two separate runs were completed at equilibrium then the results were assessed via nonlinear regression and compiled into a data set (Table 4.1).

Table 4.1: Compilation of regression equations and binding constant values for nonlinear regression plots of FACE data for the interaction of indol and indol45 with LPS (n=2).

Peptide	Regression Type	Regression Equation	Average K_b (M^{-1}) × 10^4
Indol	*Nonlinear*	$y = \frac{ax}{1+bx}$	2.30 ± 0.20
Indol45	*Nonlinear*	$y = \frac{ax}{1+bx}$	12.35 ± 0.98

Several experimental factors were taken into consideration when developing the FACE methodology. A phosphate buffer (pH 7.2) was chosen for analysis due to its strong buffering capacity and how it best simulated physiological conditions. The phosphate buffer concentration was found to be most effective at 10 mM based on previous studies.[12] A thorough rinse protocol was also required to reduce protein adsorption to the inner capillary wall. With injection times at 120

s, a large mass of peptide would be in the capillary increasing the odds of adsorption. Fortunately, the extensive rinsing mitigated the amount of protein adsorption.

Based on the FACE results, an obvious interaction between indol/indol45 and LPS can be observed visually in both Figures 4.8 and 4.9. The plateaus illustrate a strong interaction between indol/indol45 and LPS, respectively. The shoulder displayed in Figure 4.8 and 4.9 on each of plateaus 3 - 7 indicates free indol or indol45. This change in plateau height is indicative of the free ligand leaking out of the injection plug. The increasing height of the latter plateau demonstrates that this is undoubtedly the free ligand plateau. At equilibrium it is determined that a specific amount of indol/indol45 is bound to LPS, therefore, as indol/indol45 increased in concentration the excess will be displayed by a growing plateau.

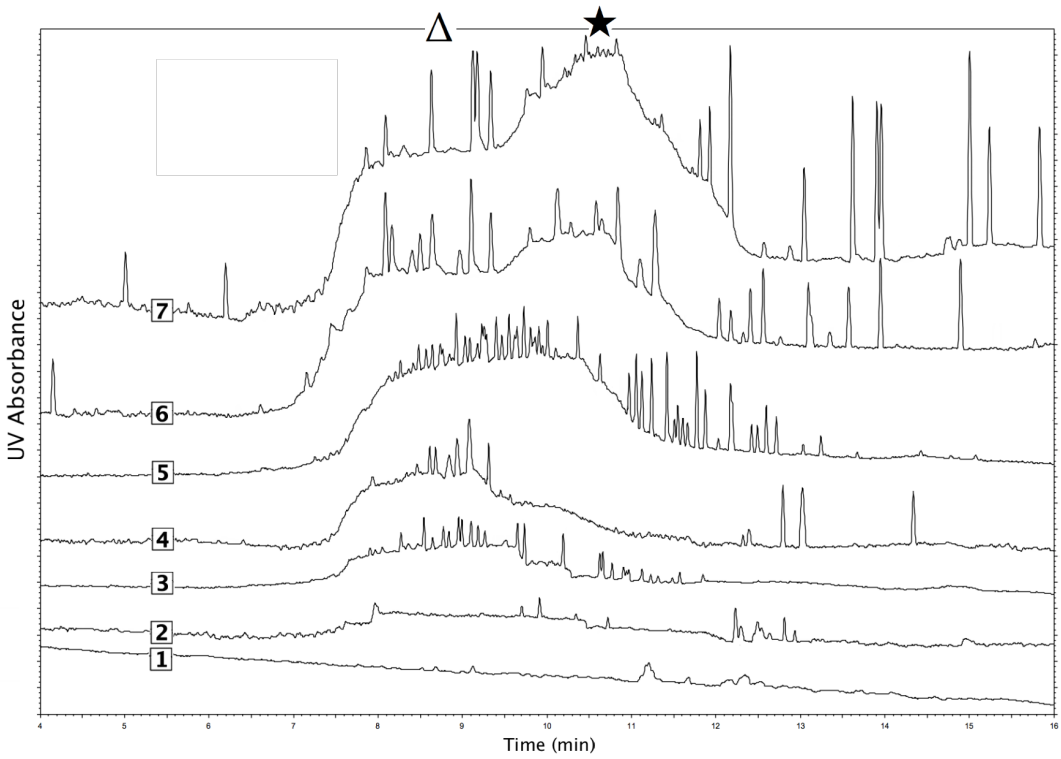

Figure 4.8: Overlay of electropherograms from samples of varying concentrations of indol with constant 285 mg/L concentration of LPS. [Δ]: LPS/LPS-indol complex, [★]: Free indol. Indol concentrations were: 1) 0, 2) 100, 3) 200, 4) 300, 5) 400, 6) 500, 7) 600 mg/L. Sample were injected for 120 s duration at 1.0 psi, 10 kV separation voltage, normal polarity, UV detection at 214 nm, BGE 10 mM PO_4^{-2} (pH 7.2).

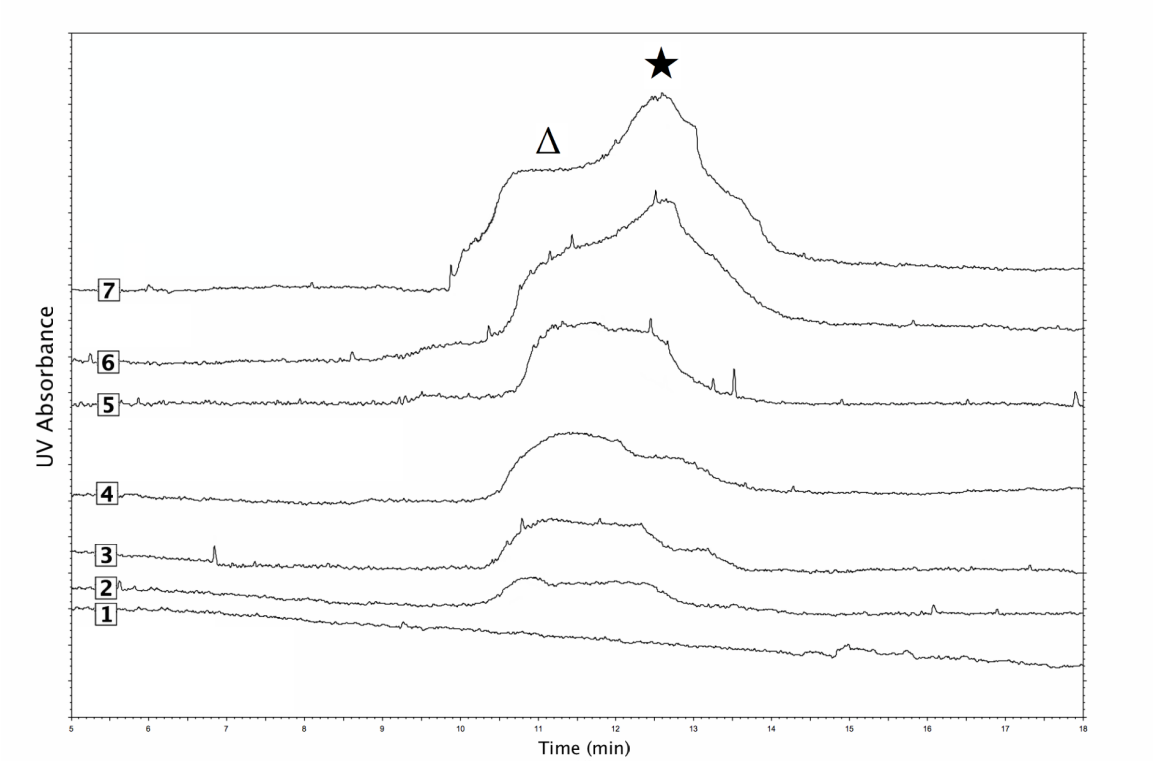

Figure 4.9: Overlay of electropherograms from samples of varying concentrations of indol45 with constant 285 mg/L concentration of LPS. [Δ]: LPS/LPS-indol45 complex, [★]: Free indol45. Indol45 concentrations were: 1) 0, 2) 100, 3) 200, 4) 300, 5) 400, 6) 500, 7) 600 mg/L. Sample were injected for 120 s duration at 1.0 psi, 10 kV separation voltage, normal polarity, UV detection at 214 nm, BGE 10 mM PO_4^{-2} (pH 7.2).

The interaction between indol-LPS (K_b: 2.30 ± 0.20 × 10^4 M^{-1}) and indol45-LPS (K_b: 12.35 ± 0.98 × 10^4 M^{-1}) determined using FACE closely compares to the previous PI-ACE results (indol-LPS K_b: 3.13 × 10^4 M^{-1} & indol45-LPS K_b: 14.83 × 10^4 M^{-1}). This provides verification of both CE methods and confidence in our K_b values. Although limited data was available for FACE analysis, both methodologies show similar results indicating an interaction was observed. To improve this interaction study, more replicates and a larger sample size would be required to lower the standard deviation of K_b values and increase confidence in the calculated equilibrium constant.

The binding isotherms for both interactions (Figure. 4.10 & 4.11) were determined using nonlinear regression. It depicts the total ligands bound per receptor vs. the free ligand concentration. A strong correlation was found with $R^2 \geq 0.90$, indicating that the assumed 1:1 stoichiometry is valid.

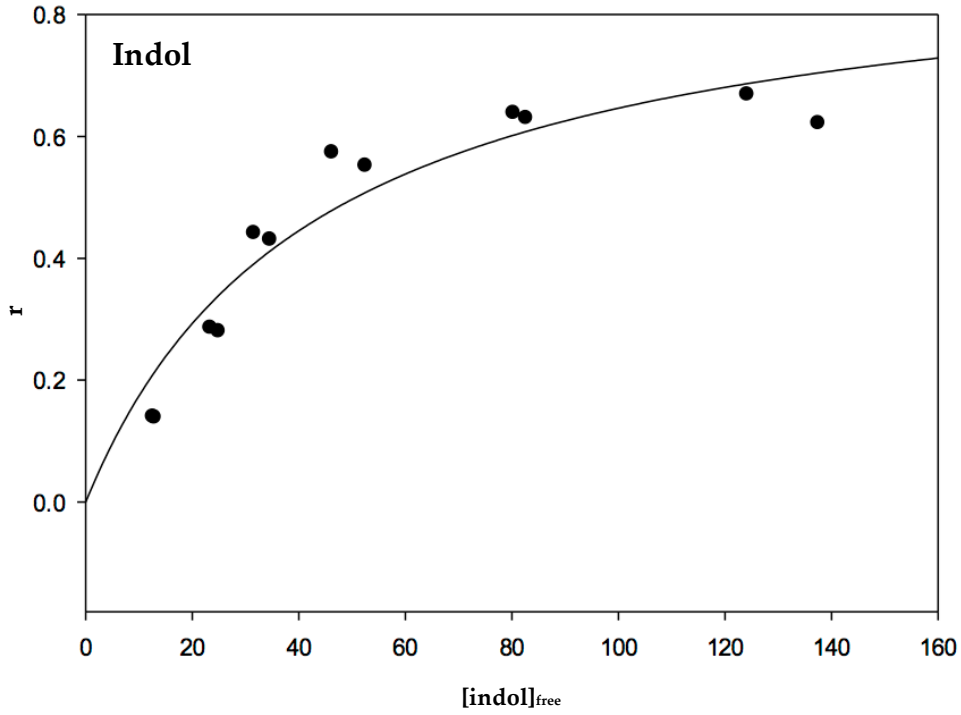

Figure 4.10: Binding isotherm for indol binding to LPS in 10 mM PO_4^{-2} buffer (pH 7.2).

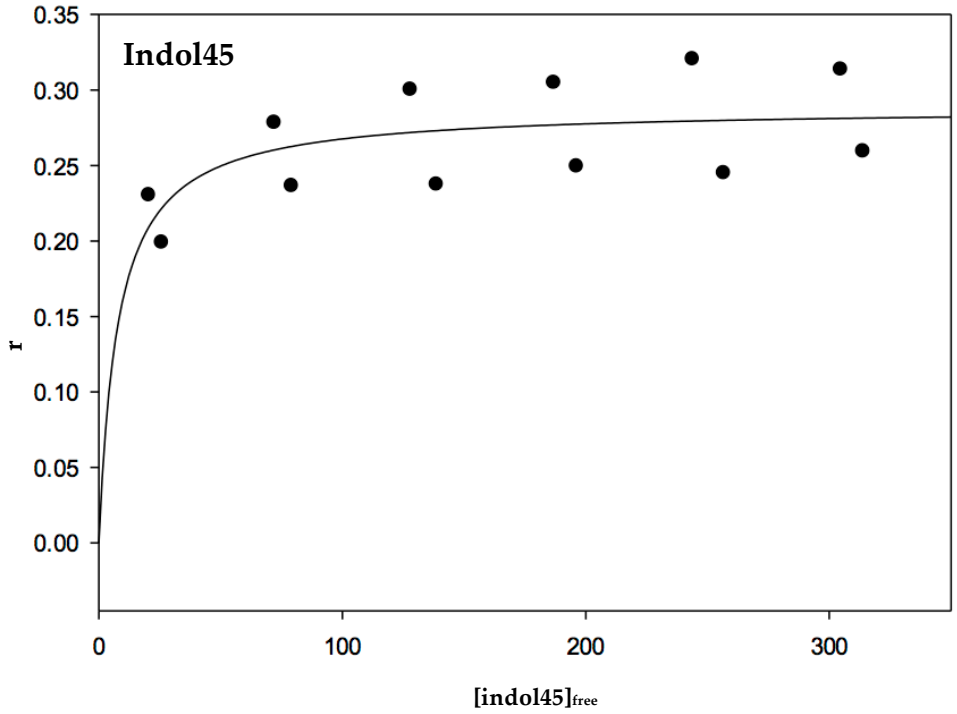

Figure 4.11: Binding isotherm for indol45 binding to LPS in 10 mM PO_4^{-2} buffer (pH 7.2).

CONCLUSION

The interaction between indol/indol45 and LPS established in Chapter 2 through PI-ACE was verified using FACE at a physiological pH. Although the FACE data is limited, a usable comparison can be made between the K_b values from both CE methods. The results from FACE displayed equilibrium constants between indol-LPS (K_b: 2.30 ± 0.20 × 10^4 M^{-1}) and indol45-LPS (K_b: 12.35 ± 0.98 × 10^4 M^{-1}), which indicate strong interactions and compare closely to the PI-ACE values of (indol-LPS K_b: 3.13 × 10^4 M^{-1} & indol45-LPS K_b: 14.83 × 10^4 M^{-1}). Based on the interactions binding isotherm, FACE displays promise as a viable technique to assess the interactions of both indol and its analogs. The plots would be more beneficial if more runs were completed with more concentrations available to analyze.

However, the FACE methodology validated the assumed 1:1 binding stoichiometry and provided confidence in the accuracy of K_b values calculated from the PI-ACE method described in Chapter 2.

FACE is a proven method to assess protein-drug interactions, however, when assessing cationic AMPs complications should be expected. Due to the high concentrations of peptide injected, coupled with long injection times, protein adsorption to the inner capillary wall occurs frequently. Many trials were deemed useless due to poor resolution of the electropherogram baseline. Prevention of adsorption occurred only when a strict rinsing protocol was in place. Another solution could be the use of capillary coatings. This was previously attempted[12], however it proved unsuccessful. Other coatings could be tested and may produce better results. If this complication can be overcome, FACE would be the primary method for assessing the binding interactions between indol/indol45 and LPS, respectively.

These findings compounded with PI-ACE analyses show the potential for indol and indol45 as suitable antimicrobial agents. Based on the strong interactions observed, both cationic AMPs may have value in pharmaceutical development. Indol45 and other indol analogs should be of principal interest because of their lack of limitations when compared to indol. These analogs should be examined further with conceivably more manipulation performed on them. With luck, a stronger and more potent antimicrobial agent will emerge that can advance the fight AMR.

REFERENCES

1. Ventola CL. The antibiotic resistance crisis: part 1: causes and threats. *P T A peer-reviewed J Formul Manag*. 2015;40(4):277-283.
2. Levy SB, Marshall B. Antibacterial resistance worldwide: causes, challenges and responses. *Nat Med*. 2004;10(1078-8956 (Print)):S122-S129. doi:10.1038/nm1145.
3. Jia Z, Ramstad T, Zhong M. Determination of protein – drug binding constants by pressure-assisted capillary electrophoresis (PACE)/ frontal analysis (FA). *J Pharm Biomed Anal*. 2002;30:405-413.
4. Deeb S El, Wätzig H, El-Hady DA. Capillary electrophoresis to investigate biopharmaceuticals and pharmaceutically-relevant binding properties. *TrAC - Trends Anal Chem*. 2013;48:112-131. doi:10.1016/j.trac.2013.04.005.
5. Østergaard J, Heegaard NHH. Capillary electrophoresis frontal analysis: principles and applications for the study of drug-plasma protein binding. *Electrophoresis*. 2003;24(17):2903-2913. doi:10.1002/elps.200305526.
6. Busch MHA, Carels LB, Boelens HFM, Kraak JC, Poppe H. Comparison of five methods for the study of drug–protein binding in affinity capillary electrophoresis. *J Chromatogr A*. 1997;777:311-328. doi:10.1016/S0021-9673(97)00369-5.
7. Martínez-Pla JJ, Martínez-Gómez MA, Martín-Biosca Y, Sagrado S, Villanueva-Camañas RM, Medina-Hernández MJ. High-throughput capillary electrophoresis frontal analysis method for the study of drug interactions with human serum albumin at near-physiological conditions. *Electrophoresis*. 2004;25(18-19):3176-3185. doi:10.1002/elps.200406049.
8. Ding YS, Zhu XF, Lin BC. Capillary Electrophoresis Study of Human Serum Albumin Binding to Basic Drugs. *Chromatographia*. 1999;49(5/6):343-346.
9. Østergaard J, Hansen SH, Jensen H, Thomsen AE. Pre-equilibrium capillary zone electrophoresis or frontal analysis: Advantages of plateau peak conditions in affinity capillary electrophoresis. *Electrophoresis*. 2005;26(21):4050-4054. doi:10.1002/elps.200500287.
10. Vuignier K, Schappler J, Veuthey JL, Carrupt PA, Martel S. Improvement of a capillary electrophoresis/frontal analysis (CE/FA) method for determining binding constants: Discussion on relevant parameters. *J Pharm Biomed Anal*. 2010;53(5):1288-1297. doi:10.1016/j.jpba.2010.07.024.

11. El-Hady D, Kühne S, El-Maali N, Wätzig H. Precision in affinity capillary electrophoresis for drug-protein binding studies. *J Pharm Biomed Anal*. 2010;52:232-241. doi:10.1016/j.jpba.2009.12.022.

12. Dufort-Lefrancois E. Exploring Capillary Electrophoresis Methods for the Affinity Interaction of Indolicidin and Lipopolysaccharide. 2015.

CHAPTER 5: CONCLUSION

Antimicrobial resistance (AMR) is a continuous challenge that threatens the efficacy of numerous medications that are used daily on a global scale.[1] This crisis places a huge health and economic burden on our health care system.[2] There is a desperate need for the development of alternative antimicrobial drugs combined with a coordinated effort of other mitigation strategies to slow the epidemic.[1] Antimicrobial peptides (AMPs) are one possible alternative that should be examined because of their broad spectrum of antimicrobial activitiy.[3–5] They are active against most Gram-negative and Gram-positive bacteria, fungi, enveloped viruses, and eukaryotic parasites.[3] The cationic AMP indolicidin (indol) is one proposed drug that has been investigated, however it is flawed for therapeutic use. It is limited in usage as an antimicrobial drug because of the toxic and hemolytic properties it displays.[6] However, it could be invaluable as a parent structure in which analogs such as indolicidin45 (indol45) can be developed from.[6] This analog has exhibited an increase in antimicrobial activity, a decrease in hemolysis, and a stronger binding potential to Lipopolysaccharide (LPS), a Gram-negative bacterial cell membrane component, when compared to indol.[6] Other analogs that have yet to be discovered could potentially be even better candidates as alternatives for antimicrobial drugs. This offers a huge potential for the pharmaceutical industry as the AMR threat continuously grows.

During the analysis of protein-based pharmaceuticals it is critical to establish quality control, perform chiral analysis, and assess non-covalent interactions.[7] To characterize these interactions, capillary electrophoresis (CE) has proven to be a powerful analytical technique due to its tremendous versatility, convenient automation, and small sample requirements.[7,8] The assessment of interactions

between proposed drugs and receptor establishes an equilibrium constant (K_b), which provides information on their strength of binding at equilibrium.[9,10] Specific CE techniques, primarily pre-incubation affinity CE (PI-ACE) and Frontal Analysis CE (FACE), have been utilized in this thesis to determine a K_b for both the interaction between indol-LPS and indol45-LPS. PI-ACE was also coupled with a thermodynamic analysis to determine the type of intermolecular interaction between indol/indol45 and LPS, respectively.

The PI-ACE methodology was thoroughly discussed in this thesis in Chapter 2. A K_b value was produced using the average of three linear regression plots (Double, Y-, and X- reciprocals) for both indol and indol45 with LPS. Analysis was completed in triplicates at 25 °C. The values obtained were: for the indol-LPS interaction (K_b: $3.13 \pm 0.77 \times 10^4\ M^{-1}$) and for the indol45-LPS interaction (K_b: $14.83 \pm 1.67 \times 10^4\ M^{-1}$). The higher K_b value for indol45 indicated a stronger binding constant at equilibrium compared to indol. This stronger binding by indol45 supports prior bioactivity studies, which showed that indol45 had a much lower minimum inhibitory concentration, i.e. greater antimicrobial activity, than that of indol against select bacteria.[6] This is most likely due to the change in hydrophobicity between indol and indol45 due to the change in amino acid content. After substituting the 4^{th} and 5^{th} tryptophan residues for alanine, indol45 became less hydrophobic. Due to the known increased antimicrobial activity of indol45 compared to indol, it can be hypothesized that indol45 kills the bacteria more efficiently. Indol45 can either permeabilize the bacterial membrane resulting in cell lysis or could cross the bacterial envelope into the cytosol and act intracellularly. As mentioned earlier, indol45 is less hydrophobic than indol and thus presumably more comfortable in the aqueous cytosol. Overall, it is probable that the mechanism of action of indol45 against bacteria is

two-fold. It can permeabilize the bacterial cell membrane and disrupt DNA function, both processes ultimately leading to cell death. Further research of indol45 is required to conclusively determine its potential therapeutic use.

After a reliable K_b was determined using PI-ACE at 25 °C, this method was utilized in a thermodynamic analysis to ascertain the type of non-covalent interaction present. K_b values were established at three temperatures (20, 25, and 30 °C) and plotted using the Van't Hoff equation to calculate the enthalpy change (ΔH°), the entropy change (ΔS°), and Gibbs' Free energy change (ΔG°).[11] With knowledge of these values, the type and spontaneity of the interaction was ascertained.[11] The results displayed an enthalpy change of $\Delta H^\circ = -22.85 \pm 0.81$ kJ×mol^{-1}, an entropy change of $\Delta S^\circ = 9.81 \pm 1.40 \times 10^{-3}$ kJ×deg^{-1}mol^{-1}, and a negative Gibbs' Free energy change for the interaction between indol and LPS. Between indol45 and LPS there was an enthalpy change of $\Delta H^\circ = -23.36 \pm 0.35$ kJ×mol^{-1}, an entropy change of $\Delta S^\circ = 20.54 \pm 1.30 \times 10^{-3}$ kJ×deg^{-1}mol^{-1}, and a negative Gibbs' Free energy change as well. These results indicate a spontaneous electrostatic interaction between both indol and indol45 with LPS, respectively. Indol45 had a slightly more negative ΔH° and ΔG° with a negligible ΔS° value, indicating a more favourable interaction than that of indol. An electrostatic interaction supports the hypothesized binding between indol/indol45 and LPS, respectively. With both peptides bearing a +4 charge, they should seamlessly interact with the negatively charged phosphate groups located on the core oligosaccharide section of LPS in the outer cell membrane.

FACE was finally used to verify the K_b established from PI-ACE analysis and to add confidence to the assumed 1:1 binding stoichiometry. A K_b value was produced using nonlinear regression for both interactions between indol and

indol45 with LPS, respectively. Analysis was completed and a usable K_b value was calculated for each peptide. More data should be acquired in order to verify the results. The results from FACE displayed equilibrium constants between indol-LPS (K_b: 2.30 ± 0.20 × 10^4 M^{-1}) and indol45-LPS (K_b: 12.35 ± 0.98 × 10^4 M^{-1}), which indicated strong interactions and compared closely to the PI-ACE values of (K_b: 3.13 ± 0.77 × 10^4 M^{-1} & 14.83 ± 1.67 × 10^4 M^{-1}). The results from both methodologies and both interactions fell within the standard deviation of each. The close comparison in values provided validation of the assumed 1:1 binding stoichiometry in PI-ACE and presented FACE as a viable method to assess the interaction between indol/indol45 and LPS, respectively.

Both CE techniques provided adequate results, however like all research, there were frequent obstacles and complications that required addressing. PI-ACE was our initial focus and provided the largest data set, but the method required an incubation phase due to the slow binding kinetics between indol/indol45 and LPS, respectively. This resulted in a long analysis time, reducing the benefit that CE typically provides with its potential for short analyses. FACE was the most promising technique, although it lacked in the quantity of data for K_b calculations. The cationic nature of indol and indol45, combined with the large concentration of peptide required during injection, frequently resulted in protein adsorption to the inner capillary wall. This resulted in several experimental results becoming unusable. To overcome this problem a longer rinse protocol was initiated, which helped some but didn't alleviate the entire problem.

The strong binding of indol45 presents a large opportunity for future exploration with possible indol analogs and how they attack bacterial cells. Changing select amino acids of an already potent cationic AMP, such as indol, has now been

shown to produce more viable options. Assessing different indol analogs with other receptors should also be examined. LPS was used as the projected receptor but other possibilities may represent bacterial cells more accurately. Wu et al. (1999) have examined proposed drugs and how they interact with bacterial membrane models.[12] These models provide a much closer representation to actual bacteria compared to strictly LPS. The binding of indol/indol45 to LPS, respectively, does however display that there would be an interaction between the proposed drugs and a Gram-negative bacterial cell. What occurs after binding occurs on an actual bacterial cell however, can only be hypothesized without live bacterial research.

Unfortunately, the development of novel antimicrobial drugs cannot exclusively thwart the progress of AMR. The implementation of multiple other practices, such as improving diagnoses, optimizing therapeutic regimens, improving prescription practices, and preventing infection transmission, are all required to provide society a chance at effectively managing the crisis.[13] Researchers combined with policy-makers need to evaluate the AMR epidemic and act as an integrated force to establish a global strategy.[14] This strategy can only hope to reduce the occurrence of the bacterial resistance we currently know rather than eliminate it. With the continuous emergence of multi-drug resistant bacteria, complete defeat of AMR is doubtful, however continuous research can hopefully prevent the fall of our health care system into a pre-antibiotic era.

REFERENCES

1. Ventola CL. The antibiotic resistance crisis: part 1: causes and threats. *P T A peer-reviewed J Formul Manag*. 2015;40(4):277-283.
2. Levy SB, Marshall B. Antibacterial resistance worldwide: causes, challenges and responses. *Nat Med*. 2004;10(1078-8956 (Print)):S122-S129. doi:10.1038/nm1145.
3. Hancock REW. Cationic peptides: Effectors in innate immunity and novel antimicrobials. *Lancet Infect Dis*. 2001;1(3):156-164. doi:10.1016/S1473-3099(01)00092-5.
4. Hancock REW. Peptide antibiotics. *Lancet*. 1997;349(9049):418.
5. Hancock REW, Sahl H-G. Antimicrobial and host-defense peptides as new anti-infective therapeutic strategies. *Nat Biotechnol*. 2006;24(12):1551-1557. doi:10.1038/nbt1267.
6. Podorieszach AP, Huttunen-Hennelly HEK. The effects of tryptophan and hydrophobicity on the structure and bioactivity of novel indolicidin derivatives with promising pharmaceutical potential. *Org Biomol Chem*. 2010;8(I):1679-1687. doi:10.1039/b921248e.
7. Altria K, Chen A, Clohs L. Capillary Electrophoresis as a Routine Analytical Tool in Pharmaceutical Analysis. *LC-GC Eur*. 2001;19(9):2-7.
8. Tanaka Y, Terabe S. Estimation of binding constants by capillary electrophoresis. *J Chromatogr B Anal Technol Biomed Life Sci*. 2002;768(1):81-92. doi:10.1016/S0378-4347(01)00488-1.
9. Rundlett KL, Armstrong DW. Examination of the origin, variation, and proper use of expressions for the estimation of association constants by capillary electrophoresis. *J Chromatogr A*. 1996;721(1):173-186. doi:10.1016/0021-9673(95)00774-1.
10. Jiang C, Armstrong DW. Use of CE for the determination of binding constants. *Electrophoresis*. 2010;31(1):17-27. doi:10.1002/elps.200900528.
11. Ross PD, Subramanian S. Thermodynamics of Protein Association Reactions: Forces Contributing to Stability. *Biochemistry*. 1981;20(11):3096-3102.
12. Wu M, Maier E, Benz R, Hancock REW. Mechanism of interaction of different classes of cationic antimicrobial peptides with planar bilayers and with the cytoplasmic membrane of Escherichia coli. *Biochemistry*.

1999;38(22):7235-7242. doi:10.1021/bi9826299.

13. Ventola CL. The antibiotic resistance crisis: part 2: management strategies and new agents. *P T*. 2015;40(5):344-352.

14. World Health Organization. Global Action Plan on Antimicrobial Resistance. 2015:28.

APPENDIX A: PI-ACE RECIPROCAL PLOTS

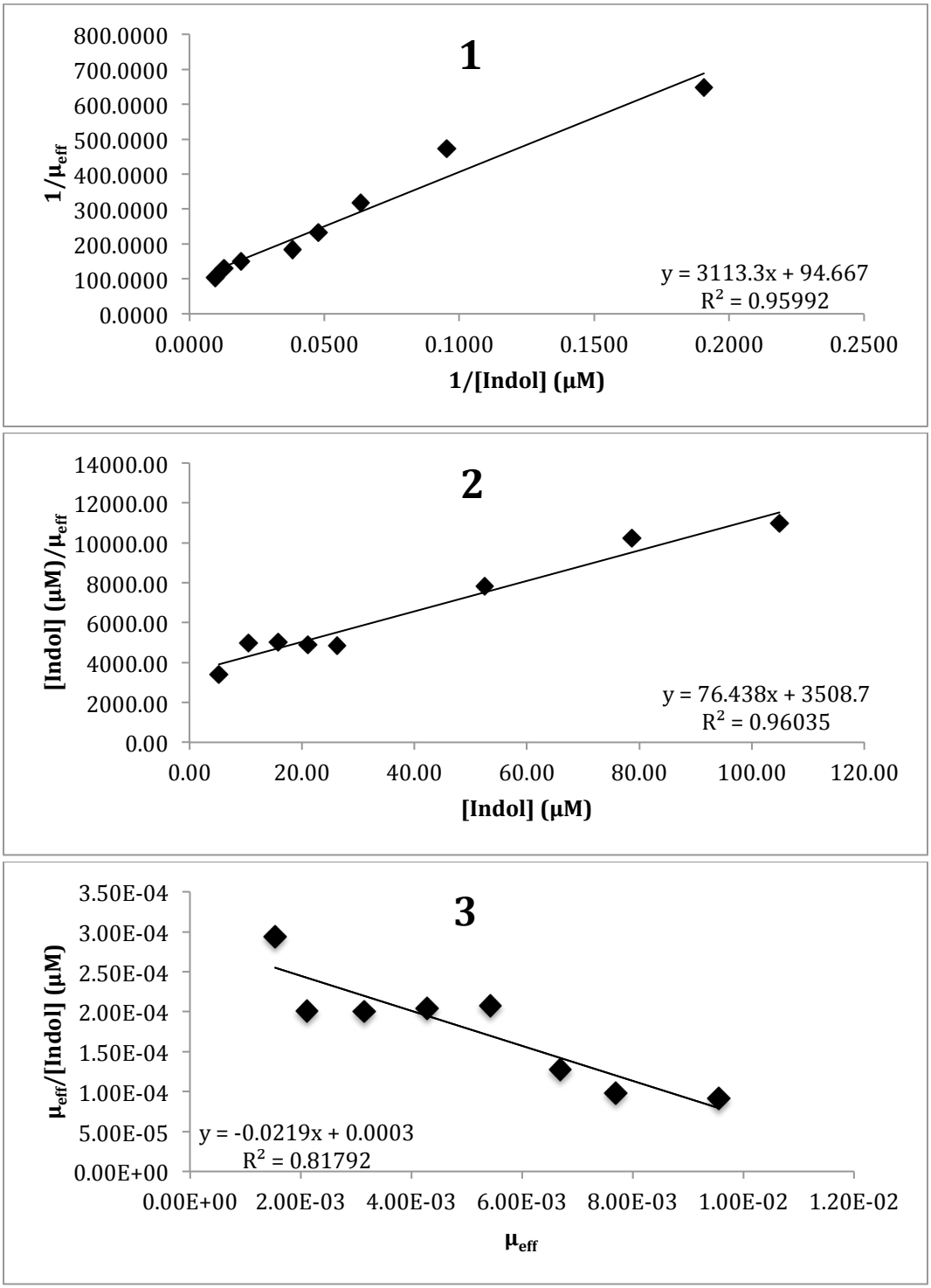

Figure A.1: Reciprocal plots for the indol-LPS interaction using PI-ACE incubated for 2 h at 25 °C. 1) Double-reciprocal 2) Y-reciprocal and 3) X-reciprocal.

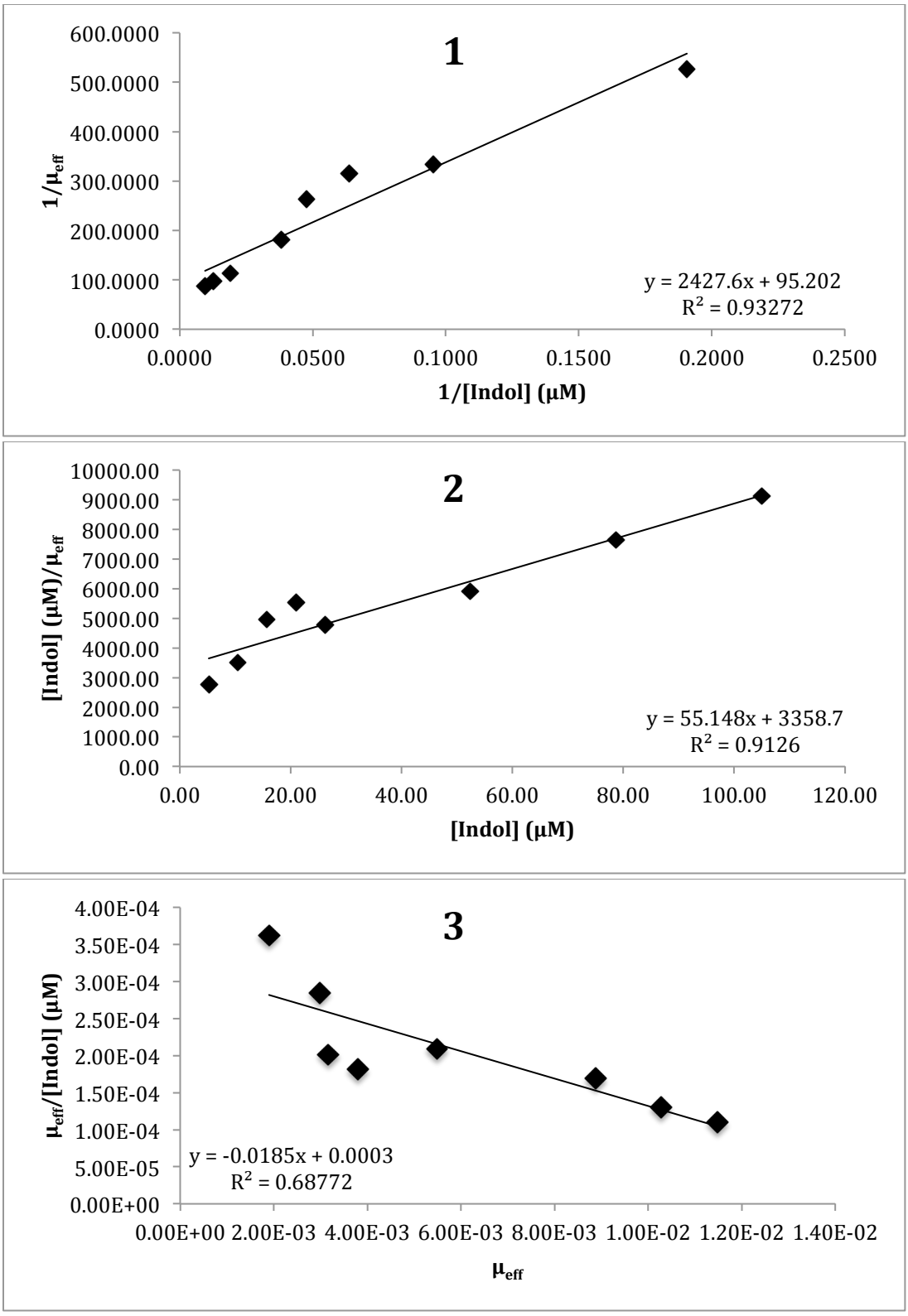

Figure A.2: Reciprocal plots for the indol-LPS interaction using PI-ACE incubated for 6 h at 25 °C. 1) Double-reciprocal 2) Y-reciprocal and 3) X-reciprocal.

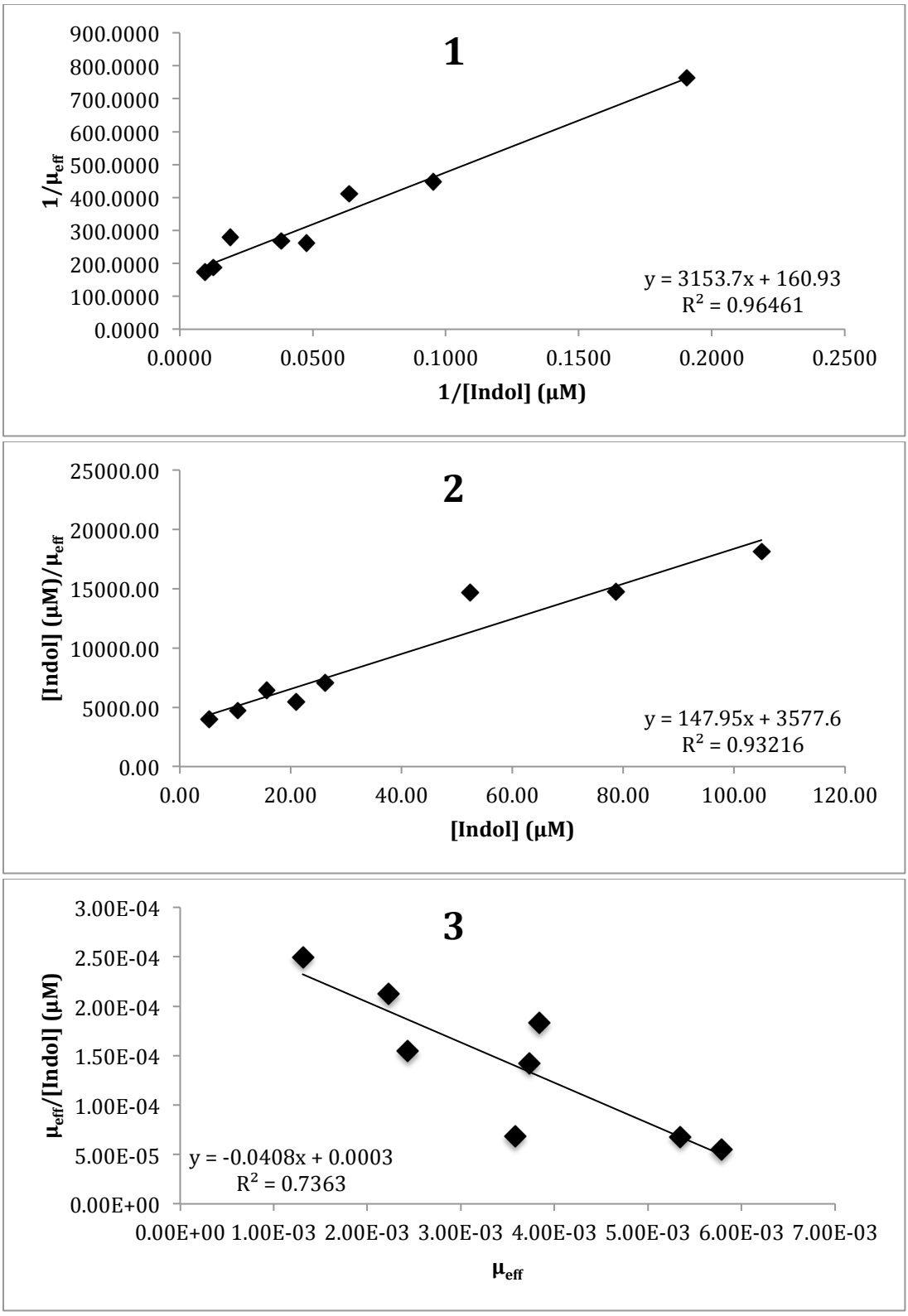

Figure A.3: Reciprocal plots for the indol-LPS interaction using PI-ACE incubated for 12 h at 25 °C. 1) Double-reciprocal 2) Y-reciprocal and 3) X-reciprocal.

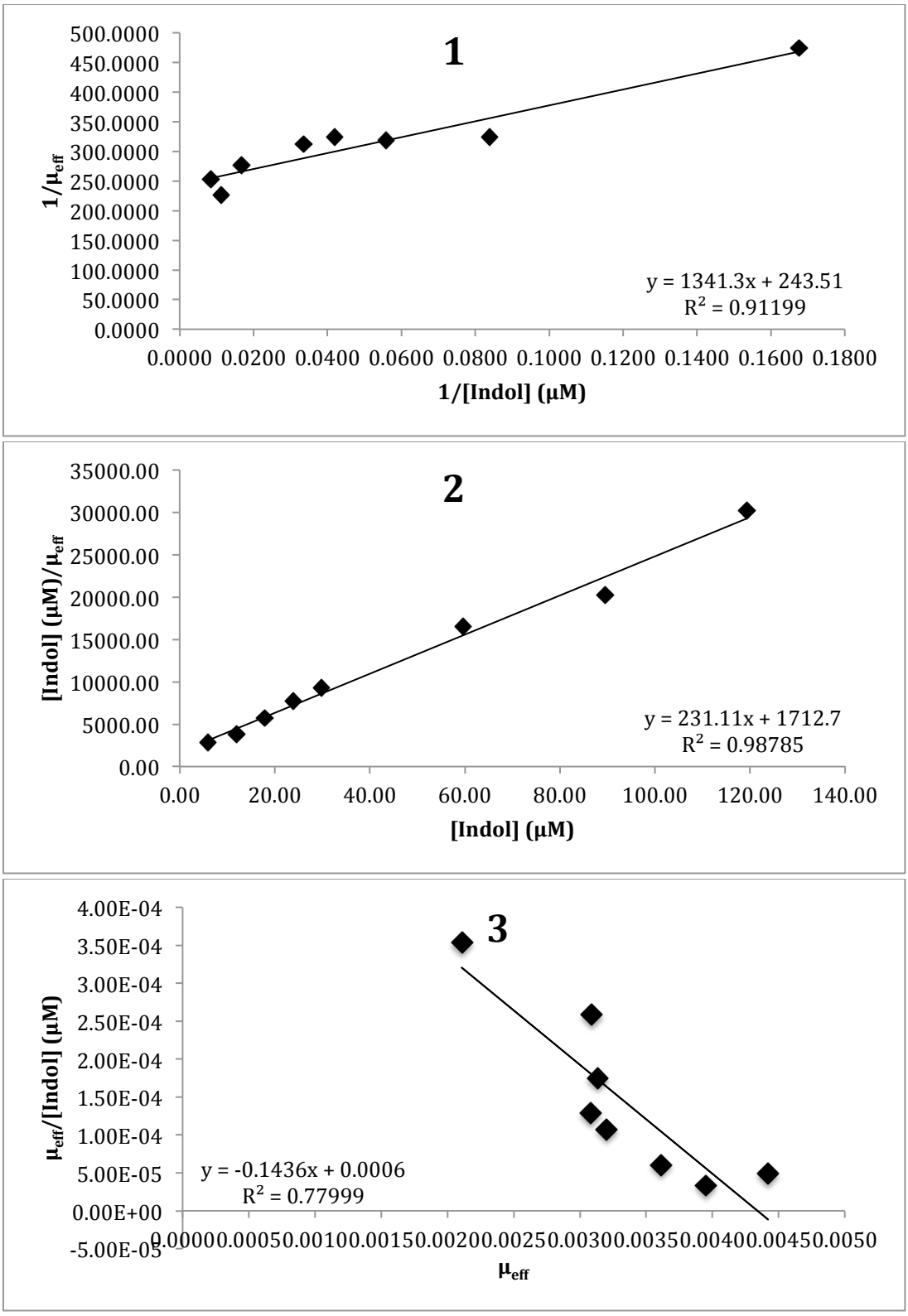

Figure A.4: Reciprocal plots for the indol45-LPS interaction using PI-ACE incubated for 2 h at 25 °C. 1) Double-reciprocal 2) Y-reciprocal and 3) X-reciprocal.

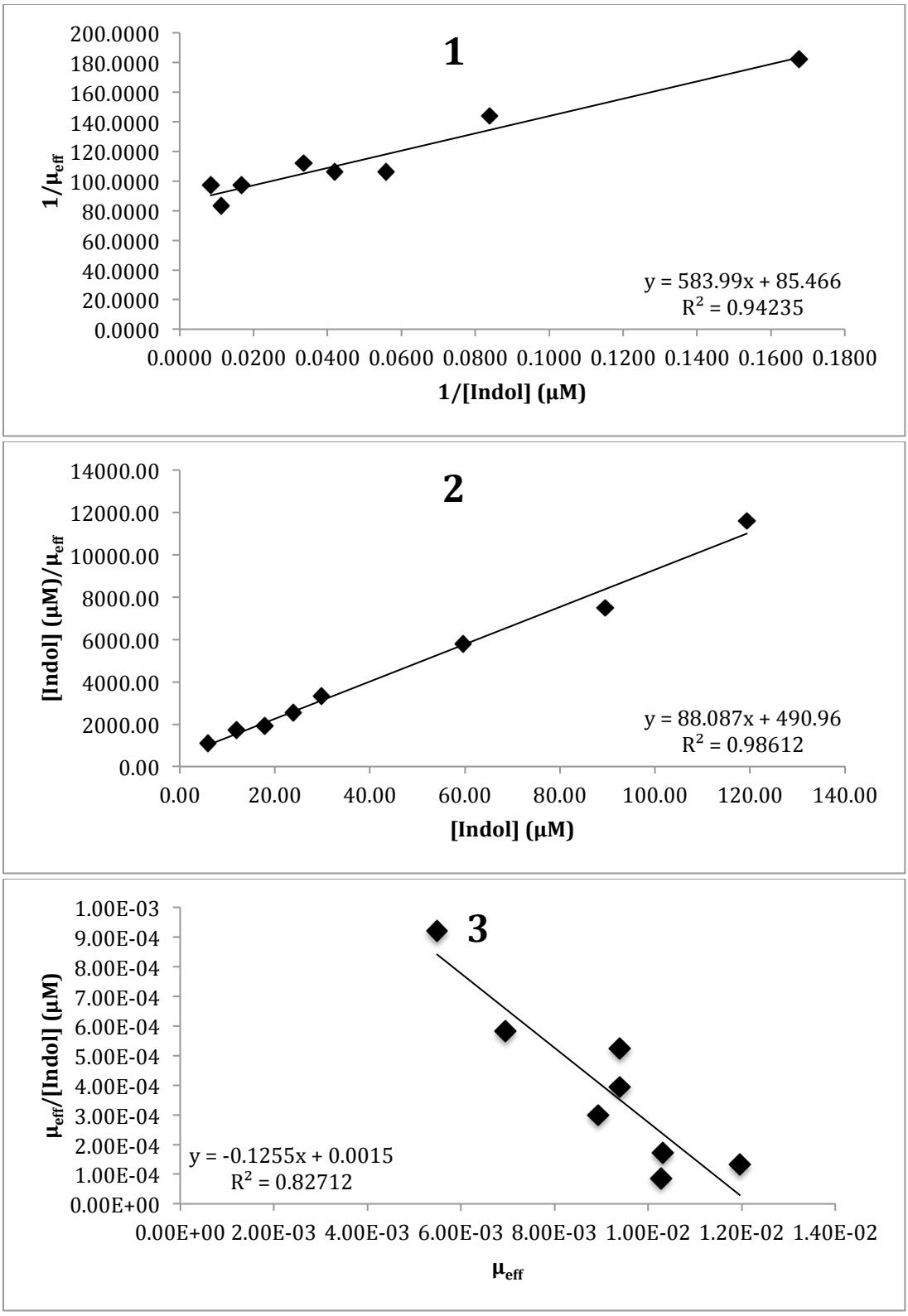

Figure A.5: Reciprocal plots for the indol45-LPS interaction using PI-ACE incubated for 6 h at 25 °C. 1) Double-reciprocal 2) Y-reciprocal and 3) X-reciprocal.

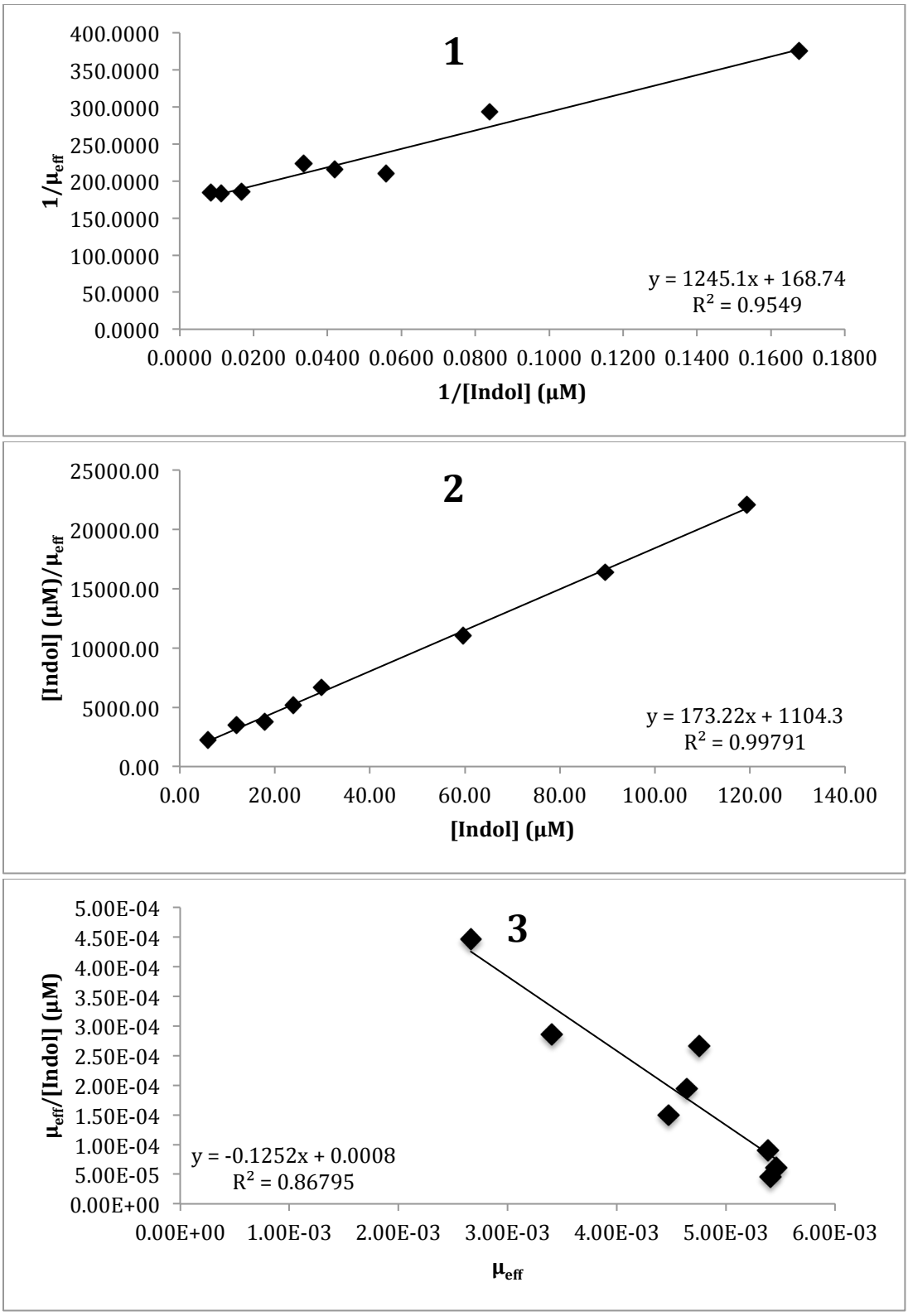

Figure A.6: Reciprocal plots for the indol45-LPS interaction using PI-ACE incubated for 12 h at 25 °C. 1) Double-reciprocal 2) Y-reciprocal and 3) X-reciprocal.

APPENDIX B: THERMODYNAMIC ANALYSIS ELECTROPHEROGRAM OVERLAYS

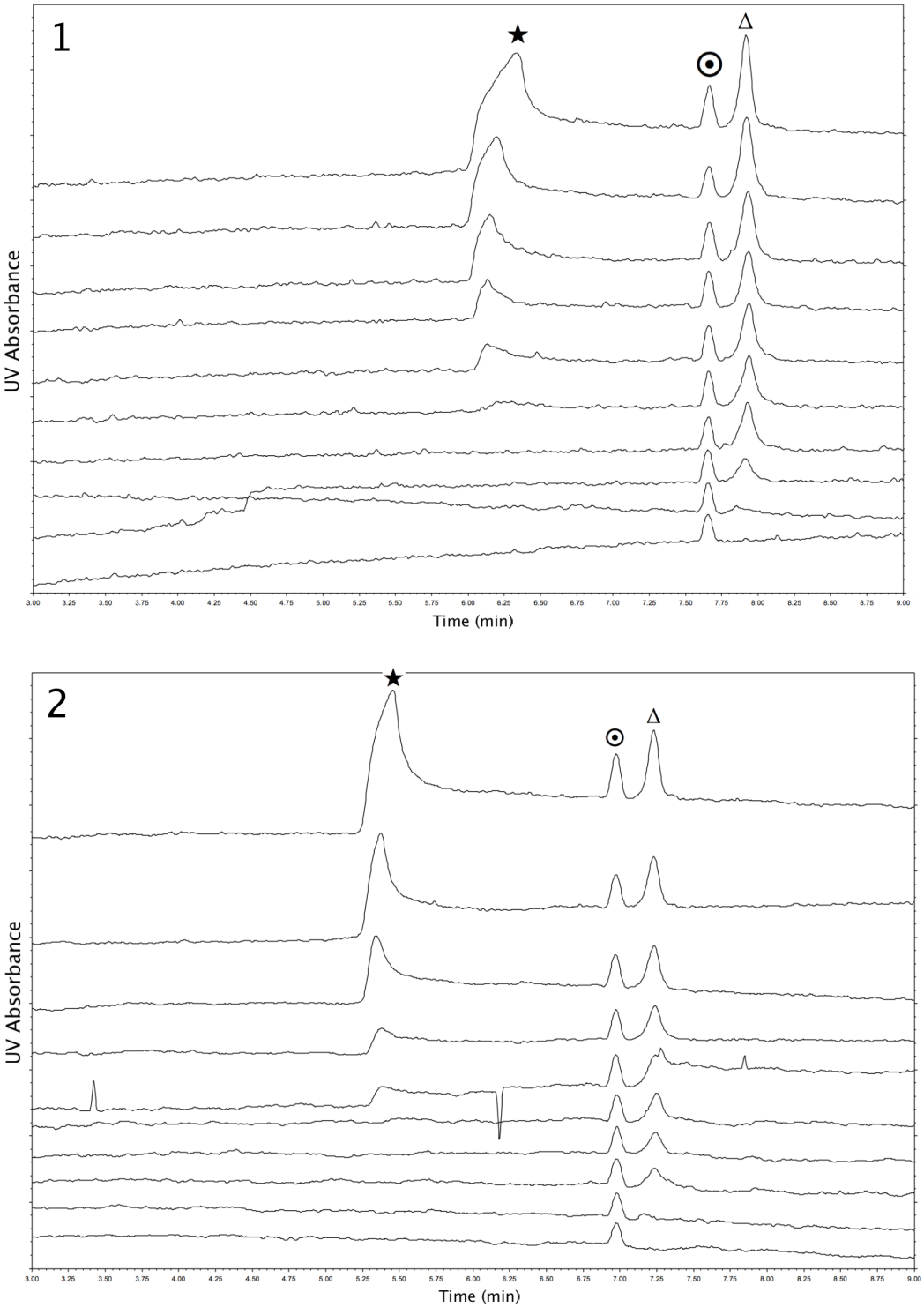

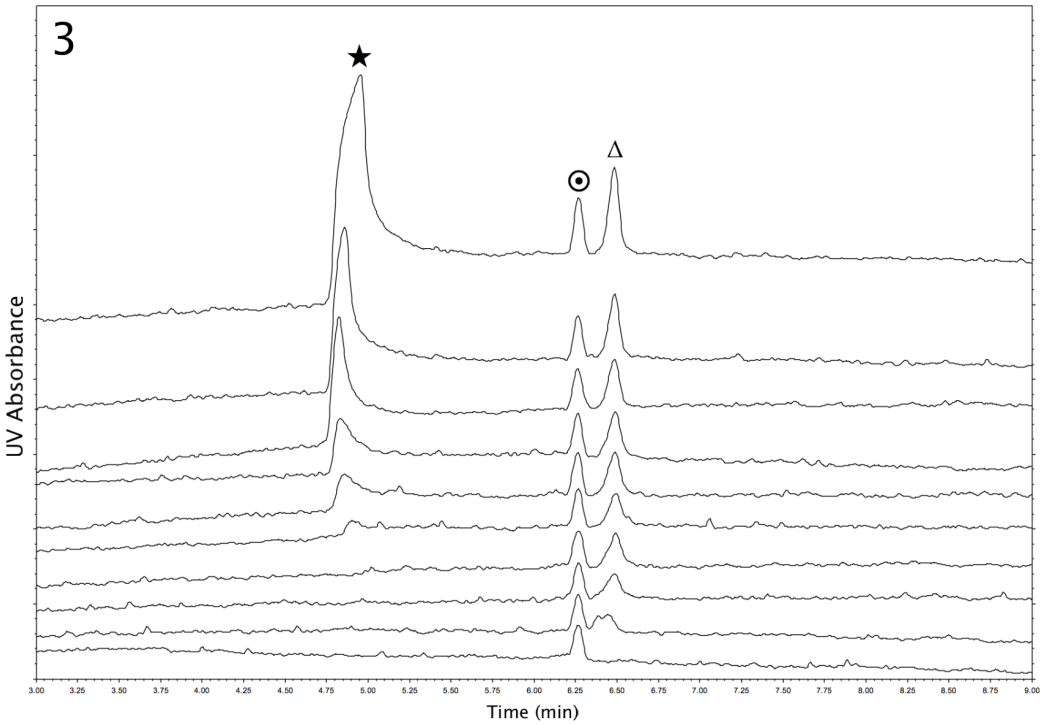

Figure B.1: Overlays of electropherograms from thermodynamic analysis of samples incubated for 2 h of 50 mg/L LPS combined with varying concentrations of indol and DMSO (0.1%v/v). [⊙]: DMSO (neutral marker), [Δ]: LPS/LPS-indol complex. [★]: Free indol. Indol concentrations incrementally increased from the first run (bottom electropherogram) to the last run (top electropherogram): 1) 0 (DMSO only), 2) 0, 3) 10, 4) 20, 5) 30, 6) 40, 7) 50, 8) 100, 9) 150, 10) 200 mg/L. Samples were injected for 5 s duration at 1.0 psi, 20 kV separation voltage, normal polarity, UV detection at 214 nm, BGE of 100 mM PO_4^{-2} (pH 7.2). Overlay 1) 20 °C, 2) 25 °C, 3) 30 °C.

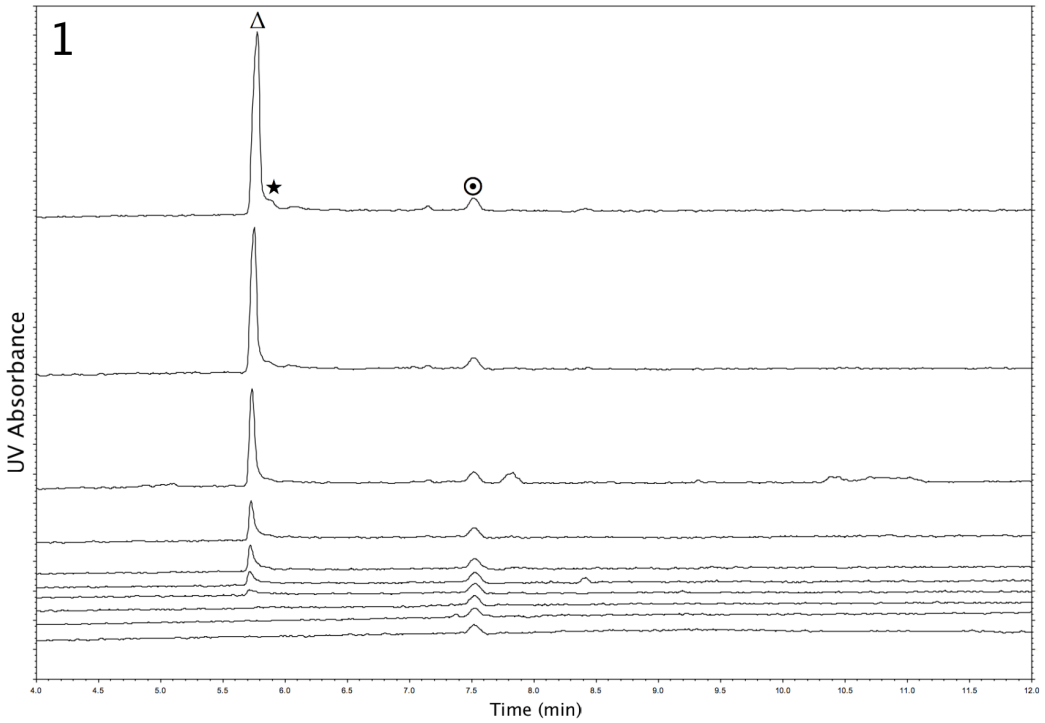
1
Δ
★
⊙
UV Absorbance
4.0
4.5
5.0
5.5
6.0
6.5
7.0
7.5
8.0
8.5
9.0
9.5
10.0
10.5
11.0
11.5
12.0
Time (min)

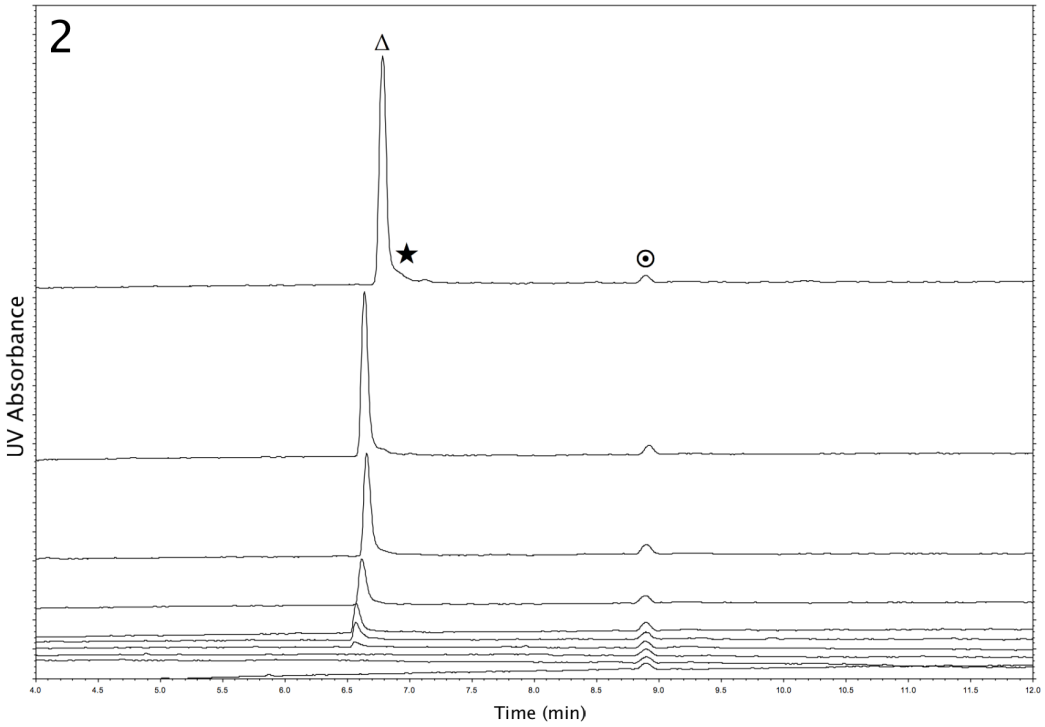
2
Δ
★
⊙
UV Absorbance
4.0
4.5
5.0
5.5
6.0
6.5
7.0
7.5
8.0
8.5
9.0
9.5
10.0
10.5
11.0
11.5
12.0
Time (min)

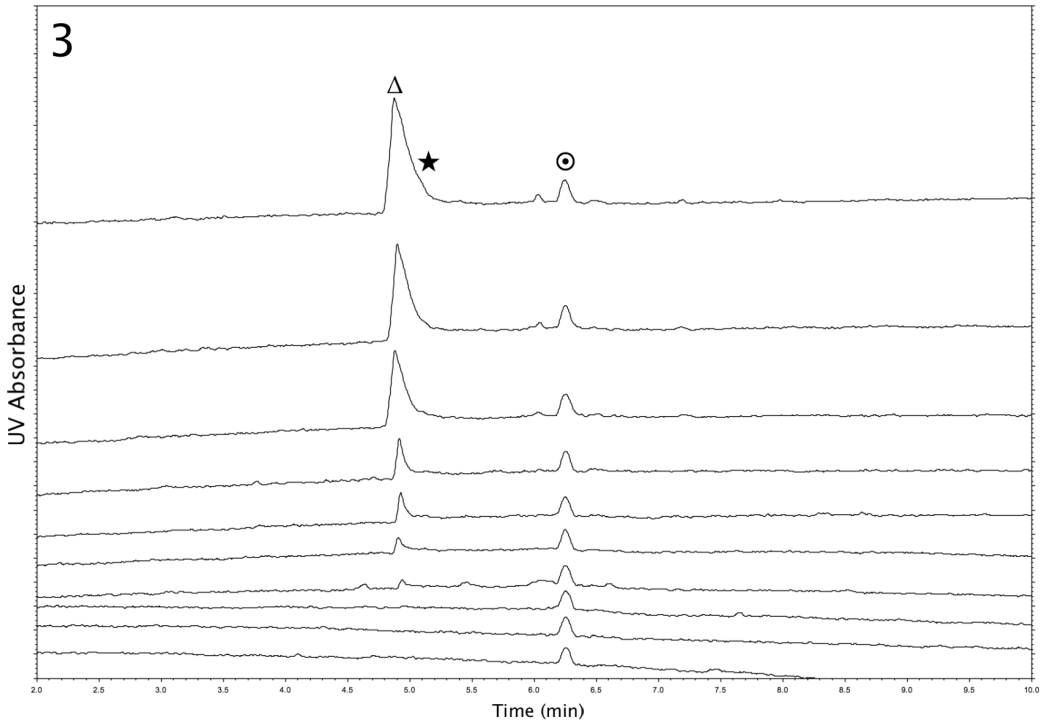

Figure B.2: Overlays of electropherograms from thermodynamic analysis of samples incubated for 2 h of 50 mg/L LPS combined with varying concentrations of indol45 and DMSO (0.1%v/v). [⊙]: DMSO (neutral marker), [Δ]: LPS/LPS-indol45 complex. [★]: Free indol45. Indol45 concentrations incrementally increased from the first run (bottom electropherogram) to the last run (top electropherogram): 1) 0 (DMSO only), 2) 0, 3) 10, 4) 20, 5) 30, 6) 40, 7) 50, 8) 100, 9) 150, 10) 200 mg/L. Samples were injected for 5 s duration at 1.0 psi, 20 kV separation voltage, normal polarity, UV detection at 214 nm, BGE of 100 mM PO_4^{-2} (pH 7.2). Overlay 1) 20 °C, 2) 25 °C, 3) 30 °C.